Interactions in D-brane Configurations

Owen, Anthony Wynne

Interactions in D-brane Configurations

A thesis presented for the degree of

Doctor of Philosophy

by

Anthony Wynne Owen

Department of Mathematics

University of Durham

May 2004

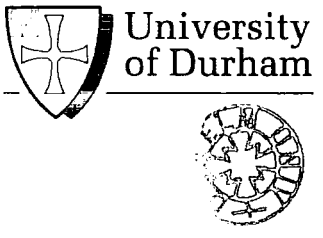

Dedicated to Mum, Dad and Michelle.

Interactions in D-brane Configurations

by

Anthony Wynne Owen

Abstract

We explore various interactions in D-brane configurations and their implications for the construction of phenomenologically viable string models.

Initially, we investigate the scenario of parallel and perpendicular stacks of D-branes located on an orbifold singularity, as in the bottom-up construction. A supersymmetric D-brane model is presented, that has CP spontaneously broken by discrete torsion. The low energy physics is largely independent of the compactification scheme and the kähler metric has 'texture zeros' dictated by the choice of discrete torsion. This motivates a simple ansatz for the kähler metric which results in a CKM matrix given in terms of two free parameters, hence we predict a single mixing angle and the CKM phase. The CKM phase is predicted to be close to $\frac{\pi}{3}$.

We then proceed to a discussion of a different class of models involving D-branes intersecting at arbitrary angles, and wrapping a compact internal space. Here we calculate tree level three and four point scattering amplitudes in type II string models with matter fields localised at D-brane intersections. We treat both the classical and quantum parts in detail, with the latter being computed using conformal field theory techniques developed for closed strings on orbifolds. Contributions from string states wrapping the internal space are also included. These calculations are then generalised to N-point amplitudes, which are determined completely.

Finally, we consider the application of these results to four fermion interactions. In particular, the implications for Higgs exchange in intersecting brane models is discussed.

Acknowledgements

First and foremost I would like to thank my supervisor, *Dr.Steven Abel*, for his patience and guidance whilst pursuing our research. Also, for his ability to strike a balance between allowing me the freedom to gain my independence as a researcher and the need to progress quickly. For assistance with computations in RGE effects utilised in chapter 3, I would like to thank *Shaaban Khalil.*

To my office mates, *David Howe, Jonathan Levell* and *Ben Schofield*, I give a special thanks for help with aspects of physics that stumped me and for generally keeping me sane. Thanks also to *Paul Bostock* for being a source of immediate aid during my first year. Finally, for light relief, I would like to thank *John Carmack* and *Tufty.*

This thesis is dedicated to Mum and Dad, whose emotional and financial support throughout my life is the foundation of my achievements. This dedication is shared with *Michelle Fong*, who makes me laugh every single day and without whom this thesis would never have been completed.

Declaration

I declare that the work in this thesis has not previously been submitted for a degree at this or any other university.

The research described in this thesis is the result of collaboration between S.A.Abel and the author and has been published in the following papers:

- S.A.Abel and A.W.Owen,
  "CP Violation and CKM Predictions from Discrete Torsion"
  Nucl. Phys. **B651** (2003) 191-210 [hep-th/0205031]

- S.A.Abel and A.W.Owen,
  "Interactions in Intersecting Brane Models"
  Nucl. Phys. **B663** (2003) 197-214 [hep-th/0303124]

- S.A.Abel and A.W.Owen,
  "N-point Amplitudes in Intersecting Brane Models"
  Nucl. Phys. **B682** (2004) 183-216 [hep-th/0310257]

Some of the results have been presented by the author at the following conference and written up in the conference report

- A. W. Owen,
  "Interactions in Intersecting Brane Models"
  Proceedings of the second International Conference on String Phenomenology. Durham 2003.

Contents

List of Figures

List of Tables

Chapter 1

Introduction and Motivation

1.1 The Standard Model and String Theory

The Standard Model of particle physics is one of the greatest intellectual triumphs of the twentieth century. Predictions for interactions between elementary particles are seen to be in remarkable agreement with what we observe in nature. Furthermore, the Standard Model achieves this using a very simple structure. It is based on the principal of local gauge invariance and contains three interactions, mediated by gauge vector bosons, described by the gauge group $SU(3)_c \times SU(2)_L \times U(1)_Y$. These fundamental forces are supplemented with matter fields, described by Weyl fermions charged under the gauge groups as follows,

$$\begin{array}{llllll} Q_L^i & (3,2)_{1/6} & u_R^i & (\bar{3},1)_{1/3} & d_R^i & (\bar{3},1)_{-2/3} \\ L_L^i & (1,2)_{-1/2} & e_R^i & (1,1)_1. & & \end{array} \tag{1.1}$$

The subscript denotes $U(1)_Y$ hypercharge and the superscript runs from one to three labelling the three generations of matter fields observed in nature. One important feature of this arrangement is *chirality*. That is, left-handed and right-handed fields possess different charges. This protects fermion masses, which through the Higgs mechanism receive a mass of the order of electroweak symmetry breaking.

Despite its remarkable empirical success the Standard Model has a number of important shortcomings. For instance, there are nineteen independent parameters in the Standard Model that need to be tuned by experiment.

Furthermore, if we assume that mass is generated by a Higgs mechanism and that there exists a cut-off scale for the Standard Model, we require extensions such as supersymmetry to avoid the hierarchy problem. There are also the 'why' questions,

- why the above choices of gauge fields?
- why the particular pattern of matter fields we observe, and no others?
- why do we live in a four dimensional world?

However, arguably its greatest shortcoming is it excludes the most pervasive of all fundamental forces, gravity. This is because there is no quantum field theory that can successfully describe gravity at the quantum scale and as such it does not fit naturally within the framework of the Standard Model.

The problem of finding a quantum theory of gravity is probably the most challenging and fundamentally important issue facing modern theoretical physics. There have been a number of promising ideas put forward, each with its own advantages and disadvantages. Here, I will concentrate on one approach, string theory, which has received a huge amount of attention from particle physicists since the 1970s. The basic idea is to replace the point particles of quantum field theory with extended one dimensional objects, known as strings. The main advantage of this description is that, while there are many particles there is only one string. This acts as a strong unification principle. Our current limited understanding of string theory is illustrated in figure 1.1. Here, we depict the five different types of weakly coupled ten dimensional string theories and M-Theory whose low energy limit is eleven dimensional supergravity theory [1]. These are thought to be different limits of some underlying unknown theory and are related to one another by various non-perturbative and perturbative dualities [2, 3]. These dualities allow us insights into the non-perturbative structure of the various string theories. For example, M-Theory compactified on S_1 is the strongly coupled Type IIA theory. In addition to the fundamental strings, these theories admit a variety of extended non-perturbative objects. For instance, there exists hypersurfaces in spacetime where open strings end. These are called 'Dp-branes', where p is the number of spatial dimensions. Also, there are NS-branes and M-branes, however we will be concerned mostly with Dp-branes.

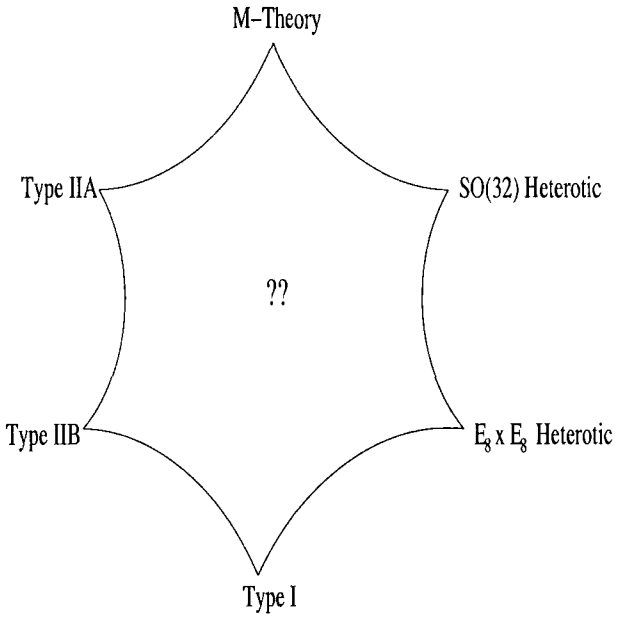

Figure 1.1: All string theories, and M-Theory, as limits of one unknown theory.

String theory is a promising candidate for new physics beyond the Standard Model, as it provides a framework within which it is possible to describe consistently both quantum gravity and the gauge interactions contained in the Standard Model of particle physics. It also has the nice feature of being UV finite at all orders in perturbation theory. This is due to the fact that the strings have a length, which acts as a high energy cut-off for the theory. Furthermore, it also provides an approach to explaining the 'why' questions described above. The reason for this, is that whichever string theory we choose, it must be compactified down to four dimensions. The details of the compactification often determines the gauge group and matter content of the low energy theory. Thus the possibility arises that there exists some ground state in a string theory, for which the compactification automatically gives rise to the gauge groups and matter content of the Standard Model. However a selection principle to determine a compactification space that does this is not yet available. It is possible that this may only be achieved through a thorough understanding of the string moduli space depicted in figure 1.1, and hence the non-perturbative structure of the various string theories.

1.2 Why String Phenomenology?

Formulating a non-perturbative version of some string theory, finding its ground state and compactifying to obtain the Standard Model is a formidable task. Therefore, a simpler alternative, which will help achieve this goal, is to 'manually' construct and examine *string models*. By a string model, I mean a specific consistent set-up, which has been constructed to resemble the Standard Model or supersymmetric extensions thereof (whether it achieves this, is another matter). For example, $E_8 \times E_8$ Heterotic string compactified on a particular orbifold. In effect, we let experiment guide us, rather than attempting to fundamentally determine our ground state. The aim of String Phenomenology is therefore to find a string model, or class of models, which is in agreement with the Standard Model and to correctly predict some feature of our universe not previously observed. If this can be achieved, we could replace the Standard Model with a more satisfactory model of nature and shed light on the underlying non-perturbative structure of string theory.

Progress towards this goal has been achieved. There are large classes of string models which do indeed resemble our observable universe. For instance, compactifying ten dimensional $E_8 \times E_8$ Heterotic string theory on a Calabi-Yau manifold (which is a manifold with $SU(3)$ holonomy) can lead to models, which after breaking supersymmetry, resemble the Standard Model at low energies. However they often contain extended gauge groups and matter content. These models have the beautiful geometric feature of relating the Euler number of the Calabi-Yau manifold to the number of generations of particles [4], thus providing a partial geometric explanation to the 'why' questions listed above. Furthermore, if we consider eleven dimensional M-theory and its low energy supergravity limit, we may also obtain semi-realistic models by compactifying seven dimensions using a manifold of G_2 holonomy [5].

In fact, one of the greatest strengths of string theory is the way in which it often translates our 'why' questions into questions about geometry. Another example of this arises through string models based on the idea of D-branes. A Dp-brane is simply a (p+1)-dimensional hypersurface where open string endpoints are constrained to move. They have an interesting connection to gauge theories, in fact a stack of N D-branes has a U(N) gauge theory on it's world volume (see section 2.3). Hence, we can construct string models by choosing the required D-branes to provide us with interesting gauge groups.

For example, a stack of three, a stack of two and a single D-brane gives rise to the gauge group $U(3) \times U(2) \times U(1)$, which often can be related to the Standard Model gauge group. Hence, a geometrical choice (i.e. the number of D-branes in the model) can account for the gauge groups in the Standard Model.

This type of construction contains two large (overlapping) classes of string models,

1. Type IIA/B theory with parallel and perpendicular D-branes on orbifolds and orientifolds.

2. Type IIA/B theory with D-branes intersecting at arbitrary angles and wrapping a compact internal space.

In this thesis, we shall study interactions in both these classes of string models. This will lead us to explore some generic features of these models, and to construct specific examples with low energy physics close to that of the Standard Model. Furthermore, the results of this research will allow for future improvements in the construction of such models. As a final remark, another promising class of model which contains hypersurfaces with localised gauge fields is Horava-Witten M-theory [6], but these models lie outside the scope of this thesis.

1.3 Layout of this thesis

This thesis has six chapters in total. After the introduction and motivation in this chapter, we briefly survey the necessary background material in Chapter 2. This includes the basic formalism required for constructing and analysing string models. In particular, section 2.1 contains a brief review of the Neveu-Schwarz-Ramond Superstring, including its quantisation. This is used in determining the string spectrum of our model in chapter 3. Then we discuss how to calculate string amplitudes in section 2.2, which will be required in chapters 4 and 5. Finally, we give a brief motivational discussion of D-branes, which are the essential ingredients of the models discussed in this thesis.

Chapter 3 is concerned with the first class of string models listed above. Here we construct a D-brane model using the *bottom-up approach* [7]. This model was presented in [8] and is a supersymmetric model, that has CP

spontaneously broken by discrete torsion. The construction of this model is described in detail in section 3.4 where it is shown that discrete torsion can give rise to CP violation. This is pursued in section 3.5, where we examine the phenomenological implications. In particular, we use the fact that the low energy physics is largely independent of the compactification scheme and the kähler metric has 'texture zeros' dictated by the choice of discrete torsion. This motivates a simple ansatz for the kähler metric which results in a CKM matrix given in terms of two free parameters, hence we predict a single mixing angle and the CKM phase. The CKM phase is predicted to be close to $\frac{\pi}{3}$. This model can be seen as a first step in a new way to avoid the traditional supersymmetric CP and flavour problems typically found in attempts to incorporate supersymmetry breaking and flavour structure in a high energy model.

In chapter 4, we proceed to the second class of string models, known as intersecting brane models, involving D-branes intersecting at arbitrary angles. In particular, we calculate three and four point scattering amplitudes in type II string models with matter fields localised at the intersections of D-brane wrapping cycles. This work was published in [8,9]. In section 4.4, we calculate three point tree level scattering amplitudes. This includes the case of Yukawa interactions which are seen to give rise to a natural mechanism for the generation of a mass hierarchy [10]. Next, we determine the four point function in section 4.5. The quantum contribution is determined using conformal field theory techniques developed in [11, 12] for closed strings on orbifolds.

In chapter 5 we generalise these calculations to N-point amplitudes involving string states at D-brane intersections. These results were published in [9]. We finish in section 5.4 with an application of our results to the analysis of Higgs exchange in intersecting brane models. Our results are then summarised, along with a conclusion and prospects for future work in chapter 6.

Chapter 2

An Introduction to String Theory

We now proceed to a brief review of the necessary background material in string theory, required to understand the constructions and calculations presented in the later chapters. The main references are [13–17].

2.1 The Neveu-Schwarz-Ramond Superstring

2.1.1 The classical action

We begin with an overview of the basic construction of the Neveu-Schwarz-Ramond (NSR) superstring. From this construction, we can obtain all five weakly coupled string theories. A string may be discussed in terms of a two dimensional field theory, defined on a worldsheet with coordinates $\sigma \in [0, \pi]$ and $\tau \in (-\infty, \infty)$. There are D bosonic fields, X^μ, which can also be interpreted as the embedding of the string worldsheet in the target spacetime. These transform as vectors under Lorentz transformations in the target spacetime. We also have D anticommuting Majorana fermions, ψ^μ, which transform as spinors under coordinate transformations in the two-dimensional worldsheet and as vectors under Lorentz transformations in the target spacetime. The action, in conformal gauge (i.e. the metric, γ_{ab}, on the two-dimensional worldsheet is conformally flat), is given by

$$S = -\frac{T}{2} \int d^2\sigma \, \left(\partial_a X^\mu \partial^a X_\mu - i\overline{\psi}^\mu \, \rho^a \, \partial_a \psi_\mu \right), \tag{2.1}$$

where $T = \frac{1}{2\pi\alpha'}$ is the tension of the string, $\alpha'^{1/2}$ is the string length and $a = 0, 1$ sums over the worldsheet coordinates. The matrices ρ^a are 2×2 Dirac matrices which in a convenient basis for the worldsheet spinors can be taken to be,

$$\rho^0 = \begin{pmatrix} 0 & -i \\ i & 0 \end{pmatrix}, \quad \rho^1 = \begin{pmatrix} 0 & i \\ i & 0 \end{pmatrix}. \tag{2.2}$$

These matrices obey,

$$\{\rho^a\,,\,\rho^b\} = -2\,\eta^{ab}\,, \tag{2.3}$$

where the signature for the Lorentzian metric, η^{ab}, is taken to be (- +). In this basis, the action (2.1) is real provided the fermion field

$$\psi^\mu = \begin{pmatrix} \psi^\mu_- \\ \psi^\mu_+ \end{pmatrix}, \tag{2.4}$$

is a two-component Majorana spinor as stated above. Hence, $\psi^\mu_\pm$ are real and $\overline{\psi} = \psi^T\rho^0$.

2.1.2 Equation of motion and boundary conditions

As a first step towards determining the spectrum of this theory, we must consider the equation of motion and boundary conditions for the worldsheet fields. Let us first consider the bosonic part of the action (2.1),

$$S_B = -\frac{T}{2}\int d^2\sigma\partial_a X^\mu \partial^a X_\mu. \tag{2.5}$$

Varying this action with respect to X^μ we obtain,

$$\delta S_B = T\int d\sigma d\tau \delta X_\mu \left(\partial_\sigma^2 - \partial_\tau^2\right) X^\mu - T\int d\tau \left[\partial_\sigma X^\mu \delta X_\mu\right]_{\sigma=0}^{\sigma=\pi}. \tag{2.6}$$

The first term provides us with the equation of motion for X^μ, which is simply the free two-dimensional wave equation. As such, the general solution is comprised of arbitrary left and right moving functions,

$$X^\mu(\tau,\sigma) = X^\mu_L(\sigma^+) + X^\mu_R(\sigma^-), \tag{2.7}$$

where we have defined worldsheet light-cone coordinates, $\sigma^{\pm} = \tau \pm \sigma$. Introducing, $\partial_{\pm} = \frac{1}{2}(\partial_{\tau} \pm \partial_{\sigma})$, we obtain

$$\partial_{+}\partial_{-}X^{\mu} = 0. \tag{2.8}$$

The second term in (2.6) provides us with the boundary conditions for the bosonic worldsheet fields. There are two main possibilities,

- **Open Strings** with one of the following,
  1. *Neumann* boundary conditions, $\partial_{\sigma}X^{\mu}(\tau,\sigma)|_{\sigma=0,\pi} = 0$.
  2. *Dirichlet* boundary conditions, $\partial_{\tau}X^{\mu}(\tau,\sigma)|_{\sigma=0,\pi} = 0$.
- **Closed Strings** with periodic boundary conditions,

$$\begin{aligned} X^{\mu}(\tau,0) &= X^{\mu}(\tau,\pi), \\ \partial_{\sigma}X^{\mu}(\tau,0) &= \partial_{\sigma}X^{\mu}(\tau,\pi). \end{aligned} \tag{2.9}$$

Proceeding to the fermionic part of the action, using the conventions in subsection 2.1.1, we have

$$S_F = iT \int d^2\sigma \left(\psi_{+}\partial_{-}\psi_{+} + \psi_{-}\partial_{+}\psi_{-}\right), \tag{2.10}$$

where the index μ has been suppressed for clarity. Using the variational principle, we see that the fermionic fields also split up into left and right movers satisfying the two dimensional massless Dirac equation,

$$\partial_{-}\psi_{+} = \partial_{+}\psi_{-} = 0. \tag{2.11}$$

The boundary term is,

$$[\psi_{+}\delta\psi_{+} - \psi_{-}\delta\psi_{-}]_{\sigma=0}^{\sigma=\pi} = 0. \tag{2.12}$$

In the open string case, the relative sign between ψ_{+}^{μ} and ψ_{-}^{μ} is purely a convention and we may impose $\psi_{+}^{\mu}(\tau,0) = \psi_{-}^{\mu}(\tau,0)$. Then, we have the following possible boundary conditions for the fermionic fields,

- **Open Strings** have the two distinct possibilities,
  1. *Ramond* (periodic) boundary conditions, $\psi_{+}^{\mu}(\tau,\pi) = \psi_{-}^{\mu}(\tau,\pi)$.

2. *Neveu-Schwarz* (anti-periodic) boundary conditions, $\psi_+^\mu(\tau,\pi) = -\psi_-^\mu(\tau,\pi)$.

- **Closed Strings**, each component of ψ is periodic or anti-periodic separately.

Now that we have obtained the equation of motion and boundary conditions for the bosonic and fermionic worldsheet fields we turn our attention to their mode expansions. This will allow us, along with mass-shell constraints, to quantise the two dimensional field theory on the string worldsheet.

2.1.3 Mode expansions of the worldsheet fields

We first focus our attention on the closed string. The periodicity of the bosonic fields leads to the mode expansions,

$$\begin{aligned} X_L^\mu(\sigma^+) &= \tfrac{1}{2}x_0^\mu + \alpha' p^\mu \sigma^+ + i\sqrt{\tfrac{\alpha'}{2}}\textstyle\sum_{n\neq 0}\frac{\tilde{\alpha}_n^\mu}{n}e^{-2in\sigma^+}, \\ X_R^\mu(\sigma^-) &= \tfrac{1}{2}x_0^\mu + \alpha' p^\mu \sigma^- + i\sqrt{\tfrac{\alpha'}{2}}\textstyle\sum_{n\neq 0}\frac{\alpha_n^\mu}{n}e^{-2in\sigma^-}, \end{aligned} \tag{2.13}$$

where x_0^μ and p^μ are the centre of mass position and momentum of the string respectively. For the zero mode, we have the relation $\tilde{\alpha}_0^\mu = \alpha_0^\mu = \sqrt{\frac{\alpha'}{2}}p^\mu$. Also, for X^μ to be real we require,

$$(\tilde{\alpha}_n^\mu)^* = \tilde{\alpha}_{-n}^\mu, \quad (\alpha_n^\mu)^* = \alpha_{-n}^\mu. \tag{2.14}$$

The mode expansions (2.13) describe left and right moving waves travelling independently and in opposite directions around the closed string.

The fermionic fields have the mode expansions,

$$\psi_+^\mu = \textstyle\sum_r \tilde{\psi}_r^\mu e^{-2ir\sigma^+}, \quad \psi_-^\mu = \sum_r \psi_r^\mu e^{-2ir\sigma^-}, \tag{2.15}$$

where $r \in \mathbb{Z}$ when $\psi_\pm$ is in the periodic (Ramond) sector and $r \in \mathbb{Z} + 1/2$ when $\psi_\pm$ is in the anti-periodic (Neveu-Schwarz) sector. Note that, there are four distinct closed string sectors corresponding to the possible permutations for pairing up Neveu-Schwarz (NS) and Ramond (R) boundary conditions in the left and right movers. Finally, the Majorana condition requires that,

$$(\tilde{\psi}_r^\mu)^* = \tilde{\psi}_{-r}^\mu, \quad (\psi_r^\mu)^* = \psi_{-r}^\mu. \tag{2.16}$$

Next, consider the open string with Neumann boundary conditions for the bosonic fields. In this case, the left and right movers combine to form standing waves, hence

$$X^\mu(\tau,\sigma) = x_0^\mu + 2\alpha' p^\mu \tau + i\sqrt{2\alpha'}\sum_{n\neq 0}\frac{\alpha_n^\mu}{n}e^{-in\tau}cos(n\sigma). \tag{2.17}$$

Hence, there are no longer independent left and right movers as appeared in the closed string case, and the zero mode is now given by $\alpha_0^\mu = \sqrt{2\alpha'}p^\mu$. We return to the case of Dirichlet boundary conditions in section 2.3, where we discuss D-branes.

For the fermionic fields on the open string, we again have a single set of oscillators,

$$\psi_\pm^\mu(\tau,\sigma) = \frac{1}{\sqrt{2}}\sum_r \psi_r^\mu e^{-ir\sigma^\pm}, \tag{2.18}$$

where again we have $r \in \mathbb{Z}$ when $\psi_\pm$ is in the Ramond sector and $r \in \mathbb{Z}+1/2$ when $\psi_\pm$ is in the Neveu-Schwarz sector. This notation will be assumed implicitly from now on. Note, we still have the same reality conditions on the oscillators as in (2.16).

2.1.4 The super-Virasoro algebra and mass-shell constraints

The final ingredient required for the quantisation of worldsheet fields, is obtained by a consideration of constraints arising from conserved currents on the worldsheet.

The string action given in (2.1) has a *global world-sheet supersymmetry*, i.e. it is invariant under the infinitesimal transformations,

$$\begin{aligned}\delta X^\mu &= \bar{\epsilon}\psi^\mu,\\ \delta\psi^\mu &= -i\rho^\alpha\partial_\alpha X^\mu\epsilon,\end{aligned} \tag{2.19}$$

where ϵ is a constant anticommuting spinor. These transformations mix bosonic and fermionic fields and hence are termed, supersymmetric. Any global symmetry gives rise to a conserved current via the 'Noether method'. In this case we obtain the supercurrent, which in light cone coordinates is

given by,

$$J_{\pm}(\sigma^{\pm}) = \psi_{\pm}^{\mu}\partial_{\pm}X_{\mu}. \tag{2.20}$$

This is obviously conserved since, $0 = \partial_{-}J_{+} = \partial_{+}J_{-}$.

Another conserved quantity, the energy-momentum tensor, arises from worldsheet coordinate invariance. Utilising the Noether method we obtain, in light cone coordinates, the following conserved currents

$$\begin{aligned} T_{\pm\pm} &= \partial_{\pm}X^{\mu}\partial_{\pm}X_{\mu} + \tfrac{i}{2}\psi_{\pm}^{\mu}\partial_{\pm}\psi_{\pm\mu}, \\ T_{+-} &= T_{-+} = 0. \end{aligned} \tag{2.21}$$

These conserved quantities give rise to constraints on the bosonic and fermionic fields. In fact, we will demand that,

$$0 = J_{+} = J_{-} = T_{++} = T_{--}, \tag{2.22}$$

on the physical states. These constraints can be derived systematically by a gauge fixing of a suitable supergravity lagrangian [13]. However, we will take them as postulates and see that they lead to consistent and interesting string theories.

To achieve this, define the *super-Virasoro generators*, which are the modes of $T_{\alpha\beta}$ and J_{α}. For open strings, the bosonic operators are given by,

$$L_n = \frac{1}{\pi}\int_0^{\pi} d\sigma \left(e^{in\sigma}T_{++} + e^{-in\sigma}T_{--}\right) = \frac{1}{\pi}\int_{-\pi}^{\pi} d\sigma e^{in\sigma}T_{++}, \tag{2.23}$$

and the fermionic operators,

$$G_r = \frac{\sqrt{2}}{\pi}\int_0^{\pi} d\sigma \left(e^{ir\sigma}J_{+} + e^{-ir\sigma}J_{-}\right) = \frac{\sqrt{2}}{\pi}\int_{-\pi}^{\pi} d\sigma e^{ir\sigma}J_{+}. \tag{2.24}$$

In terms of oscillators from the mode expansions,

$$\begin{aligned} L_n &= \tfrac{1}{2}\textstyle\sum_{m=-\infty}^{\infty}\alpha_{n-m}\cdot\alpha_m + \tfrac{1}{4}\sum_r(2r-n)\psi_{n-r}\cdot\psi_r, \\ G_r &= \textstyle\sum_{m=-\infty}^{\infty}\alpha_m\cdot\psi_{r-m}, \end{aligned} \tag{2.25}$$

where the index r takes it's normal values according to the boundary conditions of the fermionic fields. In the closed string case, there are two sets of super-Virasoro generators, one given by the modes of T_{++} and J_{+} and the

other by the modes of T_{--} and J_-.

As a consequence of our postulate (2.22), these operators give an infinite number of constraints corresponding to an infinite number of conserved currents of the (1+1)-dimensional field theory. They are associated with the *super-conformal symmetry* of the action (2.1). A detailed exposition of this can be found in [14].

2.1.5 Covariant quantisation

To finally quantise the two-dimensional worldsheet field theory, we must promote the modes of the bosonic and fermionic fields to the level of operators. This can be achieved by canonical quantisation of the bosonic and fermionic coordinates of the string. Since, in the conformal gauge, we have a free field theory the modes of the bosonic fields must be the quantum mechanical raising and lowering operators for the simple harmonic oscillator, hence

$$\begin{aligned} &[\alpha_m^\mu, \alpha_n^\nu] = [\tilde{\alpha}_m^\mu, \tilde{\alpha}_n^\nu] = m\delta_{m+n,0}\eta^{\mu\nu}, \\ &[\alpha_m^\mu, \tilde{\alpha}_n^\nu] = 0. \end{aligned} \tag{2.26}$$

Similarly, for the fermionic modes, we obtain the anti-commutators,

$$\begin{aligned} &\{\psi_r^\mu, \psi_s^\nu\} = \{\tilde{\psi}_r^\mu, \tilde{\psi}_s^\nu\} = \delta_{r+s,0}\eta^{\mu\nu}, \\ &\{\psi_r^\mu, \tilde{\psi}_s^\nu\} = 0, \end{aligned} \tag{2.27}$$

where r, s have the usual values dependent on the boundary conditions of the fermionic fields.

After quantisation, we must be careful with our expressions for the Virasoro generators (2.25). In particular, we see that L_0 is not well defined. We conventionally define

$$L_0 = \frac{1}{2}\sum_{m=-\infty}^{\infty} :\alpha_{-m}\cdot\alpha_m: + \frac{1}{4}\sum_r (2r) :\psi_{-r}\cdot\psi_r:, \tag{2.28}$$

where $:\ :$ denotes normal ordering, i.e. the prescription that places $m, r > 0$ operators to the right. Since an arbitrary constant could have been present here, we must add a to-be-determined constant to all formulas containing L_0.

We can now determine the *super-Virasoro algebra* generated by the super-

Virasoro generators. This is given by,

$$\begin{aligned}
[L_m, L_n] &= (m-n)L_{m+n} + A_r(m)\delta_{m+n,0} \\
[L_m, G_r] &= (\tfrac{1}{2}m - r)G_{m+r} \\
\{G_r, G_s\} &= 2L_{r+s} + B_r(r)\delta_{r+s,0},
\end{aligned} \tag{2.29}$$

where A_r and B_r are anomaly terms which depend on the boundary conditions of the fermionic fields. These are given by,

$$\begin{array}{llll}
A_r(m) = \frac{1}{8}D(m^3 - m) & B_r(r) = \frac{1}{2}D(r^2 - \frac{1}{4}) & r \in \mathbb{Z} + \frac{1}{2} & \text{(NS)}, \\
A_r(m) = \frac{1}{8}Dm^3 & B_r(r) = \frac{1}{2}Dr^2 & r \in \mathbb{Z} & \text{(R)},
\end{array} \tag{2.30}$$

where D is the number of spacetime dimensions. These anomalies are most easily determined by evaluating expectation values in the Fock-space ground state.

The constraints (2.22) can now be incorporated into our quantised theory by requiring that their positive frequency components annihilate physical states, i.e.

$$\begin{aligned}
G_r|\phi>= 0 \qquad & r > 0, \\
L_n|\phi>= 0 \qquad & n > 0, \\
(L_0 - a)|\phi>= 0, &
\end{aligned} \tag{2.31}$$

where a is a constant to be determined.

We can determine a and D by considering states in our Fock-space. For certain values of a and D we obtain unphysical negative norm states, for other values all states have positive norms. At the boundary between these two regions are extra zero norm states that occur for special values of a and D. These are associated with gauge invariance and are important for including gauge fields in our theory. As a consequence, it is these values of a and D which give rise to interesting physical theories. Let us consider the NS sector. The ground state $|0;k\rangle$, is on-shell if $(L_0 - a)|0;k\rangle = \alpha' k^2 - a = 0$, since $\alpha_0^2 = 2\alpha' k^2$. Furthermore, the excited state $|\phi\rangle = G_{-1/2}|0;k\rangle$ is on-shell if $\alpha' k^2 = a - \frac{1}{2}$. Now, if $a = \frac{1}{2}$ then not only does $|\phi\rangle$ satisfy the physical state condition $G_{1/2}|\phi>= 0$, but also it is a zero norm state, i.e. $\langle\phi|\phi\rangle = 0$. In fact, if we choose $a = 1/2$, there is an infinite family of physical states with zero norm given by $G_{-1/2}|\tilde{\phi}>$, where $|\tilde{\phi}\rangle$ satisfies $G_{1/2}|\tilde{\phi}\rangle = G_{3/2}|\tilde{\phi}\rangle = L_0|\tilde{\phi}\rangle$. For example, $|\tilde{\phi}>= (G_{-1/2})^n|0;k\rangle$ where $n \in \mathbb{Z}$. Hence, it seems that $a = \frac{1}{2}$

is a good value to consider.

Next, we can similarly determine the spacetime dimensionality, by looking for extra zero norm states. Consider the following family of states,

$$|\sigma\rangle = (G_{-3/2} + \lambda G_{-1/2}L_{-1})|\tilde{\sigma}\rangle, \tag{2.32}$$

where,

$$G_{1/2}|\tilde{\sigma}\rangle = G_{3/2}|\tilde{\sigma}\rangle = (L_0 + 1)|\tilde{\sigma}\rangle = 0. \tag{2.33}$$

Using the super-Virasoro algebra it can be shown that,

$$\begin{aligned} G_{1/2}|\sigma >= (2 - \lambda)L_{-1}|\tilde{\sigma}\rangle, \\ G_{3/2}|\sigma >= (D - 2 - 4\lambda)|\tilde{\sigma}\rangle. \end{aligned} \tag{2.34}$$

Hence $|\sigma\rangle$ is a zero norm state for $\lambda = 2$ and hence $D = 10$. A similar procedure, for the fermionic (Ramond) sector, leads to the critical values $a = 0$ and again $D = 10$.

Thus, the critical values of a and D that give rise to physically interesting theories are,

$$\begin{aligned} a &= \begin{cases} 0 & \text{(R)} \\ \frac{1}{2} & \text{(NS)} \end{cases} \\ D &= 10. \end{aligned} \tag{2.35}$$

2.1.6 The open string spectrum

We can now proceed to a determination of the spectrum of states for the open superstring. We restrict our attention to massless states, as these are the only states which will appear in the low energy field theory limit, $\alpha' \to 0$. The $L_0 = a$ constraint can be rewritten as the open string mass formula,

$$m^2 = \frac{1}{\alpha'}(N - a), \tag{2.36}$$

where,

$$N = \sum_{n=1}^{\infty} \alpha_{-n} \cdot \alpha_n + \sum_{r>0} r\psi_{-r} \cdot \psi_r, \tag{2.37}$$

counts the level number of a physical state. The open string spectrum has two independent sectors, which we now consider separately.

Firstly, let us consider the NS sector, in this case $a = \frac{1}{2}$. Hence, the

ground state $|0;k\rangle_{NS}$ is tachyonic, this state is removed from the spectrum by the GSO projection which we will discuss shortly. The first excited state is $\psi^{\mu}_{-1/2}|0;k\rangle_{NS}$, which is massless. Due to its index μ, this state transforms as a vector in the transverse $SO(8)$ rotation group. This group corresponds to the Little group of $SO(1,9)$ that leaves the light-cone momentum invariant. We can also consider excitations of the bosonic field, however these states are not massless. For example, $\alpha^{\mu}_{-1}|0;k\rangle_{NS}$ has $m^2 = \frac{1}{2\alpha'}$. All states in the NS sector transform as spacetime bosons i.e. they are given by irreducible vectorial and tensorial representations of $SO(8)$.

We now move on to the Ramond sector. From the anti-commutation relations (2.27) we see that the zero modes ψ^{μ}_0 satisfy the ten dimensional Clifford algebra,

$$\{\psi^{\mu}_0, \psi^{\nu}_0\} = \eta^{\mu\nu}. \tag{2.38}$$

Hence, we can identify the zero modes with Dirac matrices via $\psi^{\mu}_0 = \frac{1}{\sqrt{2}}\Gamma^{\mu}$. The states at each mass level must furnish representations of this $D = 10$ Clifford algebra. It follows that these states transform as spinors under $SO(1,9)$. Hence, the Ramond sector gives rise to spacetime fermions.

In particular, the Ramond ground state is massless (since $a = 0$) and degenerate as ψ^{μ}_0 maps ground states to ground states. We can choose a useful basis as follows,

$$\begin{aligned} d^{\pm}_i &= \tfrac{1}{\sqrt{2}}(\psi^{2i}_0 \pm i\psi^{2i+1}_0) \quad i = 1,..,4, \\ d^{\pm}_0 &= \tfrac{1}{\sqrt{2}}(\psi^{1}_0 \mp \psi^{0}_0). \end{aligned} \tag{2.39}$$

In this basis, the Clifford algebra takes the form,

$$\{d^{+}_i, d^{-}_j\} = \delta_{ij}. \tag{2.40}$$

Hence, the $d^{\pm}_i$, $i = 0,..,4$ act as raising and lowering operators generating 32 Ramond ground states. We can denote these states as,

$$|s_0, s_1, s_2, s_3, s_4\rangle = |\mathbf{s}\rangle, \tag{2.41}$$

where each $s_i = \pm\frac{1}{2}$ can be raised or lowered by $d^{\pm}_i$. To understand the usefulness of this notation consider the fermionic part of the ten-dimensional

Lorentz generators,

$$S^{\mu\nu} = -\frac{i}{2}\sum_r [\psi_r^\mu, \psi_r^\nu]. \tag{2.42}$$

The eigenstates of $S_0 = iS^{01}$ and $S_i = S^{2i,2i+1}$ are the corresponding s_i. These generators always flip an even number of the s_i, hence the Dirac representation decomposes into a **16** and a **16'**.

The physical state condition $G_0|\phi\rangle = 0$ gives us the massless Dirac equation in momentum space, $p_\mu \psi_0^\mu = 0$. If we pick a massless frame of reference we obtain,

$$p_\mu \psi_0^\mu = \frac{p_1 \Gamma^0}{\sqrt{2}}(1 - \Gamma^0\Gamma^1) = \sqrt{2} p_1 \Gamma^0 (\frac{1}{2} - S_0) = 0, \tag{2.43}$$

hence $s_0 = \frac{1}{2}$, resulting in a sixteen fold degeneracy for the physical Ramond ground state. This is a spinor representation of $SO(8)$ which decomposes into $\mathbf{8_s}$ with an even number of $-\frac{1}{2}$'s and $\mathbf{8_c}$ with an odd number. One is in the **16** and the other in **16'** differing only by a spacetime parity transformation.

2.1.7 The GSO projection

The superstring spectrum admits a consistent truncation, called the Gliozzi-Scherk-Olive (GSO) projection, which is demanded by consistency of the string theory. This projection removes those states with an even number of ψ oscillator excitations. Hence,

$$P_{GSO} = \frac{1}{2}\left(1 - (-1)^F\right), \tag{2.44}$$

where F is fermion number operator.

In the NS sector, we have

$$F = \sum_{r>0} \psi_{-r} \cdot \psi_r, \tag{2.45}$$

which satisfies,

$$\left\{(-1)^F, \psi^\mu\right\} = 0. \tag{2.46}$$

We now see that the GSO projection has the attractive feature of projecting out the tachyon (since $F = 0$) as mentioned previously.

For the R sector, we must define

$$(-1)^F = \pm\Gamma^{11}(-1)^{\sum_{r\geq 1}\psi_{-r}\cdot\psi_r}, \tag{2.47}$$

where

$$\Gamma^{11} = \Gamma^0\Gamma^1\ldots\Gamma^9, \tag{2.48}$$

is the ten dimensional chirality operator. The sign choice in (2.47) leads to different chirality projections on the spinors. This has important consequences in the case of the closed string, as will be discussed in the next subsection.

Applying the GSO projection to the open superstring spectrum leads to an equal number of bosons and fermions at the massless level. In fact, it can be shown that the open superstring with GSO projection has $D = 10$, $N = 1$ spacetime supersymmetry. This construction can be then shown to lead (on anomaly cancellation) to the Type I $SO(32)$ superstring theory.

2.1.8 The closed string spectrum: Type IIA and Type IIB

As a closed string is effectively two copies of an open string, we can determine its spectrum by taking the tensor product of left-movers with right-movers, each of which is described by the open string spectrum as above. However, there is also a constraint relating the left and right movers. Consider the physical state conditions $(L_0 - a)|\phi\rangle = (\tilde{L}_0 - a)|\phi\rangle = 0$, subtracting and adding gives,

$$\begin{aligned}(L_0 - \tilde{L}_0)|\phi\rangle &= 0,\\ (L_0 + \tilde{L}_0 - 2a)|\phi\rangle &= 0.\end{aligned} \tag{2.49}$$

The first constraint results in a level matching condition, i.e.

$$N = \tilde{N}, \tag{2.50}$$

and the second yields the closed string mass formula,

$$m^2 = \frac{4}{\alpha'}(N - a). \tag{2.51}$$

In the case of the closed string, we have a choice to make regarding the

Sector	SO(8) Representation	Massless Field	Boson/Fermion
NS-NS	$\mathbf{8_v} \otimes \mathbf{8_v} = \mathbf{35} \oplus \mathbf{28} \oplus \mathbf{1}$	$g_{\mu\nu}$, $B_{\mu\nu}$, Φ	Boson
NS-R	$\mathbf{8_v} \otimes \mathbf{8_s} = \mathbf{8_s} \oplus \mathbf{56_s}$	Ψ_μ, λ	Fermion
R-NS	$\mathbf{8_s} \otimes \mathbf{8_v} = \mathbf{8_s} \oplus \mathbf{56_s}$	Ψ'_μ, λ'	Fermion
R-R	$\mathbf{8_s} \otimes \mathbf{8_{s/c}} = p - forms$	Ramond-Ramond fields	Boson

Table 2.1: Closed string massless states.

GSO projection on the R sector. Taking the same GSO projection (i.e the same sign in (2.47)) on both left movers and right movers results in the Type IIB superstring theory, while taking opposite signs results in the Type IIA theory. This gives rise, along with the level matching conditions, to the following massless closed string states,

$$\begin{aligned} &\text{Type IIA:} \quad (\mathbf{8_v} \oplus \mathbf{8_s}) \otimes (\mathbf{8_v} \oplus \mathbf{8_c}) \\ &\text{Type IIB:} \quad (\mathbf{8_v} \oplus \mathbf{8_s}) \otimes (\mathbf{8_v} \oplus \mathbf{8_s}). \end{aligned} \tag{2.52}$$

These massless states are summarised in table 2.1 and fill out supermultiplets of a D=10, IIA (non chiral) and IIB (chiral) supergravity theory. The graviton arises from the NS-NS sector and the gravitinos from the NS-R and R-NS sectors. Hence, the closed string theories have N=2 supersymmetry in D=10.

Here, we also come across a hint to the existence of extended objects, known as D-branes. These turn out to be $(p+1)$-dimensional sources for the p-form fields in the Ramond-Ramond sector. This will be elaborated on in section 2.3.

2.2 Calculation of String Amplitudes

We now proceed to a discussion of the methodology required in the calculation of string scattering amplitudes. This is a complicated and expansive subject, and as such we will only present a brief and heuristic overview here. More computational detail will be provided in the concrete calculations performed in chapters 4 and 5.

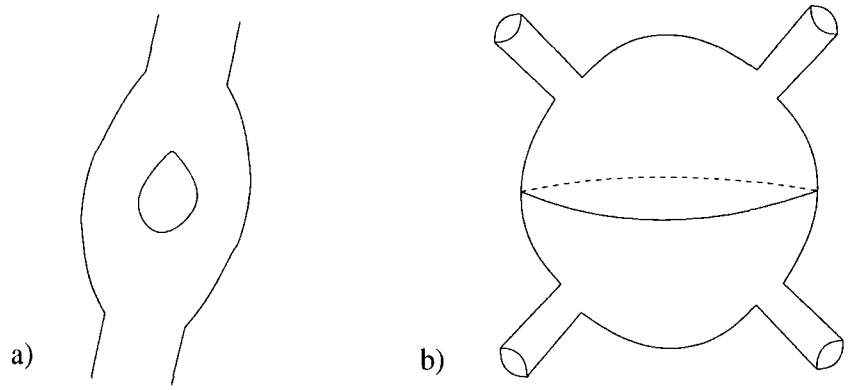

Figure 2.1: a) Open string one-loop vacuum amplitude. b) Closed string four-point tree level interaction.

2.2.1 String perturbation theory

Following the path integral approach used in representing a quantum theory, we can define an amplitude in string theory by summing over all possible worldsheet configurations between the initial and final states, weighted by the classical action. Figure 2.1 depicts examples of such possible worldsheet configurations in open and closed string interactions. An important feature of these diagrams, is that there is no specific Lorentz invariant interaction point which marks the splitting and joining of strings. In effect, the interaction is 'smeared out'. This removes the UV divergences that plague point particle interactions and leads to string theory being UV finite at all orders in perturbation theory.

We can classify our string interaction diagrams according to their topology, and then sum over all worldsheets with a particular topology by integrating over size and shape moduli. In fact, it is a feature of string theory that a single string diagram with a fixed topology can often represent a large number of point particle feynman diagrams, corresponding to different limits of the moduli. As an example, in the theory of oriented closed strings, there is one and only one feynman diagram at any given order of perturbation theory. This corresponds to the fact that oriented two-dimensional manifolds are completely specified by a given number of handles and the number of holes. For example, the one-loop vacuum amplitude is simply given by a torus, the two-loop vacuum amplitude by two tori sewn together, etc.

The classification of diagrams is more complicated in the case of open strings and unoriented closed strings. For instance, figure 2.2 depicts one-

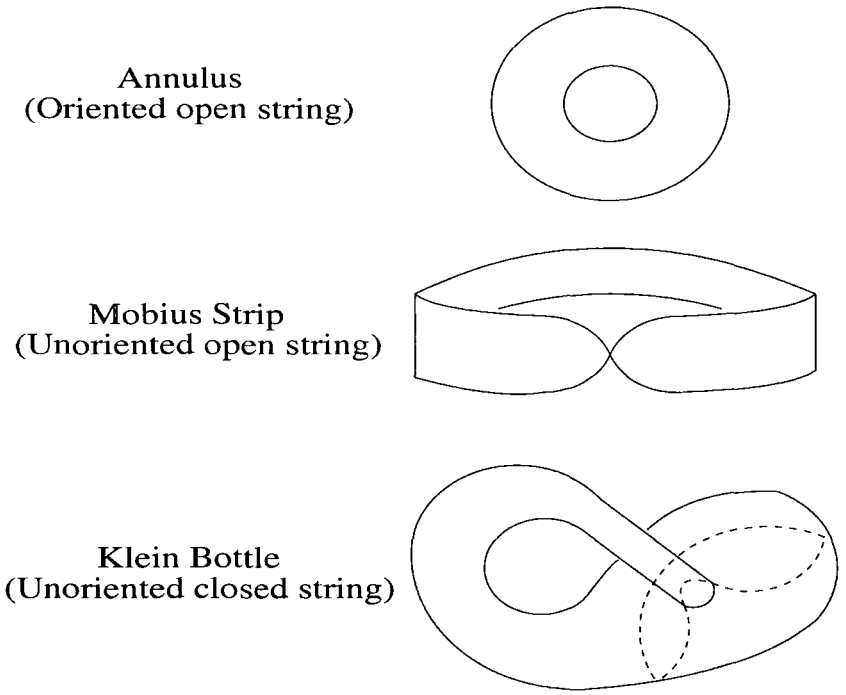

Figure 2.2: Contributions to tadpole divergences.

loop vacuum amplitudes that may give rise to tadpoles. That is, an amplitude for the creation of a single particle from the vacuum, induced by quantum effects. For a consistent theory these diagrams must cancel and this puts constraints on possible string models, this will be discussed further in chapter 3. Notice that, if we have unoriented closed strings we also have a Klein bottle contribution to the one-loop vacuum amplitude for the closed string, in addition to the torus.

2.2.2 Vertex operators

The problem of summing over all possible worldsheets is simplified by the invariance of the string action under a conformal rescaling of the worldsheet metric, i.e. $\gamma_{\alpha\beta} \rightarrow e^{\Phi}\gamma_{\alpha\beta}$ (this is also known as a Weyl transformation). Thus, we can map any worldsheet configuration to any conformally equivalent configuration and still obtain the same contribution to the string amplitude. To see how this simplifies matters, let us consider the four point closed string interaction depicted in figure 2.1. In all string amplitude calculations we will assume the simplified case of string sources taken off to infinity. This corresponds to an S-matrix element. In this case, we can conformally map

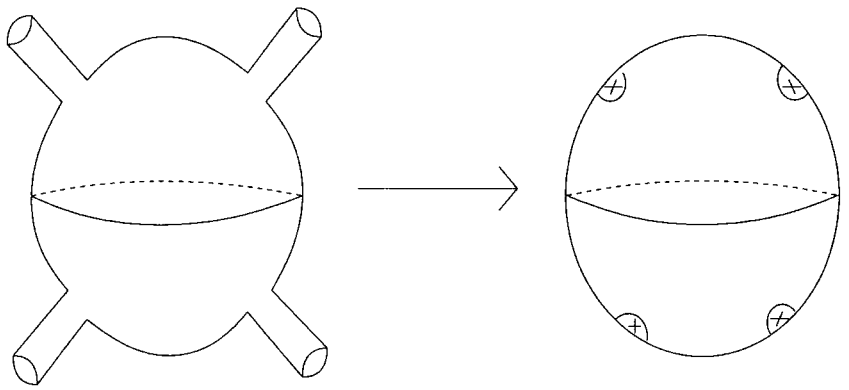

Figure 2.3: External string states are described by local operators on the worldsheet.

the outgoing legs described by the cylinder,

$$Im(w) \in [0, -\infty), \quad w \sim w + 2\pi, \tag{2.53}$$

to the unit disc given by,

$$z = e^{-iw}, \quad 0 \leq |z| \leq 1. \tag{2.54}$$

The external state is then mapped to the origin of the unit disc. Therefore, each external state becomes a local 'disturbance' on the worldsheet, as depicted in figure 2.3. A similar approach gives the same result for external open strings, except in this case the local disturbance resides on the boundary of the resulting worldsheet.

In conformally mapping the external string states to points on the worldsheet, we do not simply lose the quantum numbers of the external string state. Hence, there must exist a state-operator correspondence whereby for each string state there exists a corresponding local operator in the (1+1)-dimensional quantum field theory that describes the string propagation. Thus, for an external state with momentum k^μ and internal state j, there exits a local *vertex operator* $V_j(k)$ for emission and absorption of that state.

In conclusion, due to the conformal invariance of the worldsheet we may restrict our sum over worldsheets to *compact* worldsheets, with legs replaced with local vertex operators.

2.2.3 The Polyakov path integral

We now proceed to formulate the path integral required to sum over worldsheets. As we have seen, it is important to classify the contributions to a string amplitude by the topology of the worldsheet. Hence, we now must consider the possible addition of a non-dynamical extra term to the string action (2.1). Such an extra term will only be important when comparing worldsheets of different topology. The only possibility consistent with worldsheet symmetries is,

$$\chi = \frac{1}{4\pi\alpha'}\int_M d^2\sigma(-\gamma)^{1/2}R + \frac{1}{2\pi\alpha'}\int_{\partial M} dsK, \tag{2.55}$$

where R is the Ricci scalar for the worldsheet M and K is the extrinsic curvature integrated over the boundary, ∂M of the worldsheet.

In the path integral, we must sum over the dynamical fields on the string worldsheet, these include the bosonic and fermionic fields and also the metric. In order to better define the path integral we must work with Euclidean metrics. That is, the Minkowskian metric γ_{ab} is replaced with a Euclidean worldsheet metric g_{ab} with signature (++). In this two-dimensional theory, it can be shown that the Euclidean path integral gives the same amplitude as the Minkowski one [14]. Then, our new Euclidean string action with topological term is given by,

$$S_E = S_B + S_F + \lambda\chi, \tag{2.56}$$

where,

$$\begin{aligned} S_B &= \tfrac{1}{4\pi\alpha'}\textstyle\int_M d^2\sigma g^{1/2}g^{ab}\partial_a X^\mu \partial_b X_\mu, \\ S_F &= -\tfrac{1}{4\pi\alpha'}\textstyle\int_M d^2\sigma g^{1/2}g^{ab} i\bar{\psi}^\mu \rho_b \partial_a \psi_\mu, \\ \chi &= \tfrac{1}{4\pi\alpha'}\textstyle\int_M d^2\sigma (g)^{1/2}R + \tfrac{1}{2\pi\alpha'}\textstyle\int_{\partial M} dsK. \end{aligned} \tag{2.57}$$

Note that, we are no longer working in the conformal gauge as we will be summing over all possible metrics.

As mentioned above, χ is a non-dynamical term and does not affect our previous determination of the string spectrum. In fact, it is purely a topological term and can be identified with the *Euler number* of the worldsheet. In the path integral, the factor $e^{-\lambda\chi}$ affects the relative weighting of worldsheets

with different topologies. The Euler number is given by,

$$\chi = 2 - 2h - b - c, \tag{2.58}$$

where h, b and c are the number of handles, boundaries and crosscaps respectively. Hence, we see that emission and reabsorption of an open string results in $\delta\chi = -1$. Relative to the open string tree amplitude, such a process is weighted by e^{λ} in the path integral. Similarly, the emission and reabsorption of a closed string results in $\delta\chi = -2$. Therefore we have,

$$g_o^2 \sim g_c \sim e^{\lambda}, \tag{2.59}$$

where g_o, g_c are the open and closed string coupling constants respectively.

Finally we can express an n-particle S-matrix element as follows,

$$S_{j_1..j_n}(k_1,..,k_n) = \tag{2.60}$$
$$\sum_{\text{compact topologies}} \int \mathcal{D}X^{\mu}\mathcal{D}\psi^{\mu}\mathcal{D}g_{ab} e^{-S_E[X^{\mu},\psi^{\mu},g_{ab}]} \prod_{i=1}^{n} \int d^2\sigma_i g^{1/2} V_{j_i}(k_i,\sigma_i).$$

In order for the vertex operator insertions to be diffeomorphism invariant, they must be integrated over the worldsheet. However, this is not quite the end of the story. The problem is that (2.60) contains a large overcounting from equivalent configurations related through worldsheet symmetries. In effect, we need to divide by the volume of this symmetry group. This can be carried out by integrating over a slice that cuts through each gauge equivalence class once, and obtaining the correct measure on the slice by the Faddeev-Popov method. The details for this procedure are not necessary for our requirements but are covered in detail in [14]. We now proceed to briefly discuss the actual form of the vertex operators.

2.2.4 State-operator mapping

As we have seen, there exists a state-operator correspondence, whereby we may identify quantum fields and quantum states via a one to one mapping. The states may then be regarded as being created from the vacuum state by these quantum fields or vertex operators. We now investigate this correspondence in more detail in the context of the bosonic sector of the superstring,

with vertex operators for the worldsheet fermionic states being discussed in the next section.

In order for us to quantify the state-operator correspondence we must introduce a new coordinate system for the worldsheet. We first obtain a Euclidean signature by the Wick rotation $\tau \to i\tau$, and then we define $z = e^{\tau - i\sigma}$. This maps the closed string to the complex plane and the open string to the upper half complex plane. Our bosonic mode expansions for the closed string (2.13) then becomes (with a redefinition of the zero mode),

$$\begin{aligned} \partial X^\mu(z) &= -i\left(\tfrac{\alpha'}{2}\right)^{1/2} \textstyle\sum_{n=-\infty}^{\infty} \alpha_n^\mu z^{-n-1}, \\ \bar{\partial} X^\mu(\bar{z}) &= -i\left(\tfrac{\alpha'}{2}\right)^{1/2} \textstyle\sum_{n=-\infty}^{\infty} \tilde{\alpha}_n^\mu \bar{z}^{-n-1}. \end{aligned} \tag{2.61}$$

Here we have introduced a notation that will be used throughout this thesis. Any function of z ($\bar{z}$) only, is holomorphic (anti-holomorphic) respectively and we define, $\partial = \partial_z$ and $\bar{\partial} = \partial_{\bar{z}}$. These expressions can be inverted to obtain,

$$\begin{aligned} \alpha_{-n}^\mu &= \left(\tfrac{2}{\alpha'}\right)^{1/2} \oint \tfrac{dz}{2\pi} z^{-n} \partial X^\mu(z), \\ \tilde{\alpha}_{-n}^\mu &= \left(\tfrac{2}{\alpha'}\right)^{1/2} \oint \tfrac{d\bar{z}}{2\pi} \bar{z}^{-n} \bar{\partial} X^\mu(\bar{z}), \end{aligned} \tag{2.62}$$

where we integrate counterclockwise around a circle centred on the origin. Thus, using the Cauchy-Integral formula, we can identify our raising operators with quantum fields as follows,

$$\begin{aligned} \alpha_{-n}^\mu &\to i\left(\tfrac{2}{\alpha'}\right)^{1/2} \tfrac{1}{(n-1)!} \partial^n X^\mu(0), \quad n \geq 1 \\ \tilde{\alpha}_{-n}^\mu &\to i\left(\tfrac{2}{\alpha'}\right)^{1/2} \tfrac{1}{(n-1)!} \bar{\partial}^n X^\mu(0), \quad n \geq 1. \end{aligned} \tag{2.63}$$

For the closed string ground state, the vertex operator is given by,

$$|0; k> \quad \leftrightarrow \quad \int d^2z : e^{ik.X} :, \tag{2.64}$$

since this form provides the right behaviour under spacetime translations and contains no derivatives of X^μ, which would correspond to an excited state. Using (2.63) and (2.64) we can easily construct the necessary vertex operators. For example, the emission or absorption of the first excited state of the closed string is described by,

$$\zeta_{\mu\nu} \alpha_{-1}^\mu \tilde{\alpha}_{-1}^\nu |0; k> \quad \leftrightarrow \quad \int d^2z \zeta_{\mu\nu} : \partial X^\mu \bar{\partial} X^\nu e^{ik.X} : \tag{2.65}$$

where $\zeta_{\mu\nu}$ is a polarisation tensor. Note, we integrate over the worldsheet so that the vertex operator is invariant under a diffeomorphism.

For the open string, we have a similar story. However, in this case we must integrate the fields over the boundary of the worldsheet. For example,

$$\zeta_\mu \alpha^\mu_{-1}|0;k> \quad \leftrightarrow \quad \int dl \zeta_\mu : \partial_t X^\mu e^{ik.X} : \tag{2.66}$$

where we integrate along the real line, which corresponds to the open string boundary. Also, ∂_t is the derivative tangential to the boundary.

2.2.5 Fermionic vertex operators

We now move on to a basic discussion of the vertex operators for states corresponding to excitations of the worldsheet fermionic fields. Expressing our worldsheet fields in terms of Laurent expansions gives[1],

$$\psi^\mu(z) = \sum_r \frac{\psi^\mu_r}{z^{r+1/2}}, \quad \tilde{\psi}^\mu(\bar{z}) = \sum_r \frac{\tilde{\psi}^\mu_r}{\bar{z}^{r+1/2}}. \tag{2.67}$$

As before, r sums over integers/half-integers depending on whether we are considering the Ramond/Neveu-Schwarz sectors respectively. The tilde distinguishes between left and right-movers. The state-operator correspondence in the NS sector is given by,

$$\begin{aligned} \psi^\mu_{-r} &\rightarrow \tfrac{1}{(r-1/2)!}\partial^{r-1/2}\psi^\mu(0), \\ \tilde{\psi}^\mu_{-r} &\rightarrow \tfrac{1}{(r-1/2)!}\bar{\partial}^{r-1/2}\tilde{\psi}^\mu(0), \end{aligned} \tag{2.68}$$

where again we have used the Cauchy-Integral formula.

It is somewhat more difficult to construct vertex operators for the Ramond sector as the Laurent expansion has a branch cut. However, we can make use of a surprising equivalence known as *bosonization*. This equivalence is between bosons and fermions and occurs frequently in two dimensional conformal field theories. Consider the conformal field theory of two Majorana-Weyl fermions $\psi^{1,2}(z)$ and form the complex combinations,

$$\psi = \tfrac{1}{\sqrt{2}}(\psi^1 + i\psi^2), \quad \bar{\psi} = \tfrac{1}{\sqrt{2}}(\psi^1 - i\psi^2), \tag{2.69}$$

[1]The extra factor of $\frac{1}{2}$ arises from these fields transforming with half the weight of a vector.

then the operator product expansions (OPEs) of these fields have exactly the same form to those of $e^{\pm iH(z)}$, where $H(z)$ is the holomorphic part of a scalar field on the worldsheet. We can then make the identification,

$$\psi(z) \cong e^{iH(z)}, \quad \bar{\psi}(z) \cong e^{-iH(z)}. \tag{2.70}$$

All of this applies equally to the antiholomorphic case.

This bosonization applies to the NS and R sectors. However, since we are now grouping fermions into complex pairs we may generalise our boundary conditions to,

$$\psi(\sigma + 2\pi) = e^{2\pi i\nu}\psi(\sigma), \tag{2.71}$$

where $\nu \in \mathbb{R}$. This is useful in less symmetric cases, e.g. for a compactification space which includes an orbifold factor. The Laurent expansions are now modified to,

$$\psi(z) = \sum_{r\in\mathbb{Z}+\nu} \frac{\psi_r}{z^{r+1/2}}, \quad \bar{\psi}(z) = \sum_{r\in\mathbb{Z}-\nu} \frac{\bar{\psi}_r}{\bar{z}^{r+1/2}}. \tag{2.72}$$

We can uniquely define a ground state by,

$$\psi_{n+\nu}|0>_\nu = \bar{\psi}_{n+1-\nu}|0>_\nu = 0, \quad n = 0, 1, ... \tag{2.73}$$

The OPEs of the fermion fields with the operator corresponding to $|0>_\nu$ allows us to make the identification,

$$|0>_\nu \cong e^{i(-\nu+1/2)H}. \tag{2.74}$$

Hence, for the $D = 10$ superstring we can bosonise the fermionic fields as follows,

$$\begin{aligned} &\tfrac{1}{\sqrt{2}}(\pm\psi^0 + \psi^1) \cong e^{\pm iH^0}, \\ &\tfrac{1}{\sqrt{2}}(\psi^{2a} \pm i\psi^{2a+1}) \cong e^{\pm iH^a}, \quad a = 1, .., 4. \end{aligned} \tag{2.75}$$

With the Ramond sector ($\nu = 0$) ground state, $|\mathbf{s}>$, having the corresponding vertex operator,

$$\Theta_{\mathbf{s}} \cong e^{i\sum_a s_a H^a}. \tag{2.76}$$

This vertex operator is often called the *spin-twist* operator. It is also necessary to incorporate ghosts in both the fermionic and bosonic vertex operators, more details can be found in [14].

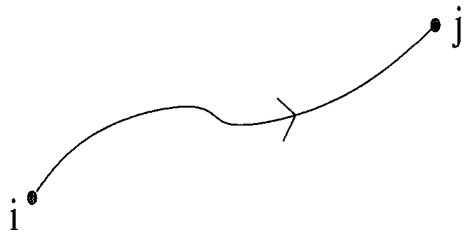

Figure 2.4: Chan-Paton degrees of freedom for an oriented string.

2.2.6 Chan-Paton factors and gauge invariance

While we are discussing string interactions and vertex operators we may take a convenient detour to discuss the incorporation of gauge invariance in open string theories.

The distinguishing feature of open strings are their two distinct endpoints. It is possible to exploit this feature by adding non-dynamical (i.e. with zero Hamiltonian) degrees of freedom to the string endpoints. That is, we demand that each endpoint is in a state i or j such that $i, j = 1, .., N$, as depicted in figure 2.4. It is then possible to decompose an open string wavefunction in a basis λ^a_{ij} of $N \times N$ matrices,

$$|k; a >= \sum_{i,j=1}^{N} |k; ij > \lambda^a_{ij}, \tag{2.77}$$

where $|k, ij >$ is the open string state with endpoints in the states i and j. Note that, in this notation we have suppressed information on the oscillator excitations. The matrices λ^a_{ij} are called *Chan-Paton factors*. All open string vertex operators must carry these factors.

Chan-Paton factors have an important consequence for open string amplitudes. Each such amplitude must be weighted by a trace of a product of Chan-Paton factors. For example, consider the four-point interaction depicted in figure 2.5. To sum over all states involved in the interaction we must sum over all possible string endpoint configurations. However, since the Chan-Paton factors are non-dynamical, each string inherits the state of

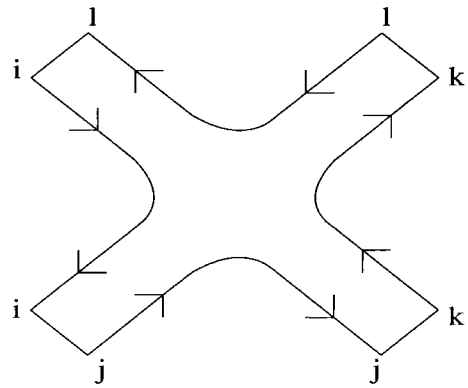

Figure 2.5: A tree-level four point interaction with Chan-Paton factors.

it's endpoints from it's neighbours. As a result the amplitude is weighted by,

$$\sum_{i,j,k,l} \lambda^1_{ij}\lambda^2_{jk}\lambda^3_{kl}\lambda^4_{li} = Tr(\lambda^1\lambda^2\lambda^3\lambda^4). \tag{2.78}$$

This factor is invariant under a global $U(N)$ worldsheet symmetry,

$$\lambda^a \rightarrow U\lambda^a U^{-1}, \quad U \in U(N), \tag{2.79}$$

under which the endpoints transform in the fundamental, $\mathbf{N}$, and anti-fundamental, $\bar{\mathbf{N}}$, representations of the unitary group, $U(N)$.

Now, the vertex operator corresponding to the massless vector boson in the NS sector must be generalised to,

$$V^{a,\mu}_{ij} = \int dl \lambda^a_{ij}\psi^\mu : e^{ik.X} : . \tag{2.80}$$

This vertex operator then transforms under the adjoint representation $\mathbf{N}\otimes\bar{\mathbf{N}}$ of $U(N)$. Hence, the global $U(N)$ worldsheet symmetry is promoted to a local $U(N)$ *gauge* symmetry in spacetime. It follows that, the introduction of Chan-Paton factors allows us to incorporate non-abelian gauge fields in open string theory.

2.3 An Introduction to D-branes

We now give a brief introduction to the non-perturbative objects known as D-branes. A *Dp-brane* is a $(p+1)$-dimensional hypersurface in spacetime on

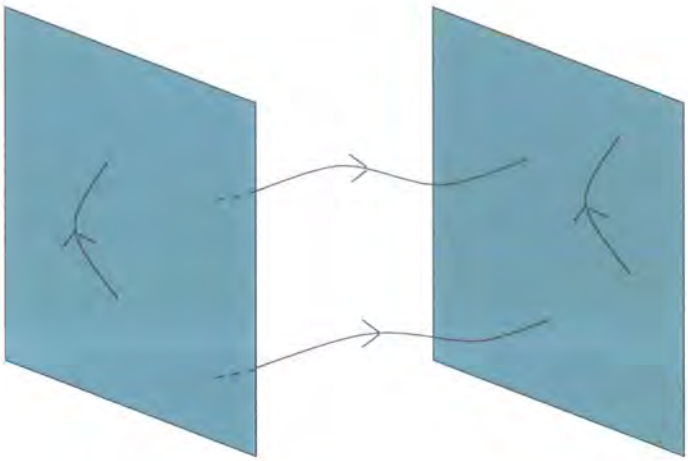

Figure 2.6: A pair of D-branes. Open string endpoints are always confined to the D-brane worldvolume.

which open string endpoints are confined, a possible configuration is shown in figure 2.6. Let us begin by examining the need for such objects in string theories which contain open strings.

2.3.1 The case for D-branes

We have already come across a number of hints to the existence of such objects in our overview of the NSR superstring. The first is the possibility of *Dirichlet* boundary conditions,

$$\partial_\tau X^\mu(\tau, \sigma)|_{\sigma=0,\pi} = 0, \tag{2.81}$$

for open string endpoints. Such a condition constrains the ends of the string to a hypersurface in spacetime. This hypersurface then has the basic characteristic of a Dp-brane as described above. Hence, it is necessary in the presence of a Dp-brane to have spacetime coordinates which parallel to a D-brane have Neumann boundary conditions, and perpendicular to the D-brane have Dirichlet boundary conditions. This is the origin of the terminology *Dirichlet-brane* or *D-brane*.

Next, we consider the Ramond-Ramond p-forms mentioned in the description of the closed string spectrum in subsection 2.1.8. The p-form potentials

arising from $\mathbf{8_s} \otimes \mathbf{8_{s/c}}$ are,

$$\begin{array}{ll} \text{Type IIA:} & C_1, C_3, C_5, C_7 \\ \text{Type IIB:} & C_0, C_2, C_4, C_6, C_8, \end{array} \tag{2.82}$$

where in both cases the last two p-forms are Hodge dual to the first two and C_4 is self-dual. It can be shown that the elementary perturbative string states cannot carry any charge with respect to the R-R gauge fields C^{p+1}. Hence we expect that there should be $(p+1)$-dimensional extended sources which couple to these potentials via a coupling of the form,

$$S_{WZ} = Q_p \int_{M_{p+1}} C_p, \tag{2.83}$$

where M_{p+1} is the worldvolume of a Dp-brane and Q_p is it's Ramond-Ramond charge. This is indeed the case as first discussed in [18]. It follows that we have the following species of Dp-branes,

$$\begin{array}{ll} \text{Type IIA:} & 0, 2, 4, 6, 8 \\ \text{Type IIB:} & -1, 1, 3, 5, 7, 9. \end{array} \tag{2.84}$$

Here $p = 8$ describes a "domain wall" in ten dimensional spacetime. The $p = 9$ case corresponds to a spacetime filling brane, with no coupling to any R-R field strength. Also, the $p = -1$ case describes an object which is localized in time and corresponds to a "D-instanton".

Finally, if we consider a situation where we have a number of distinct D-branes, then there must exist a label for each string endpoint determining which D-brane it is constrained to move on. These are identical to the Chan-Paton degrees of freedom mentioned in subsection 2.2.6. Hence, it is sensible to reinterpret the Chan-Paton degrees of freedom as labelling which D-brane a string endpoint is confined to. For example, a state $|k, ii>$ has it's endpoints on the same D-brane, while a state $|k, ij>$ has it's endpoints on two distinct, and not-necessarily coincident, D-branes. This also suggests a link between gauge theories and D-branes. This will be the subject of the next subsection.

This evidence for the existence of D-branes in string theories can be put on a firmer foundation by the study of *T-duality*. This allows an explicit

construction of D-branes. However, this is not required for an understanding of the following chapters and we leave this to the references [14–17].

2.3.2 D-branes and gauge theory

Consider open string states in the presence of two non-coincident D-branes, as depicted in figure 2.6. The string states stretched between the two D-branes are of the form $oscillators|k, ij>$. The string tension contributes an energy to stretched string states and therefore these states are massive. Focusing our attention on massless states with both endpoints lying in the same Dp-brane, we have the states,

$$\begin{aligned} &\psi^{a}_{-1/2}|k, ii>_{NS}, \quad a = p+1, .., 9 \\ &\psi^{\hat{\mu}}_{-1/2}|k, ii>_{NS}, \quad \hat{\mu} = 0, .., p \end{aligned} \tag{2.85}$$

and their fermionic superpartners from the Ramond sector. These states are just the components of $\psi^{\mu}_{-1/2}|k, ii>_{NS}$ parallel and perpendicular to the brane.

The first set of states correspond to a set of $9-p$ scalars from the point of view of the D-brane worldvolume. These are the collective coordinates of the Dp-brane and describe its embedding in spacetime. These open string states therefore correspond to fluctuations in the D-brane shape. Hence D-branes are dynamical objects as would be expected in a theory which contains gravity. The second state transforms as a vector under $SO(1,p)$ and gives rise to a $U(1)$ gauge field on the D-brane worldvolume.

Next, consider the case of a stack of N-coincident D-branes. There are now additional massless states, since strings stretched between these branes can achieve vanishing length. We now have $N^2(9-p)$ massless scalars and each coordinate of the Dp-brane is promoted to a matrix. This non-commutative geometry has proven to play a key role in the dynamics of D-branes. Also, there are now N^2 vectors. These give rise to a matrix valued vector boson field, $\lambda_{ij}\psi^{\hat{\mu}}_{-1/2}|k, ij>$. In an identical manner to that discussed in subsection 2.2.6, this state transforms as a $U(N)$ gauge field in the D-brane worldvolume. Hence, a stack of N coincident D-branes has a $U(N)$ gauge theory in it's worldvolume. This is extremely important for string model construction, since it allows the simple construction of models

with gauge groups close to that of the Standard Model. For example, if we consider three stacks of D-branes with $N_1 = 3$, $N_2 = 2$ and $N_3 = 1$, we obtain a $U(3) \times U(2) \times U(1)$ gauge group on the D-brane worldvolume. This will be an essential feature of the string models explored in this thesis.

2.4 Obtaining four dimensional string models

As we have seen perturbative string theories are defined in ten dimensions. It is therefore necessary to 'hide' six spatial dimensions in order to obtain a model with (3+1) spacetime dimensions. This can be achieved in a number of ways which will be discussed heuristically in this section.

2.4.1 Compactification and the string scale

To begin with, a relatively simple method of obtaining a (3+1) dimensional model is to utilise D3-branes. As discussed above we can consider stacks of D-branes giving rise to a $U(3) \times U(2) \times U(1)$ gauge group on their worldvolume. This allows us to construct standard-like models on D3-branes, which we would therefore associate with our observable universe. Matter fields such as quarks and leptons as well as gauge bosons would correspond to open strings attached to the D3-brane, and therefore are unable to feel the extra spatial dimensions. Closed strings on the other hand would be free to move away from the D-brane giving rise to ten dimensional gravity. This scenario will be analysed further in chapter 3, where a specific example will be given following the bottom-up approach discussed in [7]. In order to obtain a fully realistic model we must also compactify the extra spatial dimensions in order to obtain four dimensional gravity.

For closed string models without D-branes our only option is to compactify all the extra spatial dimensions from the outset. This can be achieved using a variety of compact manifolds. In this case, and for the embedding of D-branes in a compact space to obtain $D = 4$ gravity, there is a tendency to concentrate on tori, orbifolds or Calabi-Yau manifolds. The torus is often chosen for simplicity but often has the drawback of leaving too many unbroken supersymmetries in the effective four dimensional model (e.g. heterotic strings). An orbifold is usually defined by a group action (with fixed points) on a flat space such as $\mathbb{R}^n$ or a torus, T^{2n}. For example, $\mathbb{C}^3/\mathbb{Z}_3$ is an orbifold

defined by the action

$$z_i \sim g.z_i = e^{2\pi i v_i} z_i, \tag{2.86}$$

where g is the generator of the cyclic group $\mathbb{Z}_3$ and $v = \frac{1}{3}(a_1, a_2, a_3)$ is a twist vector describing the action of the generator on each complex dimension. The benefit of compactifying on an orbifold is that the group action can be made to break supersymmetry down to $N = 1$ (allowing for a chiral model) and the manifold has a flat metric away from fixed points, thus simplifying some string calculations. An excellent review of this subject can be found in [19]. A slight generalisation of this idea is that of orientifolds. This can be applied in the case of models with D-branes and involves combining the group action with worldsheet parity reversal, for example [20].

Orbifolds are actually limits of a more complicated class of manifold known as Calabi-Yau manifolds. These are Kähler manifolds with $SU(3)$ holonomy, which is a requirement to obtain $N = 1$ supersymmetry when compactifying Heterotic $E_8 \times E_8$ string theory [4]. An example of such a manifold is the subspace of $\mathbb{C}P^4$ defined by,

$$\sum_{i=1}^{5} z_i^5 = 0. \tag{2.87}$$

In general however, these manifolds have complex metrics which do not allow for simple (or often even tractable) string calculations.

An interesting consequence of these differing methods of 'hiding' the six extra dimensions is the wide range of possible values for the string scale. It is possible to have a string scale much lower than the Planck scale if gravity feels a large internal volume, with the Standard Model being restricted to some smaller sub-volume of spacetime. This class of setup is easily realised utilising D3-branes as described above. In particular, if we locate our Standard Model on a set of D3-branes (as in the bottom-up approach) we obtain the following relation

$$M_p^2 \sim \frac{M_s^2 V_6}{\lambda^2}, \tag{2.88}$$

where V_6 is the volume of the compact internal space. Therefore provided our compact space is large, we may still obtain a Planck scale of the order of 10^{19} GeV with a small string scale. In fact, the string scale is only constrained by experiment to be greater than 1 TeV. This case contrasts with models without

D-branes such as the perturbative Heterotic string. Here both gravity and gauge degrees of freedom are the results of closed string excitations and hence feel the compact internal space equally. This leads to the following relation,

$$M_p \sim M_s \sim V_6^{1/6} \tag{2.89}$$

resulting in a string scale of the same order as the Planck scale. A useful overview of string models with vastly different string scales is given by [21].

2.4.2 Low energy effective actions

Since we will be focusing on the low energy phenomenological implications of various string models, we will be primarily concerned with the limit as $\alpha' \to 0$. In this limit only the massless degrees of freedom of the superstring survive. Then, once we have hidden the extra spatial dimensions, we will be left with an effective four-dimensional field theory. This can often be described in terms of an $N = 1$ supergravity theory, which is a gauged version of supersymmetry which incorporates gravity.

The most general action coupling $N = 1$ supergravity to gauge and chiral multiplets was constructed in [22, 23]. It can be described in terms of three functions of the chiral superfields,

1. The *Kähler potential*, $K(\phi, \phi^*)$, which is a real function. This determines the kinetic terms of the chiral fields,

$$\mathcal{L}_{kin} = K_{\alpha\bar{\beta}} \partial^\mu \phi^\alpha \partial_\mu \phi^{*\beta}, \tag{2.90}$$

   where

$$K_{\alpha\bar{\beta}} = \frac{\partial^2 K}{\partial\phi^\alpha \partial\phi^{*\beta}}, \tag{2.91}$$

   is known as the Kähler metric. The Kähler potential is very model dependent and has only been computed in the simplest of cases.

2. The *superpotential*, $W(\phi)$, which is a holomorphic function of the chiral fields. Due to it's holomorphicity, the superpotential does not depend on the string coupling and therefore we only need compute W at the tree level in string perturbation theory [24]. Furthermore, it can be

shown that it must be of the form,

$$W(\phi) = y_{abc}\phi^a\phi^b\phi^c \tag{2.92}$$

plus higher order non-renormalisable corrections [25, 26].

3. Finally, we have the *gauge kinetic function*, $f_{ab}(\phi)$, which is also holomorphic. This function determines the gauge coupling constants,

$$\mathcal{L}_{gauge} = Re(f_{ab})F^a_{\mu\nu}F^{\mu\nu b} + Im(f_{ab})F^a_{\mu\nu}\tilde{F}^{\mu\nu b}. \tag{2.93}$$

In the next chapter, we construct a specific string model which has a low energy effective field theory described in terms of a four dimensional $N = 1$ supergravity action. The superpotential and Kähler potential will be studied to see how they may give rise to Yukawa type couplings.

Chapter 3

CP violation and Discrete Torsion

We now begin our study of D-brane configurations by exploring a particular string construction which provides a geometric approach to understanding the phenomenon of CP violation, and the closely related subject of quark masses. The string construction we investigate is based on methods first discussed in [7] and the results presented in sections 3.4.4-3.5.5 were first published in [27].

3.1 Introduction and motivation

The phenomenon of CP violation, i.e. the non-invariance of nature under combined charge conjugation and parity reversal, and the numerical values of the quark masses, are aspects of nature which are not satisfactorily explained within the context of the Standard Model. For example, baryogenesis almost certainly indicates additional sources of CP violation beyond that which has been established by experiment to exist in the CKM matrix (see next section) [28–30]. Therefore, it becomes necessary to seek answers in physics beyond the Standard Model. Interestingly, the absence of electric dipole moments (EDMs) seems to indicate that the additional CP violation required must have a very constrained form. This can put strong constraints on models which attempt to go beyond the Standard Model.

Our focus on string theory, as a candidate for physics beyond the Standard Model, may provide us with an important insight into the nature of CP

violation. In string theory, what we call 4 dimensional CP is actually a gauge transformation plus Lorentz rotation of the 10 dimensional theory [31, 32]. Thus, CP is a discrete gauge symmetry and as such, can only be broken in a consistent manner by spontaneous symmetry breaking [32]. A number of authors have attempted to exploit this fact by spontaneously breaking CP in the effective supergravity approximation to various string models [33–40]. However, there is a problem not easily overcome. That is, whatever fields break CP and generate flavour structure also contribute to supersymmetry breaking, often giving rise to large contributions to CP violation and hence EDMs. In effect, the supersymmetry breaking 'knows about' the flavour and CP structure. Thus, it is difficult to construct a model which simultaneously has phenomenologically viable CP violation and quark masses and satisfactory suppression of EDMs and flavour changing neutral currents.

These problems may be avoided if one instead establishes the flavour and CP structure at the string theory level rather than the supergravity level. This is because, as we will see, string theory allows us to separate CP violation and flavour from supersymmetry breaking. In this chapter, we take a first step in this direction by constructing a supersymmetric MSSM-like model which has a full flavour structure and broken CP.

Our framework will be the 'bottom-up' approach to string model building developed in [7]. This approach allows the construction of a local configuration of D-branes that reproduces most of the phenomenological features of the MSSM without having to worry about the global properties of the compactification space. This helps us to avoid some of the problems associated with not knowing the correct compactification to take as the ground state. The source of spontaneous CP violation will be discrete torsion, a choice of orbifold group action on the B-field background, analogous to Wilson lines for gauge fields [41]. One nice feature of this, is that the Yukawa couplings contain a non-trivial complex phase, with the breaking of 4 dimensional CP appearing as a phase in the CKM matrix. With a rather simple ansatz dictated by our choice of discrete torsion (similar to 'texture zero' models in the MSSM) we find a CKM matrix defined by two free parameters. As a result, we predict a single mixing angle and the CKM phase, both of which lie within current experimental limits. Furthermore, quark mass ratios are determined and are seen to be reasonably close to experimental values.

This chapter is organized as follows, we first give a brief account of CP violation in the Standard Model. Then, we discuss CP violation and discrete torsion in the context of closed string theories. This provides a background for similar features which will appear in our model with D-branes. Following this, we introduce the model that will be a focus for this chapter. Particular attention is paid to the effect of discrete torsion on the superpotential and it's role in breaking 4 dimensional CP. We then proceed to a more phenomenological discussion, including Yukawa couplings and the CKM matrix.

3.2 CP violation in the Standard Model

The lack of invariance in nature under the combined transformation of charge conjugation and spatial inversion, is an outstanding problem in particle physics. As mentioned above, the Standard Model can accommodate CP violation, however it contains no fundamental explanation of the phenomenon. We will now explore CP in the Standard Model [42], in preparation for our study of CP in the context of string theory.

A CP transformation is a transformation which reverses all gauge charges, exchanges left and right handed fermions and reverses the orientation of space. In particular, we have

$$\psi_L(x_\mu) \rightarrow i\sigma^2\psi_L^*(x^\mu) \quad \psi_R(x_\mu) \rightarrow -i\sigma^2\psi_R^*(x^\mu) \quad \phi(x_\mu) \rightarrow \phi^\dagger(x^\mu), \tag{3.1}$$

where σ^2 is a Pauli matrix and ψ, ϕ are fermionic and complex scalar fields respectively. A CP-invariant Lagrangian, $\mathcal{L}$, transforms as $\mathcal{L}(x_\mu) \rightarrow \mathcal{L}(x^\mu)$, under (3.1).

In the Standard Model, the only source of CP violation arises from the Yukawa terms,

$$\mathcal{L}_{Yukawa} = Y_{ij}^d \overline{Q_{Li}^I} \phi d_{Rj}^I + Y_{ij}^u \overline{Q_{Li}^I} \tilde{\phi} u_{Rj}^I + Y_{ij}^l \overline{L_{Li}^I} \phi l_{Rj}^I + h.c, \tag{3.2}$$

where I stands for interaction eigenstates, and Y_{ij}^f are Yukawa couplings. The fields,

$$\phi = \begin{pmatrix} \phi^+ \\ \phi^0 \end{pmatrix} \quad \tilde{\phi} = \begin{pmatrix} -\bar{\phi}^0 \\ \phi^- \end{pmatrix}, \tag{3.3}$$

are complex scalars charged under $SU(2)_L \times U(1)_Y$. That these terms are able

to give rise to CP violation, follows from the fact that a CP transformation exchanges the operators,

$$\overline{\psi_{Li}}\phi\psi_{Rj} \leftrightarrow \overline{\psi_{Rj}}\phi^{\dagger}\psi_{Li}, \tag{3.4}$$

thus (3.2) is invariant only if $Y^f_{ij} \in \mathbb{R}$, which is not necessarily the case. It follows that complex Yukawa couplings tend to signal CP violation. However, this is not the full story.

The three Yukawa matrices give rise to 27 real and 27 imaginary parameters, but these are not all physical. If we switch off the Yukawa matrices then the Standard Model Lagrangian has the global family symmetry,

$$G^{SM}_{global}(Y^f = 0) = U(3)_Q \times U(3)_{\bar{d}} \times U(3)_{\bar{u}} \times U(3)_L \times U(3)_{\bar{l}}. \tag{3.5}$$

Thus, $\mathcal{L}_{Yukawa}$ is invariant under a change of Yukawa matrices given by,

$$\tilde{Y}^d = V_Q^{\dagger}Y^dV_{\bar{d}}, \quad \tilde{Y}^u = V_Q^{\dagger}Y^uV_{\bar{u}}, \quad \tilde{Y}^l = V_L^{\dagger}Y^lV_{\bar{l}}, \tag{3.6}$$

where V are all unitary matrices. This freedom allows us to remove 15 real and 30 imaginary parameters. However, this global symmetry is broken down to,

$$G^{SM}_{global} = U(1)_B \times U(1)_e \times U(1)_\mu \times U(1)_\tau, \tag{3.7}$$

when the Yukawas are switched on. So, in total we can remove 15 real and 26 imaginary parameters from the Yukawa couplings. This gives rise to 12 real parameters and 1 phase in the Yukawa terms. It is this single phase that can give rise to CP violation. More concretely, it can be shown that CP is violated if and only if [43],

$$Im\left\{det[Y^dY^{d\dagger}, Y^uY^{u\dagger}]\right\} \neq 0, \tag{3.8}$$

which is referred to as the Jarlskog invariant. Note, it follows that complex Yukawas do not necessarily imply CP violation.

Giving the scalar fields a vacuum expectation value, $Re(\phi^0) \rightarrow (v + H^0)/\sqrt{2}$, the Yukawa terms give rise to the mass terms,

$$\mathcal{L}_{Mass} = (M_d)_{ij}\overline{d^I_{Li}}d^I_{Rj} + (M_u)_{ij}\overline{u^I_{Li}}u^I_{Rj} + (M_l)_{ij}\overline{l^I_{Li}}l^I_{Rj} + h.c.. \tag{3.9}$$

Here,

$$M_f = \frac{v}{\sqrt{2}} Y^f, \tag{3.10}$$

and we have split the $SU(2)_L$ doublets as,

$$Q^I_{Li} = \begin{pmatrix} u^I_{Li} \\ d^I_{Li} \end{pmatrix}, \quad L^I_{Li} = \begin{pmatrix} \nu^I_{Li} \\ l^I_{Li} \end{pmatrix}. \tag{3.11}$$

The mass matrices can be diagonalised using unitary matrices V_{fL}, V_{fR},

$$V_{fL} M_f V^\dagger_{fR} = M^{diag}_f. \tag{3.12}$$

Then the mass eigenstates are given by $f_{L/Ri} = (V_{fL/R})_{ij} f^I_{L/Rj}$.

We can now define the Cabibbo-Kobayashi-Maskawa (CKM) matrix,

$$V_{CKM} = V_{uL} V^\dagger_{dL}, \tag{3.13}$$

which is unitary and hence depends on three real angles and six phases. Again, some of these parameters can be removed using the freedom to permute between various generations and the freedom in the phase structure of V_{CKM}. Defining P_f to be a diagonal unitary matrix, we can redefine the rotation of our interaction eigenstates into mass eigenstates by,

$$\tilde{V}_{fL/R} = P_f V_{fL/R}, \tag{3.14}$$

leaving M^{diag}_f unchanged. However, this redefinition results in

$$V_{CKM} \to P_u V_{CKM} P^*_d, \tag{3.15}$$

allowing us to remove five phases (there exists fives phase differences between P_u and P_d). Thus, V_{CKM} has three real angles and one phase. In the standard parametrisation the CKM matrix is written as,

$$V_{CKM} = \begin{pmatrix} c_{12}c_{13} & s_{12}c_{13} & s_{13}e^{-i\delta} \\ -s_{12}c_{23} - c_{12}s_{23}s_{13}e^{i\delta} & c_{12}c_{23} - s_{12}s_{23}s_{13}e^{i\delta} & s_{23}c_{13} \\ s_{12}s_{23} - c_{12}c_{23}s_{13}e^{i\delta} & -c_{12}s_{23} - s_{12}c_{23}s_{13}e^{i\delta} & c_{23}c_{13} \end{pmatrix}, \tag{3.16}$$

where $c_{ij} \equiv \cos\theta_{ij}$, $s_{ij} \equiv \sin\theta_{ij}$ and δ is the Kobayashi-Maskawa phase,

which is the single source of CP violation in the Standard Model [44].

3.3 Closed string models

We will now briefly discuss CP and discrete torsion in the context of closed string models. This will provide us with a useful background to understanding these features in our case of D-brane models containing open strings.

3.3.1 CP as a gauge symmetry

In the heterotic string, it is well known that a four dimensional CP conjugation corresponds to a rotation in the full 10 dimensional theory and a gauge transformation, and thus 4 dimensional CP turns out to be a discrete gauge symmetry [31, 32] (i.e. part of the 10D Poincare group). The situation is heuristically as shown in figure 3.1. The three non-compact space dimensions are labelled x_i, with y_i and w_i labelling 6 internal compact dimensions. Parity is defined as a reflection in one direction, x_1 say. By a rotation through π in the x_2x_3 plane, four dimensional parity is equivalent to a reflection in all the space directions, the more conventional definition (valid when the number of space dimensions is odd). However if we simultaneously reflect in an odd number of internal compact dimensions the total is a rotation in three orthogonal planes. Complexifying the internal space as

$$z_i = w_i + iy_i, \tag{3.17}$$

we can, without loss of generality, choose the additional reflection corresponding to a CP transformation to act on the y_i coordinates, with

$$\text{CP} : x^\mu \rightarrow x_\mu,\ z_i \rightarrow z_i^*. \tag{3.18}$$

By supersymmetry we must also reflect the fermionic superpartners. This, combined with a possible $E_8 \times E_8$ or $SO(32)$ gauge transformation, results in a reversal of gauge charges. The combined result of the rotation and gauge transformation is then a 4 dimensional CP transformation. It follows that CP can only be broken spontaneously.

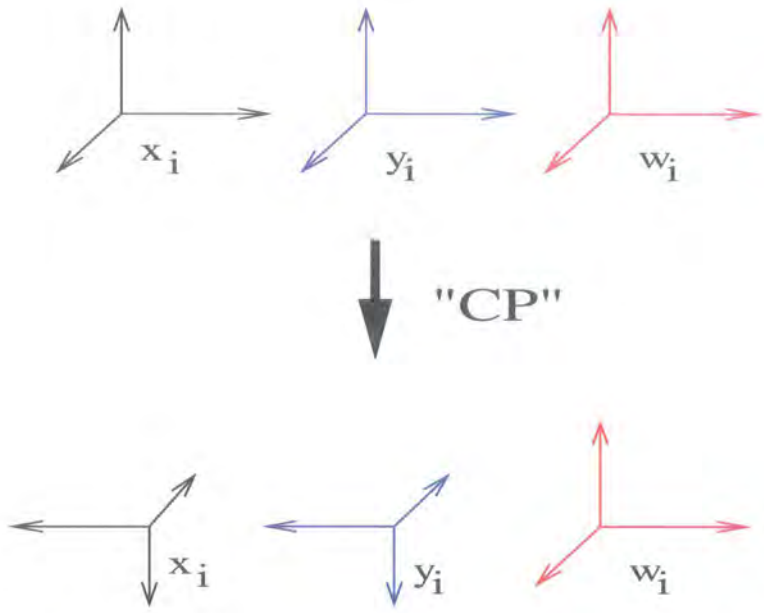

Figure 3.1: Rotations on 3 non-compact plus 3 compact directions corresponding to CP.

3.3.2 Discrete torsion

We now introduce discrete torsion through a consideration of the one-loop vacuum amplitude for a closed string theory, defined on the space $M^4 \times \mathbb{C}^3/G$. M^4 is our ordinary Minkowski space and $\mathbb{C}^3/G$ an orbifold, defined through the identification

$$z_i \sim g.z_i \quad g \in G. \tag{3.19}$$

This action must also possess a number of fixed points. The one-loop vacuum amplitude has the topology of a torus, defined by quotienting the complex plane by the equivalence relations,

$$w \sim w + 2\pi n \quad w \sim w + 2\pi m\tau, \tag{3.20}$$

where $m, n \in \mathbb{Z}$ and τ is a 'modular parameter', describing the shape of the torus. However, a single torus may be described by more than one τ. In fact, the full family of equivalent tori can be reached from any τ by the modular transformations,

$$\tau \to \tau + 1, \quad \tau \to -\tfrac{1}{\tau}. \tag{3.21}$$

The boundary conditions for the bosonic worldsheet fields are given by,

$$\left.\begin{array}{l} X^\mu(w+2\pi) = X^\mu(w+2\pi\tau) = X^\mu(w) \quad \mu = 0,1,2,3\,, \\ z^i(w+2\pi) = g.z^i(w) \\ z^i(w+2\pi\tau) = h.z^i(w) \end{array}\right\} \; i = 1,2,3\,, \tag{3.22}$$

where $g, h \in G$. Fields with periodic boundary conditions only up to the action of an orbifold group element are known as 'twisted states'. Fermionic boundary conditions can be different for left and right movers,

$$\begin{aligned} \psi_L^k(w+2\pi) &= e^{-2\pi i v_k}\psi_L^k(w), \\ \psi_R^k(w+2\pi) &= e^{-2\pi i u_k}\psi_R^k(w), \end{aligned} \tag{3.23}$$

where k runs over spacetime and internal degrees of freedom. Then the partition function is given schematically by,

$$\mathcal{Z}(\tau) = \sum_{(g,h)} \mathcal{Z}_h^g(\tau) \sum_{(u,v)} C_u^v Z_u^v(\tau), \tag{3.24}$$

where Z_u^v is the fermionic contribution and $\mathcal{Z}_h^g$ the bosonic contribution. Since, the fermionic boundary conditions get mixed up by modular transformations, we must choose C_u^v in such a way as to make (3.24) invariant under modular transformations. This is a central consistency condition in closed string theories. The partition function encodes the spectrum of the string theory. Hence modular invariance allows us to deduce all the possible closed string theories. To obtain the complete one-loop partition function, we must integrate over τ giving,

$$\mathcal{Z} = \sum_{(g,h)} \mathcal{Z}(g,h). \tag{3.25}$$

It has been discovered that (3.25) can be generalised allowing us to construct a larger class of closed string theories. This generalisation is called discrete torsion [45, 46] and arises from the possibility of weighting different twisted sectors by complex phases, i.e.

$$\mathcal{Z} = \frac{1}{|G|} \sum_{(g,h)} \beta(g,h)\mathcal{Z}(g,h), \tag{3.26}$$

whilst still retaining modular invariance. To satisfy modular invariance and

factorisation for higher loop amplitudes, these phases must satisfy

$$\beta_{g,g} = 1, \quad \beta_{g,h} = \beta_{h,g}^{-1}, \quad \beta_{g,hk} = \beta_{g,h}\beta_{g,k}, \quad \forall g, h, k \in G. \tag{3.27}$$

This implies that the phases are of the form $\beta_{g,h} = \alpha_{g,h}\alpha_{h,g}^{-1}$ where α is a 2-cocycle of the group G. The possible discrete torsions are therefore classified by the group cohomology $H^2(G, U(1))$. In the case of orbifolds, we can only have discrete torsion in the case $G = \mathbb{Z}_N \times \mathbb{Z}_M$ and is generated by one element of $\mathbb{Z}_{gcd(N,M)}$. Let ω_1, ω_2 be the generators of $\mathbb{Z}_N$ and $\mathbb{Z}_M$ respectively and $p = gcd(N, M)$. Then we can write,

$$\beta(\omega_1^a\omega_2^b, \omega_1^{a'}\omega_2^{b'}) = \varepsilon^{ab'-ba'}, \tag{3.28}$$

where $\varepsilon = e^{2\pi im/p}$, $m = 1, .., p$.

A less abstract way of looking at discrete torsion, is to consider turning on an antisymmetric tensor field $B_{\mu\nu}$. This manifests itself in the path integral by introducing the phase,

$$exp[\frac{i}{2}\int B_{\mu\nu}\partial_\alpha X^\mu \partial_\beta X^\nu \varepsilon^{\alpha\beta}]. \tag{3.29}$$

If B is flat (i.e. $dB = 0$), this phase is topological and only depends on the class of map from worldsheet to spacetime. Therefore, B has the effect of introducing different phases for different classes of embeddings of the string worldsheet into spacetime, thus giving rise to the phases in (3.26). The choices of discrete torsion can then be viewed as the choice of action of the orbifold on the B-field background [41].

We now proceed to our D-brane model where we will discuss discrete torsion in the case of open strings.

3.4 A D-Brane model with Discrete Torsion

We will begin with a descriptive overview of the string construction to be investigated. A more detailed account then follows, where we calculate the spectrum of the model, determine the form of the superpotential and explore the phenomenological consequences for CP violation.

3.4.1 A brief overview

The model we are interested in is based on the bottom-up approach to string model construction, and is a slight generalisation of the discrete torsion models discussed in [7]. This approach is based on the localisation of gauge fields to D-branes, as discussed in section 2.3. The idea is to look for D-brane configurations whose worldvolume field theories resemble the Supersymmetric Standard Model as much as possible, *before* considering the compactification of the model down to $D = 4$. In this way, some of the low energy physics in the D-brane worldvolume, is only dependent on the structure of spacetime local to the D-brane configuration. This allows us to obtain desirable phenomenological features, such as the Standard Model gauge group and three generations of quark and leptons, independently of the compactification scheme chosen. Specifically, we consider configurations of Type IIB D3-branes sitting on an orbifold singularity. By an orbifold singularity, we simply mean a fixed point of the action of G on $\mathbb{C}^3$. The reason for this choice of geometry is that D3-branes sitting in a smooth transverse space have $N = 4$ supersymmetry on their worldvolume[1]. The orbifold group acts on the string states and projects out those states not invariant under its action. This can give rise to $N = 1$ supersymmetry, allowing for chirality.

The particular model that we will be examining contains the following ingredients,

- A non-compact internal space $\mathbb{C}^3$, containing a $\mathbb{Z}_3 \times \mathbb{Z}_M \times \mathbb{Z}_M$ orbifold singularity.
- Coincident D3-branes whose world-volume theory has the gauge group $SU(3)_C \times SU(2)_L \times U(1)_Y$.
- Mutually perpendicular D7-branes[2] to cancel tadpoles, each with gauge group $U(1) \times U(2)$.

Here $\mathbb{Z}_N$ is the finite cyclic group. The generator g of this group acts on $\mathbb{C}^3$ with the action $z_i \sim e^{2\pi i v_g^i} z_i$, where $v_g = (a_1, a_2, a_3)/N$ is known as a twist vector. The D3-branes and D7-branes are located on the $\mathbb{Z}_3 \times \mathbb{Z}_M \times \mathbb{Z}_M$ orbifold singularity. This setup is depicted in figure 3.2.

[1] $N = 1$ supersymmetry in $D = 10$ gives rise to $N = 4$ supersymmetry in $D = 4$.
[2] We call a D7-brane whose worldvolume is $z_i = 0$ a D7$_i$-brane.

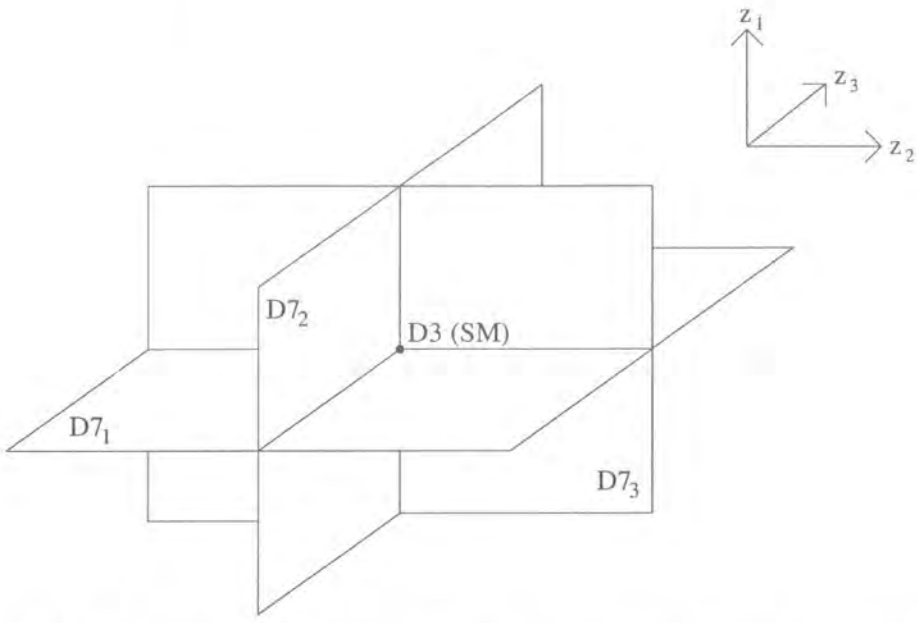

Figure 3.2: A non-compact internal space, $\mathbb{C}^3$, with Type IIB D3-branes containing the Standard Model located on an $\mathbb{Z}_3 \times \mathbb{Z}_M \times \mathbb{Z}_M$ orbifold singularity. The D7-branes are required for tadpole cancellation.

Closed strings propagate only in the bulk and are gauge singlets, whereas the open strings are localised to the D-branes. The action of the $\mathbb{Z}_3$ orbifold group divides the D3-branes into stacks of 3s, 2s and s (s will label our choice of discrete torsion). Then, the action of $\mathbb{Z}_M \times \mathbb{Z}_M$ on the string spectrum, results in the gauge group $U(3) \times U(2) \times U(1)$ on the D3-brane worldvolumes. Remarkably however, only one linear combination of the three U(1) factors is non-anomalous and this combination gives rise to the correct hypercharge assignments, resulting in a Standard Model gauge group. The choice of orbifold group also leads to a model with three quark-lepton generations, and in addition, three generations of Higgs'. Open strings with ends on D-branes within the same set give rise to the gauge bosons, and those with endpoints in different sets of D-branes give rise to matter fields in bifundamentals. This makes it very simple to identify the MSSM fields as illustrated in figure 3.3.

Finally, the $\mathbb{Z}_M \times \mathbb{Z}_M$ factor allows for a choice of discrete torsion. The discrete torsion then gives rise to a complex phase in the superpotential. These facts will all be discussed in more detail in the following sections.

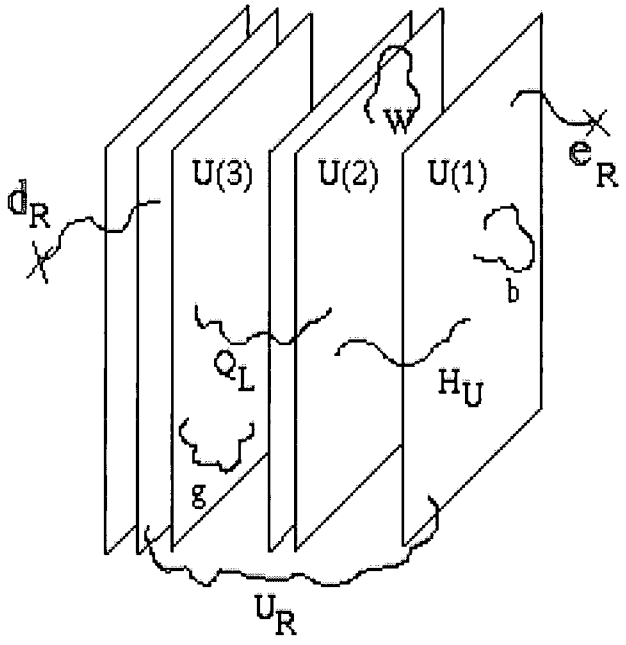

Figure 3.3: The D3-branes are shown separated for clarity, although they are in fact coincident, and the D7-branes fill the figure. The position of end points of the strings determine how they transform under the SM gauge group, with fields such as the right-handed leptons and down quarks having one end on a D3 brane and another on a D7-brane.

3.4.2 The spectrum before the orbifold projection

Let us proceed to a determination of the massless spectrum of this model, beginning with the spectrum before the orbifold projection. For the 'untwisted' 33 states, which are the open strings with both endpoints in the stack of D3-branes, we have

- world-volume gauge bosons $\lambda_{33}\psi^{\mu}_{-1/2}|0>$,
- complex scalars[3] $\lambda_{33}\psi^{i}_{-1/2}|0>$, i=1,2,3.
- Weyl fermions $\lambda_{33}|s_1, s_2, s_3, s_4>$, $s_i = \pm 1/2$ and $\sum_{i=1}^{4} s_i$ odd. With s_4 determining the space-time chirality.

Here λ_{33} are the Chan-Paton matrices, and the condition on the Weyl-fermions is the GSO projection. Note that we have defined complex fermionic fields $\psi^1 = \psi^4 + i\psi^5$, etc. These states were discussed in section 2.3.

[3]These are the coordinates of the D3-branes in the internal space.

Next, we have states in the 'twisted' 37_i and 7_i3 sectors, which come from open string states with one endpoint on a D3-brane and the other on a $D7_i$-brane. These states may achieve vanishing length and hence contribute to the massless spectrum. Such states have mixed boundary conditions. That is, one end of the string may have Neumann boundary conditions while the other has Dirichlet boundary conditions. For instance, a string state in the 37_3 sector has the following boundary conditions at the string endpoints,

$$\begin{aligned} &\mu = 0,1,2,3 \quad \text{NN}, \\ &\mu = 4,5,6,7 \quad \text{DN}, \\ &\mu = 8,9 \qquad \text{DD}, \end{aligned} \tag{3.30}$$

where D stands for Dirichlet and N for Neumann. The bosonic mode expansions for directions with mixed boundary conditions, are half-integer moded. Hence, due to superconformal invariance, the Ramond sector and Neveu-Schwarz sector oscillators are then half-integer/integer moded respectively. Therefore, the Ramond sector has fermion zero modes in the NN and DD directions, while we obtain scalars from the Neveu-Schwarz sector, which has fermion zero modes in the DN directions. This gives rise to the following massless states,

- complex scalars $\lambda_{37_i}|s_j, s_k>$, $j,k \notin \{i,4\}$ and $s_j = s_k$,
- Weyl fermions $\lambda_{37_i}|s_i, s_4>$, $s_i = s_4$,

where again λ_{37_i} are the Chan-Paton matrices and we have similar states in the 7_i3 sector.

3.4.3 The action of the orbifold on the open string states

As mentioned previously, the orbifold group acts on the string states and projects out those states not invariant under its action. The action of the orbifold group, $\mathbb{Z}_3 \times \mathbb{Z}_M \times \mathbb{Z}_M$, can be split up into the action of its separate cyclic group factors. Each of which acts independently on the Chan-Paton matrices and the string worldsheet fields. For instance, a $\mathbb{Z}_N$ orbifold with group generator g and twist vector $v_g = (a_1, a_2, a_3)/N$, requires $a_1 + a_2 + a_3 = 0$ for N=1 supersymmetry on the D3-brane worldvolume [7]. The

generator g then acts on the 33 sector by leaving the gauge boson invariant, and transforming the scalars and fermions respectively as,

$$g^k\psi^i_{-1/2}|0> = e^{2\pi i k v^i_g}\psi^i_{-1/2}|0>, \tag{3.31}$$

$$g^k|\vec{s}> = e^{2\pi i k \vec{s}.\vec{v_g}}|\vec{s}> . \tag{3.32}$$

Here $\vec{s} = (s_1, s_2, s_3)$, and the twisted 37_i states transform as the fermions above if we set any s_i not defined to be zero. These transformations are dictated by the action of the orbifold group on the bosonic coordinates and supersymmetry. For our particular case, we denote the generator for $\mathbb{Z}_3$ by θ and the generators for the two $\mathbb{Z}_M$ factors to be ω_i. We then take the twist vectors to be,

$$\begin{aligned} v_\theta &= (1,1,-2)/3, \\ v_{\omega_1} &= (1,-1,0)/M, \\ v_{\omega_2} &= (0,1,-1)/M. \end{aligned} \tag{3.33}$$

The action of θ on the Chan-Paton matrices of the twisted and untwisted states respectively is,

$$\theta\lambda_{33} = \gamma_{\theta,3}\lambda_{33}\gamma^\dagger_{\theta,3}, \tag{3.34}$$

$$\theta\lambda_{37_i} = \gamma_{\theta,3}\lambda_{37_i}\gamma^\dagger_{\theta,7_i}, \tag{3.35}$$

where the form of this action is dictated by the necessity of leaving string amplitudes invariant. We define,

$$\gamma_{\theta,3} = diag(I_{3s}, \alpha I_{2s}, \alpha^2 I_s), \tag{3.36}$$

$$\gamma_{\theta,7_i} = diag(\alpha I_s, \alpha^2 I_{2s}), \tag{3.37}$$

where $\alpha = e^{\frac{2\pi i}{3}}$. The γ_θ matrices form a unitary representation of $\mathbb{Z}_3$ and are determined by our requirement of a Standard Model gauge group, which will be explored in the next section. Furthermore, they must satisfy the tadpole cancellation condition [7],

$$\sum_{i=1}^{3} Tr(\gamma_{\theta,7_i}) + 3Tr(\gamma_{\theta,3}) = 0. \tag{3.38}$$

Since we are considering an oriented string theory, there are no contributions to tadpoles from the Klein bottle and Möbius strip. Thus, condition (3.38) simply ensures that there are no contributions to tadpoles from the cylinder diagram. In addition, this constraint ensures non-abelian anomaly cancellation. More details and explicit calculations can be found in [47, 48].

The action of the generators ω_i is the same as above. However this time the γ_{ω_i} matrices form a projective representation of $\mathbb{Z}_M \times \mathbb{Z}_M$, a possibility that arises since the action of $\mathbb{Z}_M \times \mathbb{Z}_M$ allows for a choice of discrete torsion. In the context of closed strings, we saw in section 3.3.2 that this is associated with a cocycle $\beta(g,h) \in H^2(\mathbb{Z}_M \times \mathbb{Z}_M, U(1)) \cong \mathbb{Z}_M$ [45, 46], which manifests itself in the one-loop partition function. In the case of open strings, this phase appears in the projective representation where $\gamma_g\gamma_h = \beta(g,h)\gamma_h\gamma_g$ [49, 50]. These phases are identical and are required for invariance of closed-open string interactions under the action of $\mathbb{Z}_M \times \mathbb{Z}_M$.

It follows that there are M non-equivalent choices of discrete torsion, described by distinct cocycles $\beta(\omega_1,\omega_2) = e^{2\pi i n/M} = \varepsilon$ where n=1,..,M. Such possibilities are conventionally distinguished by an integer $s = M/gcd(n,M)$. For a string endpoint residing on a generic set of $sn^{(i)}$ D3-branes, the action on the Chan-Paton factors is determined by the matrices,

$$\gamma_{\omega_1,3} = \oplus_{l,m}\omega_M^l\hat{\gamma}_{\omega_1} \otimes I_{n_{lm}^{(i)}}, \tag{3.39}$$

$$\gamma_{\omega_2,3} = \oplus_{l,m}\omega_M^m\hat{\gamma}_{\omega_2} \otimes I_{n_{lm}^{(i)}}, \tag{3.40}$$

where $\omega_M = e^{\frac{2\pi i}{M}}$, $\sum_{l,m} n_{lm}^{(i)} = n^{(i)}$, $l,m = 0,\ldots,(\frac{M}{s})-1$, and

$$\hat{\gamma}_{\omega_1} = diag(1,\varepsilon^{-1},\ldots,\varepsilon^{-(s-1)}), \tag{3.41}$$

$$\hat{\gamma}_{\omega_2} = \begin{pmatrix} 0 & 1 & 0 & \ldots & 0 \\ 0 & 0 & 1 & \ldots & 0 \\ \vdots & \ddots & \ddots & \ddots & \\ 0 & 0 & 0 & \ldots & 1 \\ 1 & 0 & 0 & \ldots & 0 \end{pmatrix}_{s\times s}. \tag{3.42}$$

Since $Tr(\gamma_{\omega_i}) = 0$, tadpoles are unaffected by discrete torsion. It follows that

there are no restrictions on the $n^{(i)}_{lm}$. For simplicity, we choose

$$n^{(i)}_{lm} = \begin{cases} n^{(i)} & \text{if l=m=0,} \\ 0 & \text{otherwise.} \end{cases} \tag{3.43}$$

Note that, in our case we have $n^{(0)} = 3, n^{(1)} = 2, n^{(2)} = 1$, arising from the gamma embedding of the $\mathbb{Z}_3$ action on the D3-branes.

Before proceeding to a determination of the open string spectrum, we first use the orbifold action to calculate the Chan-Paton factors of different states. This will aid us in not only computing the spectrum, but also deriving a complex phase in the superpotential.

3.4.4 Calculation of Chan-Paton factors

As a direct consequence of the form of the gamma embedding of the action of the $\mathbb{Z}_3$ group on the Chan-Paton factors, our D3-branes are split into stacks of $sn^{(i)}$, where $n^{(0)} = 3, n^{(1)} = 2, n^{(2)} = 1$ and the $D7_i$-branes are split into stacks of $su^{(i)}$, where $u^{(0)} = 0, u^{(1)} = 1, u^{(2)} = 2$. Now consider a generic open string state, whose Chan-Paton factor must be of size $s\alpha \times s\beta$, where $\alpha, \beta \in \{n^{(i)}, u^{(j)}\}$. If this state is to be invariant under the action of an element $g = (a, b) = \omega_1^a \omega_2^b \in \mathbb{Z}_M \times \mathbb{Z}_M$, and hence not projected out of the spectrum, we require

$$\lambda^{(k)}_{s\alpha \times s\beta} = r^{(k)}(a, b)\gamma_{g,3}\lambda^{(k)}_{s\alpha \times s\beta}\gamma^{\dagger}_{g,3}. \tag{3.44}$$

Here $r^{(k)}(a, b)$ is the phase from the action on the string worldsheet fields, and for a string endpoint on a set of $s\alpha$ D-branes we have,

$$\gamma_g = (\sqrt{\epsilon})^{-ab}\gamma^a_{\omega_1}\gamma^b_{\omega_2} \otimes I_\alpha. \tag{3.45}$$

It follows that we can factor the Chan-Paton matrix by writing,

$$\lambda^{(k)}_{s\alpha \times s\beta} = X^{(k)}_{s \times s} \otimes Y^{(k)}_{\alpha \times \beta}, \tag{3.46}$$

where $X^{(k)}$ is determined by the action of $\mathbb{Z}_M \times \mathbb{Z}_M$ and $Y^{(k)}$ may be further constrained by the θ projection. Substituting (3.46) into (3.44) removes the

dependence on $Y^{(k)}$ giving,

$$X^{(k)}\gamma^a_{\omega_1}\gamma^b_{\omega_2} = r^{(k)}(a,b)\gamma^a_{\omega_1}\gamma^b_{\omega_2}X^{(k)}. \tag{3.47}$$

Since the γ_{ω_i} matrices form a projective representation and hence satisfy $\gamma_g\gamma_h = \beta(g,h)\gamma_h\gamma_g$, we can solve (3.47) with the ansatz $X^{(k)} = \gamma^{p_k}_{\omega_1}\gamma^{q_k}_{\omega_2}$. This results in,

$$\beta(\omega_1,\omega_2)^{p_k b - q_k a} = r^{(k)}(a,b). \tag{3.48}$$

For the 33 sector fields, $\lambda^{(k)}_{33}\psi^k_{-1/2}|0>$, we have

$$r^{(k)}_{33}(a,b) = e^{2\pi i(av^k_{\omega_1} + bv^k_{\omega_2})}, \tag{3.49}$$

and for 'twisted' 37_k sector fields $\lambda_{37_k}|s_i,s_j>, i,j \notin \{k,4\}$ we have,

$$r^{(k)}_{37}(a,b) = e^{\pi i(a\sum_{i\neq k} v^i_{\omega_1} + b\sum_{i\neq k} v^i_{\omega_2})}. \tag{3.50}$$

Substituting these expressions into (3.48) we find,

$$\begin{aligned} p_k &= \begin{cases} \frac{a^k_2}{n} & \text{For 33 fields} \\ \frac{1}{2n}\sum_{i\neq k} a^i_2 & \text{For } 37_k \text{ fields} \end{cases}, \\ q_k &= \begin{cases} -\frac{a^k_1}{n} & \text{For 33 fields} \\ -\frac{1}{2n}\sum_{i\neq k} a^i_1 & \text{For } 37_k \text{ fields} \end{cases}, \end{aligned} \tag{3.51}$$

where $v_{\omega_i} = \frac{1}{M}(a^1_i, a^2_i, a^3_i)$. Hence we have, for the 33 complex scalar fields,

$$X^{(1)}_{33} = \gamma^{-\frac{1}{n}}_{\omega_2}, \quad X^{(2)}_{33} = \gamma^{\frac{1}{n}}_{\omega_1}\gamma^{\frac{1}{n}}_{\omega_2}, \quad X^{(3)}_{33} = \gamma^{-\frac{1}{n}}_{\omega_1}, \tag{3.52}$$

and for the 37 complex scalar fields,

$$X_{37_1} = \gamma^{\frac{1}{2n}}_{\omega_2}, \quad X_{37_2} = \gamma^{-\frac{1}{2n}}_{\omega_1}\gamma^{-\frac{1}{2n}}_{\omega_2}, \quad X_{37_3} = \gamma^{\frac{1}{2n}}_{\omega_1}. \tag{3.53}$$

Note that, due to $N = 1$ supersymmetry these Chan-Paton factors are also required for the chiral superfields containing the complex scalars. Finally, for the gauge bosons in the 33 and 7_i7_i sectors we have $r^{(k)}(a,b) = 1$ and hence $X = I_{s\times s}$.

3.4.5 Determining the massless open string spectrum

We are now able to compute the open string spectrum. Let us begin with the 33 sector, specifically with the gauge bosons, $\lambda_{33}\psi^{\mu}_{-1/2}|0>$. From the above we can write,

$$(\lambda_{33})_{sn^{(i)}\times sn^{(j)}} = I_{s\times s}\otimes Y_{n^{(i)}\times n^{(j)}}. \tag{3.54}$$

The projection equation for the action of θ on the gauge bosons is,

$$\lambda_{33} = \gamma_{\theta,3}\lambda_{33}\gamma^{\dagger}_{\theta,3}, \tag{3.55}$$

and the gamma embedding for θ, acting on a string endpoint attached to a stack of $s\beta$ D-branes, is given by $\alpha^i I_{s\beta}$ with $\beta \in \{n^{(i)}, u^{(j)}\}$. Then, substituting (3.54) into (3.55) we obtain $i = j$. Hence

$$(\lambda_{33})_{sn^{(i)}\times sn^{(i)}} = I_{s\times s}\otimes Y_{n^{(i)}\times n^{(i)}}, \tag{3.56}$$

giving rise to a $U(n^{(i)})$ gauge boson. Our gauge group on the D3-branes is therefore $U(3)\times U(2)\times U(1)$. A similar method applied to the 77 sector, gives the gauge groups $U(1)\times U(2)$ on the D7$_i$-branes.

For the state $\lambda^{(k)}_{33}\psi^{k}_{-1/2}|0>$ with endpoints on the stacks of D3-branes, we have

$$(\lambda^{(k)}_{33})_{sn^{(i)}\times sn^{(j)}} = (X^{(k)}_{33})_{s\times s}\otimes Y^{(k)}_{n^{(i)}\times n^{(j)}}, \tag{3.57}$$

where $X^{(k)}_{33}$ is the constant matrix computed above. The projection equation for θ then gives us,

$$(\lambda^{(k)}_{33})_{sn^{(i)}\times sn^{(j)}} = e^{2\pi i v^{k}_{\theta}}\alpha^i\alpha^{*j}(\lambda^{(k)}_{33})_{sn^{(i)}\times sn^{(j)}}. \tag{3.58}$$

Hence, we require $j = i + a^k$, where $v_\theta = (a_1, a_2, a_3)/3$. Therefore, the state $\lambda^{(k)}_{33}\psi^{k}_{-1/2}|0>$ has the Chan-Paton matrix,

$$(\lambda^{(k)}_{33})_{sn^{(i)}\times sn^{(i+a^k)}} = (X^{(k)}_{33})_{s\times s}\otimes Y^{(k)}_{n^{(i)}\times n^{(i+a^k)}}. \tag{3.59}$$

Since an open string stretched between two different stacks of D3-branes transforms as a bifundamental, this corresponds to a state which transforms

as $(n^{(i)}, \bar{n}^{(i+a^k)})$. So, the final spectrum in the 33 sector is,

$$\begin{array}{ll} \text{Vector multiplet} & U(3) \times U(2) \times U(1) \\ \text{Chiral Mulitplet} & \sum_{i=0}^{2} \sum_{k=1}^{3} (n^{(i)}, \bar{n}^{(i+a^k)}). \end{array} \tag{3.60}$$

Next, we must consider the 37_k sector. For the state, $\lambda_{37_k}|s_i, s_j > i, j \notin \{k, 4\}$, with one endpoint attached to a stack of D3-branes and the other to a stack of D7$_i$-branes, we have

$$(\lambda_{37_k})_{sn^{(i)} \times su^{(j)}} = (X_{37_k})_{s \times s} \otimes Y_{sn^{(i)} \times su^{(j)}}. \tag{3.61}$$

The θ projection equation is,

$$\lambda_{37_k} = e^{2\pi i \vec{s}.\vec{v}_\theta} \gamma_{\theta,3} \lambda_{37_k} \gamma^{\dagger}_{\theta,7}. \tag{3.62}$$

This leads to the expression,

$$(\lambda_{37_k})_{sn^{(i)} \times su^{(j)}} = \alpha^i \alpha^{*j} e^{2\pi i \vec{s}.\vec{v}_\theta} (\lambda_{37_k})_{sn^{(i)} \times su^{(j)}}, \tag{3.63}$$

hence $j = i + 3\vec{s}.\vec{v}_\theta = i - \frac{1}{2}a_k$. Therefore, for the 37_k sector we have the states,

$$\text{Chiral Mulitplet} \quad \sum_{i=0}^{2} (n^{(i)}, \bar{u}^{(i-\frac{1}{2}a_k)}). \tag{3.64}$$

There are also similar states from the 7_k3 sector given by,

$$\text{Chiral Mulitplet} \quad \sum_{i=0}^{2} (u^{(i)}, \bar{n}^{(i-\frac{1}{2}a_k)}). \tag{3.65}$$

Note that, the 77 sector states are non-dynamical before the embedding of our D-brane configuration in a compact global model.

Finally, it is important to note that there exist mixed $U(1)$-nonabelian gauge anomalies. These field theory anomalies are cancelled by a generalised Green-Schwarz mechanism mediated by closed string twisted states [51]. The anomalous $U(1)$'s get a tree-level mass of the order of the string scale [52] and hence do not appear in our low energy spectrum. In our case, it can be shown that there is only one non-anomalous $U(1)$, given by the diagonal combination

$$Y = -(\frac{1}{3}Q_3 + \frac{1}{2}Q_2 + Q_1). \tag{3.66}$$

$33\ (n^{(i)}, \bar{n}^{(i+a^k)})$	$SU(3)_c \times SU(2)_L$	Massless field
$3(3, \bar{2})$	$3(3,2)_{1/6}$	Q_L^i
$3(2, \bar{1})$	$3(1,2)_{1/2}$	H_u^i
$3(1, \bar{3})$	$3(\bar{3},1)_{-2/3}$	u_R^i
$37_k\ (n^{(i)}, \bar{u}^{(i-\frac{1}{2}a^k)})$		
$(3, \bar{1})$	$(3,1)_{-1/3}$	Non-Standard model
$(2, \bar{2})$	$(1,2;2')_{-1/2}$	H_d^k and L_L^k
$7_k3\ (u^{(i)}, \bar{n}^{(i-\frac{1}{2}a^k)})$		
$(2, \bar{3})$	$(\bar{3},1;2')_{1/3}$	d_R^k
$(1, \bar{1})$	$(1,1;1')_1$	e_R^k

Table 3.1: Open string massless states. The subscript refers to hypercharge, as defined in (3.66). Also, a prime refers to gauge groups on the $D7_k$-branes.

Here Q_i is the charge under the $U(1)$ gauge group contained in $U(n^{(i)})$. This non-anomalous $U(1)$ then gives the necessary quantum numbers to our fields to act as hypercharge. A detailed treatment can be found in [7]. So, our final gauge group is $SU(3)_c \times SU(2)_L \times U(1)_Y$. The massless spectrum is then given in table 3.1, with chiral superfields containing the Standard Model fields and their supersymmetric partners. Note in particular, that we have obtained three quark-lepton generations.

3.4.6 The superpotential

We can now discuss the form of the superpotential. Focusing on renormalisable cubic terms we have,

$$W = \varepsilon_{rst} Tr(\Phi^r_{i,i+a^r} \Phi^s_{i+a^r,i+a^r+a^s} \Phi^t_{i+a^r+a^s,i}) + \sum_{r=1}^{3} Tr(\Phi^r_{i,i+a^r} \Phi^{37_r}_{i+a^r,i+\frac{1}{2}a^r} \Phi^{7_r3}_{i+\frac{1}{2}a^r,i}). \tag{3.67}$$

Here $\Phi^r_{i,i+a^r} = \lambda^{(r)}_{33} \varphi^r_{i,i+a^r}$ is the 33 chiral multiplet transforming as $(n^{(i)}, \bar{n}^{(i+a^r)})$, and $\Phi^{37_r}_{i,i-\frac{1}{2}a^r} = \lambda_{37_i} \varphi^{37_i}_{i,i-\frac{1}{2}a^r}$ is the 37_r field transforming as $(n^{(i)}, \bar{u}^{(i-\frac{1}{2}a^r)})$, similarly for the 7_r3 field. The superpotential is easily determined by considering the fact that the above terms come from a tree-level open string interaction. This corresponds to a disc diagram with vertex operators on the boundary. A consistent boundary then requires either a (33)(33)(33) or a $(33)(37_r)(7_r3)$ interaction, leading to the above expression.

Using the expressions derived for the Chan-Paton factors in section 3.4.4,

we have

$$\begin{aligned} W &= \varepsilon_{rst} Tr((X_{33}^{(r)} \otimes Y^{(r)})(X_{33}^{(s)} \otimes Y^{(s)})(X_{33}^{(t)} \otimes Y^{(t)}))\varphi^r\varphi^s\varphi^t + \ldots \\ &= \varepsilon_{rst} Tr(X_{33}^{(r)} X_{33}^{(s)} X_{33}^{(t)}) Tr(Z^r Z^s Z^t) + \ldots, \end{aligned} \tag{3.68}$$

where $Z^i = Y^{(i)}\varphi^i$. Redefining the $Y^{(i)}$'s by a constant such that a factor of $Tr(X_{33}^{(1)} X_{33}^{(2)} X_{33}^{(3)})$ is absorbed into each term and noting that

$$\frac{Tr(X_{33}^{(2)} X_{33}^{(1)} X_{33}^{(3)})}{Tr(X_{33}^{(1)} X_{33}^{(2)} X_{33}^{(3)})} = e^{-2\pi i/M}, \tag{3.69}$$

we arrive at,

$$W = \epsilon_{abc} Tr(Z^a Z^b Z^c) + (1 - e^{-2\pi i/M}) s_{abc} Tr(Z^a Z^b Z^c) + \ldots \tag{3.70}$$

Here $s^{132} = s^{321} = s^{213} = 1$ and all other components are zero. Identifying our supersymmetric SM fields, equations (3.67) and (3.70) give us the yukawa type couplings,

$$W = h_{abc} \bar{u}_R^a Q_L^b H_u^c + f_{abc} \bar{d}_R^a Q_L^b H_d^c + \ldots, \tag{3.71}$$

where $h_{abc} = \epsilon_{abc} + (1 - e^{-2\pi i/M}) s_{abc}$ and $f_{abc} = \delta_{ab}\delta_{bc}$. Hence we have an up-quark Yukawa term containing a complex phase which gives rise to CP violation, and a prediction for the phase of the CKM matrix is presented in detail in section 3.5. Before studying the CKM matrix however, let us discuss the nature of the CP violation.

3.4.7 More on CP violation

As we saw in section 3.3.1, in closed string theories CP is a gauge symmetry which must be broken spontaneously. A similar, but even simpler, picture holds for branes at orbifold fixed points, as we shall now see, and it is the geometric configuration of torsion plus singularity that breaks CP. As an example, consider the 33 sector states $\lambda_{33}^{(k)} \psi_{-1/2}^k |0>$, which give rise to chiral multiplets transforming as $(n^{(i)}, \bar{n}^{(i+a^k)})$. The corresponding antiparticle is given by the conjugate excitation $(\lambda_{33}^{(k)})^\dagger \bar{\psi}_{-1/2}^k |0>$, and the projection

equations are reversed accordingly,

$$(\lambda_{33}^{(k)})^{\dagger}_{sn^{(j)}\times sn^{(i)}} = e^{-2\pi i v_\theta^k}(\gamma_{\theta,3})_{sn^{(j)}\times sn^{(j)}}(\lambda_{33}^{(k)})^{\dagger}_{sn^{(j)}\times sn^{(i)}}(\gamma_{\theta,3})^{\dagger}_{sn^{(i)}\times sn^{(i)}}, \quad (3.72)$$

where $(\gamma_{\theta,3})_{sn^{(l)}\times sn^{(l)}}$ is the usual action of θ on a string endpoint constrained to a stack of sn^l D-branes. This projection gives rise to a chiral mulitplet transforming as $(n^{(i+a^k)}, \bar{n}^{(i)})$, as expected.

Now consider the rotation $x^\mu \to x_\mu$, $z_i \to z_i^*$. Again by supersymmetry we transform $\psi_i \to \overline{\psi_i}$ and need to reverse the chiralities in the Ramond sector. The particle projections now trivially become antiparticle projections. To get the right antiparticles however, we also need to ensure that we have the same projective representation which is the case if the discrete torsion is unchanged (if this were not the case we would simply be unable to identify these particular rotations with CP conjugation). For open string sectors the effect of the torsion in a sector with $\mathbb{Z}_M \times \mathbb{Z}_M$ twists given by ($g \equiv \omega_1^a\omega_2^b$; $h \equiv \omega_1^{a'}\omega_2^{b'}$) can be written as

$$\beta(g,h) = \varepsilon^{ab'-ba'}. \quad (3.73)$$

The effect of the $z_i \to z_i^*$ reflection on the torsion in any sector is simply to reverse the twists, as can be seen from the orbifold action on z_i. Then, $(a,b\,;\,a',b') \to -(a,b\,;\,a',b')$ so $\beta(g,h)$ is indeed unchanged and the rotation gives us the antiparticle. Hence, 4 dimensional CP conjugation does indeed correspond to a rotation in the 10D theory, with or without discrete torsion.

It is precisely because the discrete torsion is invariant under CP conjugation that the superpotential interactions are not. Under the CP transformation we conjugate the chiral superfields but the discrete torsion remains the same. Thus

$$\int d\theta^2\, W + \int d\bar{\theta}^2\, \overline{W} \to \int d\bar{\theta}^2\, \overline{W}_{CP} + \int d\theta^2 W_{CP}, \quad (3.74)$$

where

$$W_{CP} = \epsilon_{abc}Tr(Z^aZ^bZ^c) + (1-e^{2\pi i/M})s_{abc}Tr(Z^aZ^bZ^c). \quad (3.75)$$

This should be compared to (3.70). So it is the discrete torsion term in the superpotential that is directly responsible for breaking 4 dimensional CP

and, because CP conjugation is associated with a 10D Lorentz rotation, it is a spontaneously broken symmetry. We will now divert our attention to the more phenomenological issues.

3.5 Yukawas and the CKM matrix

In this section we first discuss some theoretical considerations for obtaining the canonical Yukawa couplings. In particular, we derive bottom-up properties of the Kähler metric that have not been previously noted. We then proceed to the CKM matrix and predictions for the CKM angles and quark mass ratios. Finally we discuss radiative corrections between the string and weak scales.

3.5.1 Normalisation of Yukawas

To be consistent with $N = 1$ supersymmetry, we assume the low-energy effective field theory decribing our visible sector is an $N = 1$ SUGRA theory. It is well known that in such a theory scalar fields have a non-canonical kinetic energy term given by a Kähler metric, which is the second derivative of the Kähler potential,

$$\frac{\partial^2 K}{\partial \Phi^{\alpha *} \partial \Phi^{\beta}} \partial \phi^{\alpha *} \partial \phi^{\beta}. \tag{3.76}$$

In order to obtain a canonical kinetic energy term, we must normalise our chiral fields. This leads to an effective normalisation of couplings. In particular, if we expand the Kähler potential to first order in the charged matter fields[4], we have

$$\mathrm{K} = \hat{\mathrm{K}}(M^a, M^{a*}) + \tilde{\mathrm{K}}(M^a, M^{a*})_{\alpha\beta} Tr(\Phi^{\alpha *} \Phi^{\beta}) + ..., \tag{3.77}$$

where M^a, M^{a*} are the closed string moduli fields which describe the internal space. Then we obtain,

$$\hat{h}_{abc} = e^{\hat{K}/2} h_{lmn} (\tilde{\mathrm{K}}^{-1/2})^l{}_a (\tilde{\mathrm{K}}^{-1/2})^m{}_b (\tilde{\mathrm{K}}^{-1/2})^n{}_c, \tag{3.78}$$

where $\hat{h}_{abc}$ are the canonically normalised Yukawa couplings. It is important to note that $\tilde{\mathrm{K}}_{\alpha\beta}$ factorises into different components, one for each sector of

[4] i.e. fields charged under our visible sector gauge group.

the spectrum, e.g. in our case the 33 and 37 sector fields have the seperate kähler matter metrics, $(\tilde{\mathrm{K}}_{33})_{\alpha\beta}$ and $(\tilde{\mathrm{K}}_{37})_{\alpha\beta}$.

3.5.2 Bottom-up properties of the Kähler metric

One of the strengths of the bottom-up approach is that, until now, our discussion has been independent of any compactification scheme. In particular, the gauge group, SM spectrum and 3 generations of matter fields are all features independent of the global structure of the model. This affords us two approaches to the determination of the Yukawas,

- Select a particular compactification and calculate the exact kähler potential.
- Choose an ansatz for $\tilde{\mathrm{K}}_{33}$ and $\tilde{\mathrm{K}}_{37}$ (note that the CKM matrix is independent of $\hat{\mathrm{K}}$).

The first approach is technically difficult and only achievable in the simplest of cases, e.g. toroidal orbifolds. In addition, it goes against the bottom-up approach, which is to constrain the model as much as possible from the local rather than global properties. The second approach, at first sight, seems too arbitrary. However, the choice of possible ansätze is restricted by two observations. Firstly, the discrete torsion can constrain the form of $\tilde{\mathrm{K}}_{33}$. Such a situation arises as a consequence of $Tr(\Phi_{33}^{\alpha *}\Phi_{33}^{\beta})$ containing a factor, $Tr((X_{33}^{(\alpha)})^{\dagger}X_{33}^{(\beta)})$ arising from the Chan-Paton factors. This matrix contains 'texture zeros', dependent on the discrete torsion(n), which are inherited by $(\tilde{\mathrm{K}}_{33})_{\alpha\beta}$. It is shown in appendix A, that there exists three possible cases for the restriction of the form of $\tilde{K}_{33}$. These are

- minimal discrete torsion, i.e. $n = 1$, with $\tilde{\mathrm{K}}_{33}$ diagonal,
- $n = 2$, with two off diagonal zeros,
- and $n \geq 3$, with no off diagonal zeros.

Finally, we have the restriction that $\tilde{\mathrm{K}}_{37}$ is diagonal. $(\tilde{\mathrm{K}}_{37})_{ij}$ can be calculated from tree-level modulus-matter scattering [53]. The amplitude is given by a disc diagram with two open string vertex operators on the boundary, a (37_i) and (7_j3) vertex, and two closed string vertex operators attached to

the interior, corresponding to the moduli fields. However vertices of (37_i) and (7_i3) strings must come in pairs in order to get a consistent D-brane boundary on the disc. It follows that in this case i=j and hence $\tilde{K}_{37}$ is diagonal.

This allows us to explore possibilities for interesting flavour structure and CP violation in our Yukawas without worrying about the exact compactification scheme we are using. That is, we choose an ansatz for the Kähler metric based on our choice of discrete torsion, not our choice of compactification.

3.5.3 Explicit expressions for the Yukawa couplings

Defining the hermitian matrices,

$$\begin{aligned} t_{33} &= \tilde{K}_{33}^{-1}, \\ t_{37} &= \tilde{K}_{37}^{-1}, \end{aligned} \tag{3.79}$$

and substituting into (3.78) we obtain, in the general case, canonical up-quark Yukawas,

$$\begin{aligned} \hat{h}^{abc} &= e^{\hat{K}/2} h_{lmn} (t_{33}^{1/2})^{la} (t_{33}^{1/2})^{mb} (t_{33}^{1/2})^{nc} \\ &= e^{\hat{K}/2} (\varepsilon_{lmn} + (1 - e^{-2\pi i/M}) s_{lmn}) (t_{33}^{1/2})^{la} (t_{33}^{1/2})^{mb} (t_{33}^{1/2})^{nc}. \end{aligned} \tag{3.80}$$

Furthermore giving the three generation of Higgs fields vevs, $\langle h_u \rangle_c$, we obtain

$$(Y_u)^{ab} = e^{\hat{K}/2} (\varepsilon_{lmn} + (1 - e^{-2\pi i/M}) s_{lmn}) (t_{33}^{1/2})^{la} (t_{33}^{1/2})^{mb} (t_{33}^{1/2})^{nc} \langle h_u \rangle_c. \tag{3.81}$$

This expression also holds if we associate the actual physical Higgs fields with a linear combination of the $H_{u/d}^a$ fields. That is

$$\hat{H}_{u/d}^i = U_{u/d}^{ij} \tilde{H}_{u/d}^j, \tag{3.82}$$

where $\hat{H}_{u/d}^i$ are the physical Higgs fields and $U_{u/d}$ is a unitary matrix. Then assuming that only $\hat{H}_{u/d}^1$ is light and the other two physical Higgs' are heavy, we simply replace $\langle h_u \rangle_c$ with $(U_u^\dagger)_{c1}$.

Similarly, for the down-quark Yukawas, we obtain

$$(Y_d)^{ab} = e^{\hat{K}/2} \sum_{l=1}^{3} (t_{33}^{1/2})^{la} (t_{37}^{1/2})^{lb} (t_{37}^{1/2})^{lc} \langle h_d \rangle_c. \tag{3.83}$$

Using these formulae we can calculate the CKM matrix and determine the possiblities for CP violation in our model.

3.5.4 A simple ansatz for the CKM matrix

Using the bottom-up properties of our Kähler metric, that is

- the zeros in $\tilde{K}_{33}$ are determined by the discrete torsion,
- $\tilde{K}_{37}$ is diagonal,

we try the following simple ansatz, take M=5, n=2 and

$$t_{33}^{\frac{1}{2}} = \begin{pmatrix} \eta\alpha\varepsilon^2 & 0 & \alpha\varepsilon \\ 0 & 1 & 0 \\ \alpha\varepsilon & 0 & \alpha \end{pmatrix}, \tag{3.84}$$

$$t_{37}^{\frac{1}{2}} = diag[1, \varepsilon, 1], \tag{3.85}$$

$$\begin{aligned} \langle h_u \rangle &= (\varepsilon, 1, 0), \\ \langle h_d \rangle &= (1, \varepsilon, \varepsilon). \end{aligned} \tag{3.86}$$

Notice that our choice of discrete torsion introduces two off diagonal zeros in $\tilde{K}_{33}$ which are preserved in $t_{33}^{\frac{1}{2}}$.

Using this ansatz we can calculate the Yukawas and CKM matrix. The Yukawas have the following form,

$$Y_u = \alpha^2\varepsilon \begin{pmatrix} (1-e^{-2i\pi/5})\eta\varepsilon^2 & (1-e^{-2i\pi/5})\eta\varepsilon^3 & (1-\eta e^{-2i\pi/5})\varepsilon \\ (1-e^{-2i\pi/5})\eta\varepsilon^3 & 0 & (\eta-e^{-2i\pi/5})\varepsilon^2 \\ (\eta-e^{-2i\pi/5})\varepsilon & (1-\eta e^{-2i\pi/5})\varepsilon^2 & (1-e^{-2i\pi/5}) \end{pmatrix}, \tag{3.87}$$

and

$$Y_d = \alpha\varepsilon \begin{pmatrix} \eta\varepsilon & 0 & \varepsilon \\ 0 & \frac{\varepsilon^2}{\alpha} & 0 \\ 1 & 0 & 1 \end{pmatrix}. \tag{3.88}$$

With the freedom to rephase the right handed quark fields (because the model is supersymmetric we can make rephasings just as in the Standard Model), Y_u can be put into hermitian form. Notice that α appears only as an overall factor in Y_u and in a single entry in Y_d, as a consequence the CKM matrix is only dependent on the two parameters ε and η, with α determining the

mass of the down quark. Up to overall factors, which include the prefactors of (3.87) and (3.88), the masses of the quarks are given approximately for small η and ε by,

$$\begin{array}{lll} m_d = \frac{\varepsilon^2}{\alpha}, & m_s = \frac{\varepsilon(1-\eta)}{\sqrt{2}}, & m_b = \sqrt{2} + \frac{1}{4\sqrt{2}}\varepsilon^2 + \frac{1}{20\sqrt{2}}\eta\varepsilon^2, \\ m_u = 1.9\eta\varepsilon^4, & m_c = \sqrt{\frac{2}{3}}\varepsilon^2 - \frac{\sqrt{26}}{3}\eta\varepsilon^2 + \sqrt{\frac{2}{3}}\eta^2\varepsilon^2, & m_t = \frac{2}{\sqrt{3}} + \sqrt{\frac{2}{3}}\varepsilon^2 - \frac{1}{\sqrt{3}}\eta\varepsilon^2. \end{array} \tag{3.89}$$

The CKM matrix can be written approximately in terms of these mass eigenvalues, but it is not very illuminating to show the functional dependence here. Instead, in the next subsection, we depict graphically it's functional dependence on ε and η.

3.5.5 Predictions: CKM angles and Quark mass ratios

In the standard parametrisation, the CKM matrix is given in terms of three mixing angles, $\sin\theta_{12}$, $\sin\theta_{23}$, $\sin\theta_{13}$, and a complex phase δ. Figures 3.4 to 3.7 illustrate the dependence of these CKM angles on ε and η. The blue shaded areas highlight the regions where the CKM angles agree with experiment [54]. Since we are discussing string scale predictions we must also include RGE effects in running from the string to the weak scale. This effect is discussed in the next subsection, where we estimate that $\sin\theta_{23}$ and $\sin\theta_{13}$ are suppressed by approximately 30%. This is depicted in the figures by a red shaded region which higlights values of ε and η that will reproduce experimental values after taking into account RGE effects. This information is summarised in figure 3.8 where the regions in parameter space which produce a realistic CKM matrix are highlighted. In particular, it can be seen that δ is approximately $\pi/3$.

The quark mass ratios are also determined, $\frac{m_d}{m_b}$ can be fixed by choosing a value for α, while the rest of the quark mass ratios are dependent only on ε and η. Average values for the blue and red regions are presented in table 3.2 and compared to experimental values. As can be seen, we have good agreement with experiment except for $\frac{m_u}{m_c}$ which is too large. Note that we have not included RGE effects here, which would tend to increase the value of $\frac{m_c}{m_t}$. As we have chosen such a constrained and simple ansatz, we consider the close agreement of the CKM angles and quark mass ratios with experiment to

be successful. Furthermore, it has not been necessary to introduce any large artificial hierarchies in our ansatz (which would require similar hierarchies in the corresponding moduli fields), to achieve mass eigenvalues and mixing angles close to those of the Standard Model.

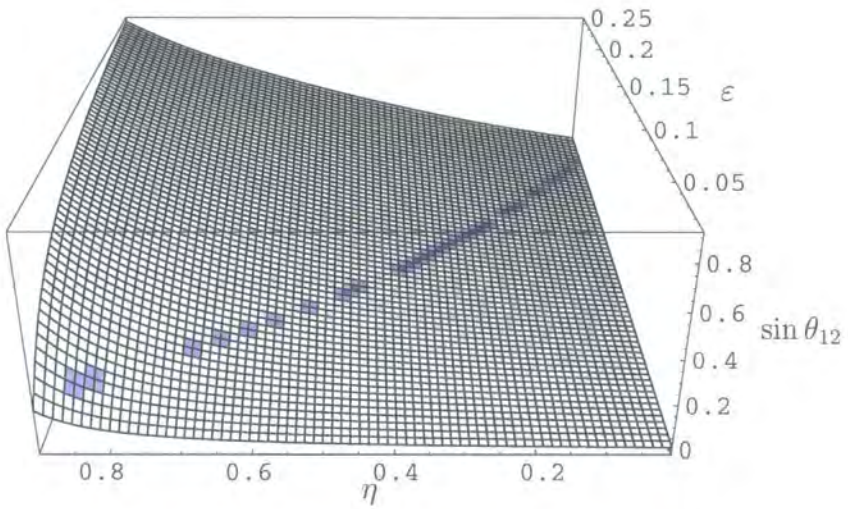

Figure 3.4: $\sin\theta_{12}$ as a function of ε and η.

Mass Ratio	Blue Region	Red Region	Experimental Value
$\frac{m_c}{m_t}$	2.5×10^{-3}	5×10^{-3}	$5.57 - 8.27 \times 10^{-3}$
$\frac{m_s}{m_b}$	0.029	0.041	$0.018 - 0.0387$
$\frac{m_u}{m_c}$	2.4×10^{-2}	2.1×10^{-2}	$1.07 - 4.5 \times 10^{-3}$

Table 3.2: Quark mass ratios

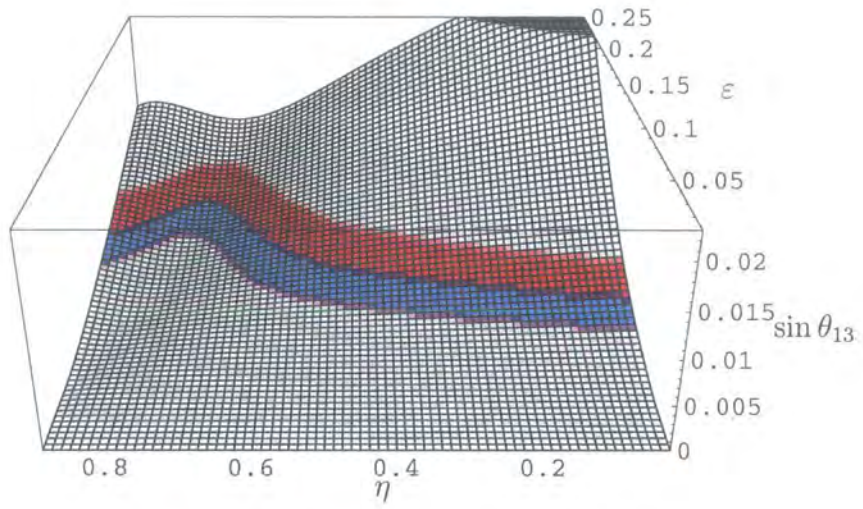

Figure 3.5: $\sin\theta_{13}$ as a function of ε and η.

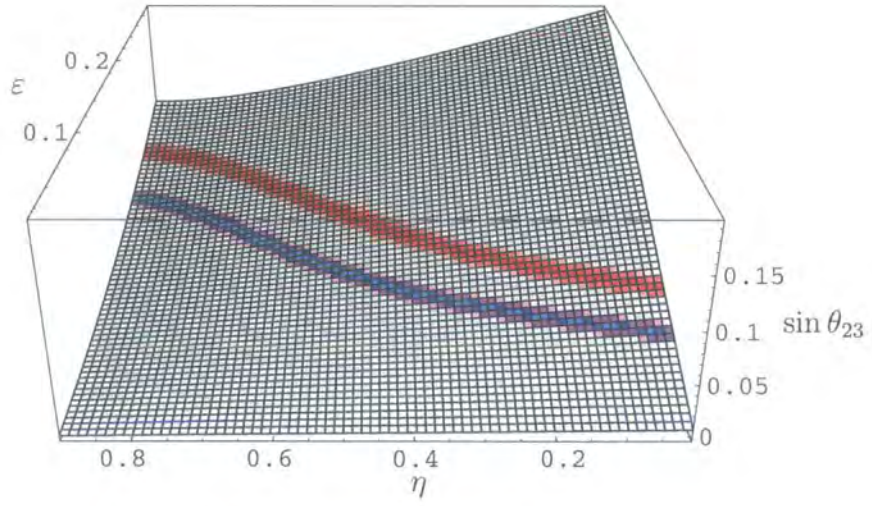

Figure 3.6: $\sin\theta_{23}$ as a function of ε and η.

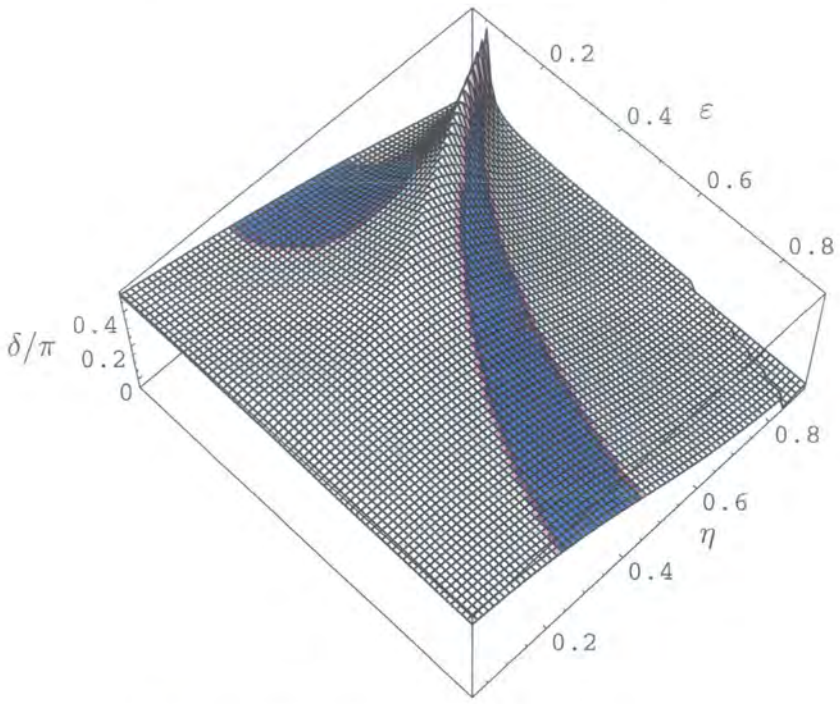

Figure 3.7: δ/π as a function of ε and η.

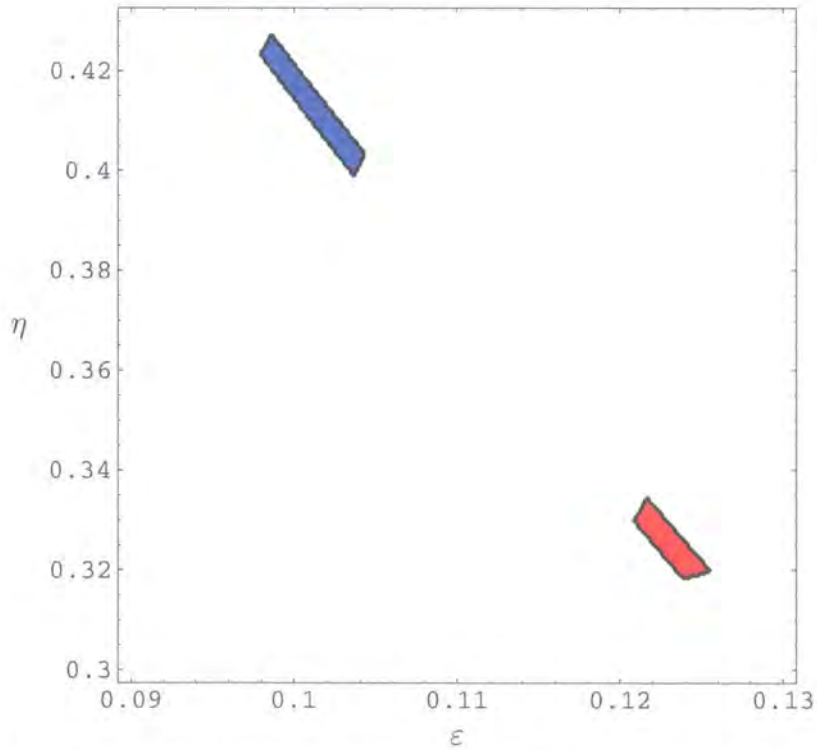

Figure 3.8: The shaded regions highlight the values of ε and η which give an agreement with experimental data. The blue/red region without/with taking into account RGE effects.

RGE effects

The CKM matrix is expected to be effected by renormalization group running. For instance, when we are close to the so-called quasifixed point, the top Yukawa is large at the GUT or string scale and runs to lower fixed point values, and hence RGE effects are important.

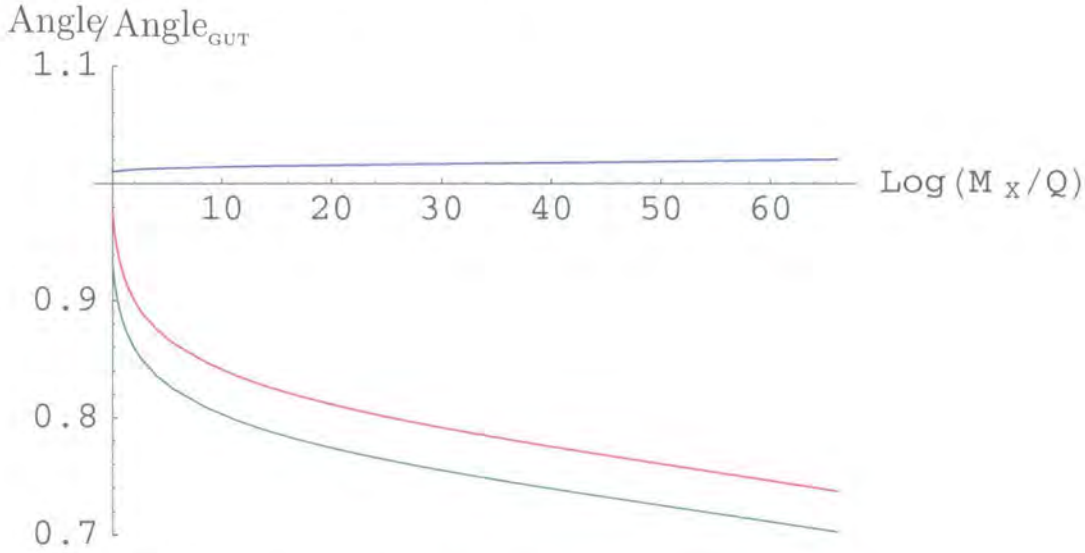

Figure 3.9: CKM running from $M_X \approx 2 \times 10^6$ GeV to M_W for a top Yukawa of $\lambda_t = 5$ at the GUT scale. red $\equiv \frac{\sin\theta_{23}}{(\sin\theta_{23})_{GUT}}$, blue $\equiv \frac{\frac{\sin\theta_{13}}{\sin\theta_{12}}}{\left(\frac{\sin\theta_{13}}{\sin\theta_{12}}\right)_{GUT}}$, green $\equiv \frac{\delta}{\delta_{GUT}}$. $\sin\theta_{12}$ does not run significantly.

However, the effect on the CKM angles is generally small, as can be seen by inspection of the RG equation. Figure 3.9 shows how the numerical values of the CKM parameters change with renormalization scale when the top quark Yukawa is close to the quasifixed point. The CKM angles are suppressed by the running and from the figure we see that the maximum reasonable suppression of the θ_{23} and θ_{13} angles is $\approx 30\%$. The phase δ does not change significantly and is expected to be close to $\frac{\pi}{3}$.

3.6 Summary and discussion

We have examined a bottom-up supersymmetric D-brane model with phenomenologically viable CP violation, broken by discrete torsion. Furthermore, a simple assumption about the form of the Kähler metric, motivated

by a choice of discrete torsion, produces a CKM matrix described by only two free parameters. As a consequence, we predict a single CKM mixing angle and the CKM phase to be close to $\pi/3$, both of which lie within current experimental limits.

Furthermore, this class of models may be a first step towards a solution of the SUSY flavour and CP problems. Generally, these problems arise because supersymmetry breaking "knows" about CP and flavour. Our approach to this problem, is to use the 'bottom-up' approach to build a supersymmetric MSSM, complete with all flavour and CP structure, *before* inputting supersymmetry breaking.

It would be interesting to investigate the dependence of these results on our choice of discrete torsion (i.e. our choice of n), and the resulting ansatz for the Kähler metrics. Finally an analysis of the possibilities for a phenomenologically viable breaking of supersymmetry has been well motivated.

Chapter 4

Interactions in Intersecting Brane Models

We now move our attention to a different class of D-brane configuration, based on D-branes intersecting at arbitrary angles. Such configurations are known as *intersecting brane worlds* [10], and have promising phenomenological features. In this chapter, we calculate tree-level three and four point amplitudes in such models [8,9], which includes the interesting cases of Yukawa interactions and four fermion contact interactions. Note, the Yukawa couplings and a more restricted class of four-point couplings (complete with normalisation factors) was discussed independently and at the same time in [55]. In chapter 5, these calculations will be generalised to N-point amplitudes, thus laying a foundation for discussing scattering amplitudes in intersecting brane models.

4.1 Introduction and Motivation

Since their discovery and subsequent relation to gauge theories, D-branes have become established as a central element in the development of phenomenologically viable string models. They facilitate the construction of models with interesting gauge groups, as seen in the previous chapter. However, the requirement of chirality in any physically realistic model leads to a restricted number of possible D-brane set-ups. One possibility is the bottom-up scenario of D-branes located on orbifold singularities, another important class are the intersecting brane models [10,56]. This scenario exploits the fact

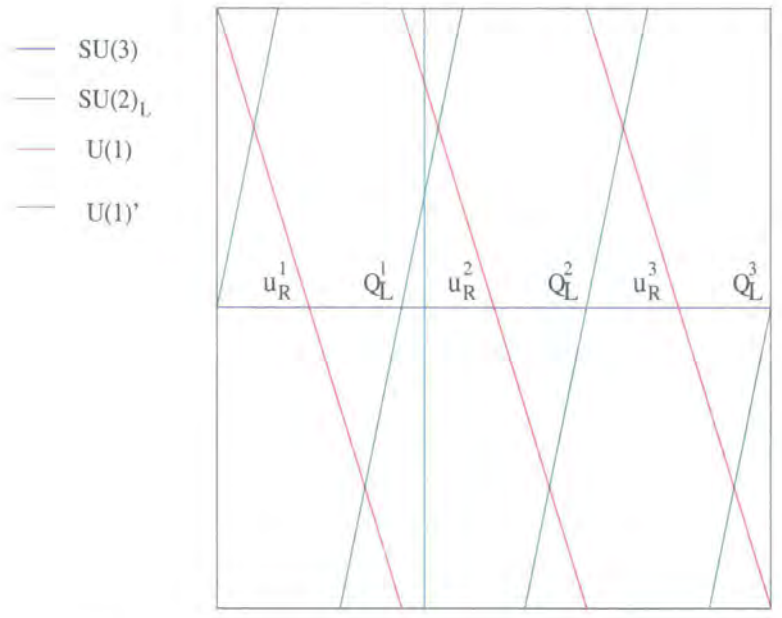

Figure 4.1: A T^2 unit cell, repeatedly intersecting branes give rise to replication of fermions.

that chiral fermions can arise at the intersection of two branes at angles [57].

A typical setup would be $D6$-branes at arbitrary angles, wrapping a compact internal space such as $T^2 \times T^2 \times T^2$, thus intersecting repeatedly. Then our quarks and leptons would be associated with open strings located at D-brane intersections and the Standard Model gauge interactions propagate on the different D6-brane worldvolumes. If all the intersections are in a single T^2 subfactor of the internal space, we have the situation depicted schematically in figure 4.1. The spectrum of fermions is generically replicated according to the intersection numbers of the D-branes which wrap the compact space. As a consequence, a simple and rather attractive topological explanation of family replication is obtained. Other scenarios are also possible, however if we use D4 or D5-branes we require a non-smooth compact space such as an orbifold in order to achieve chirality.

The intersecting brane scenario has been remarkably successful in producing semi-realistic models, for example [56, 58–70]. Models similar to the Standard Model can be obtained [71–77] and furthermore viable constructions with $N = 1$ supersymmetry have been developed [78–85], although this latter possibility is more difficult to achieve. A more detailed analysis of the phenomenology of such models is currently in progress, for example [86–89].

In this chapter we focus our attention on the case of $D6$-branes wrapping $T^2 \times T^2 \times T^2$. However, our methods can easily be adapted to more generic setups. Much of our analysis will be aided by the technology discussed in [11, 12] for closed strings on orbifolds. This is due to an analogy between twisted closed string states on orbifolds and open strings at brane intersections. This analogy is the subject of our first section. Then we proceed to a determination of the classical part of the three point function, for which the computation runs along similar lines to the closed string cases in [90, 91]. The complete calculation of the general tree-level four point function follows, with an analysis of the quantum part using conformal field theory techniques.

4.2 Closed and open string twisted states

An open string stretched between two D-branes intersecting at an angle $\pi\vartheta$, as depicted in figure 4.2, has the boundary conditions

$$\begin{aligned} &\partial_\tau X^2(0) = \partial_\sigma X^1(0) = 0, \\ &\partial_\tau X^1(\pi) + \partial_\tau X^2(\pi)\cot(\pi\vartheta) = 0, \\ &\partial_\sigma X^2(\pi) - \partial_\sigma X^1(\pi)\cot(\pi\vartheta) = 0. \end{aligned} \tag{4.1}$$

We now define $X = X^1 + iX^2$, $\bar{X} = X^1 - iX^2$ and use $z = -e^{\tau - i\sigma}$ as the worldsheet coordinate, which has domain the upper-half complex plane. Then the bosonic action (2.5) can be rewritten as,

$$S_B = \frac{1}{4\pi\alpha'} \int d^2z \left(\partial X \bar{\partial}\bar{X} + \bar{\partial} X \partial \bar{X}\right). \tag{4.2}$$

Varying with respect to X and $\bar{X}$ we obtain the string equation of motion,

$$\bar{\partial}(\partial \bar{X}) = \bar{\partial}(\partial X) = 0, \tag{4.3}$$

hence ∂X and $\partial \bar{X}$ are both holomorphic. Coupled with our boundary conditions we obtain the mode expansions,

$$\begin{aligned} \partial X(z) &= \textstyle\sum_k \alpha_{k-\vartheta} z^{-k+\vartheta-1}, \\ \partial \bar{X}(z) &= \textstyle\sum_k \bar{\alpha}_{k+\vartheta} z^{-k-\vartheta-1}. \end{aligned} \tag{4.4}$$

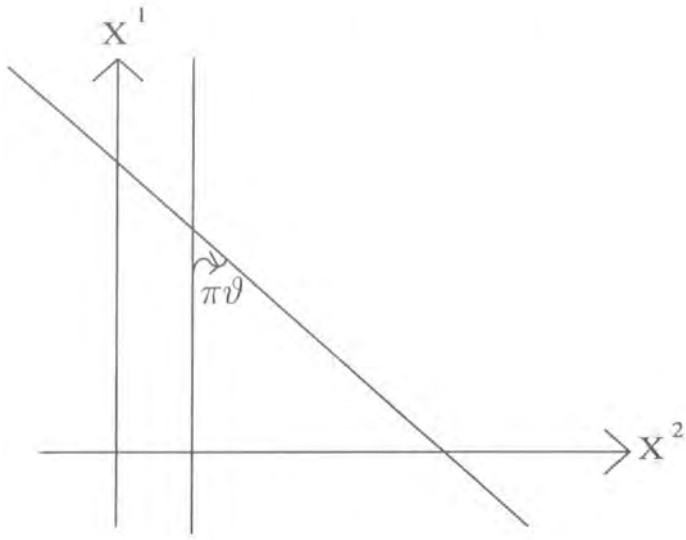

Figure 4.2: A 'twisted' open string state

The domain of these fields can be extended to the entire complex plane using the 'doubling trick', i.e. we define

$$\partial X(z) = \begin{cases} \partial X(z) & \mathrm{Im}(z) \geq 0 \\ \bar{\partial}\bar{X}(\bar{z}) & \mathrm{Im}(z) < 0 \end{cases} , \tag{4.5}$$

and similarly for $\partial\bar{X}(z)$. The mode expansion for X is then,

$$X(z,\bar{z}) = \sqrt{\frac{\alpha'}{2}} \sum_k \left(\frac{\alpha_{k-\vartheta}}{k-\vartheta} z^{-k+\vartheta} + \frac{\bar{\alpha}_{k+\vartheta}}{k+\vartheta} \bar{z}^{-k-\vartheta} \right) . \tag{4.6}$$

A similar mode expansion is obtained for the fermions with the obvious addition of $\frac{1}{2}$ to the boundary conditions for NS sectors.

Now the mode expansion of a twisted closed string state on a $\mathbb{Z}_N$ orbifold is identical to (4.4) with the replacement $\vartheta = \frac{1}{N}$. Hence, there is a natural correspondence between open strings stretched between intersecting branes and twisted closed string states on an orbifold. Therefore, as in the closed string case, we must introduce a twist field $\sigma_\vartheta(w,\bar{w})$ [11]. This field essentially changes the boundary conditions of X to be those of (4.1), where the intersection point of the two D-branes is at $X(w,\bar{w})$.

Define the twisted ground state by $|\sigma_\vartheta >= \sigma_\vartheta(0)|0>$, which is annihilated

by all the positive frequency mode operators,

$$\begin{aligned} \alpha_{k-\vartheta}|\sigma_\vartheta >= 0, \quad k > 0, \\ \bar{\alpha}_{k+\vartheta}|\sigma_\vartheta >= 0, \quad k \geq 0. \end{aligned} \tag{4.7}$$

Then we can easily obtain the OPEs,

$$\begin{aligned} \partial X(z)\sigma_\vartheta(w,\bar{w}) \sim (z-w)^{-(1-\vartheta)}\tau_\vartheta(w,\bar{w}), \\ \partial \bar{X}(z)\sigma_\vartheta(w,\bar{w}) \sim (z-w)^{-\vartheta}\tau'_\vartheta(w,\bar{w}), \end{aligned} \tag{4.8}$$

where τ'_ϑ and τ_ϑ are excited twist fields. The local monodromy conditions for transportation around $\sigma_\vartheta(w,\bar{w})$ are simply determined from the mode expansions to be,

$$\begin{aligned} \partial X(e^{2\pi i}(z-w)) = e^{2\pi i\vartheta}\partial X(z-w), \\ \partial \bar{X}(e^{2\pi i}(z-w)) = e^{-2\pi i\vartheta}\partial \bar{X}(z-w). \end{aligned} \tag{4.9}$$

The correspondence between open strings stretched between branes at angles and twisted closed strings on orbifolds (or conifolds), can also be motivated geometrically as in figure 4.3. This figure shows two identical three point diagrams which are sewn together at their edges. An open string living at the intersection is doubled up to form a twisted closed string. However, we also note that the intersection angles in this case are more general than the rather restrictive ones found in orbifolds of closed strings.

4.3 The general setup

In the proceeding computations we will use the following setup and notation. Firstly, we consider the case of an internal space which is factorizable into single tori, $T^2 \times T^2 \times T^2$, and in which only one 'extra' dimension of each $D6$-brane resides in each T^2. This allows us to factorise our amplitudes into three identical contributions, one from each torus subfactor. This allows us to focus on a single T^2, simplifying the analysis. The string states are localised at N distinct D-brane intersections. These N D-branes form the boundary

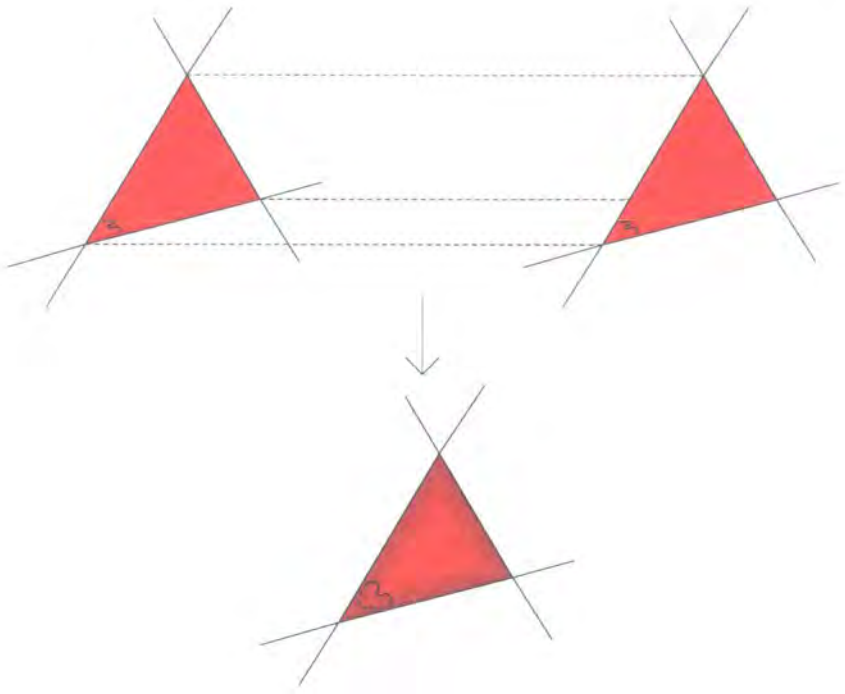

Figure 4.3: Identifying open strings to form closed strings

of an N-sided polygon with vertices f_i and interior angles $\pi\vartheta_i$, such that

$$\sum_{i=1}^{N} \vartheta_i = N - 2. \tag{4.10}$$

The D-brane intersecting f_i and f_{i+1} is labelled the i^{th} D-brane.

The torus is defined by $T^2 = \mathbb{R}^2/\Lambda$, where Λ is a lattice with basis vectors $v_x = R_x(1,0)$ and $v_y = R_y(0,1)$. Also, we denote by (n,m) a non-trivial cycle winding n times around the cycle defined by v_x and m times around the cycle defined by v_y. The i^{th} D-brane then wraps the cycle (n_i, m_i) and the number of intersections with the j^{th} D-brane is given by the intersection number,

$$I_{ij} = n_i m_j - n_j m_i. \tag{4.11}$$

We expect the amplitude to be dominated by an instanton, corresponding to the worldsheet sweeping out the area of the polygon. Then the bosonic field X can be split up into a classical piece, X_{cl}, and a quantum fluctuation, X_{qu}. Similarly for the fermionic fields. The amplitude then factorises into

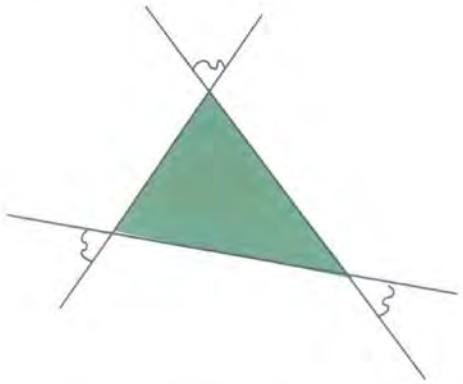

Figure 4.4: The three point interaction

classical and quantum contributions,

$$Z = \sum_{\langle X_{cl} \rangle} e^{-S_{cl}[X_{cl}]} Z_{qu}, \tag{4.12}$$

where

$$S_{cl} = \frac{1}{4\pi\alpha'} \int d^2z \left(\partial X_{cl} \bar{\partial} \bar{X}_{cl} + \bar{\partial} X_{cl} \partial \bar{X}_{cl} \right). \tag{4.13}$$

X_{cl} must satisfy the string equation of motion and possess the correct asymptotic behaviour near the triangle vertices.

Also, the D-branes wrapping cycles gives rise to an infinite number of polygons which wrap the torus and contribute to the N-point function.

4.4 The three point function

We begin with a calculation of the classical contribution to the tree-level three point function, which in particular includes Yukawa interactions. The string states are localised at the vertices of a triangle whose boundary consists of a single internal dimension from each $D6$-brane, as depicted in figure 4.4. One would expect the amplitude to be dominated by an instanton, and to be proportional to $e^{-\frac{1}{2\pi\alpha}A}$ where A is the area of the triangle worldsheet. This expectation is born out in the following calculation.

4.4.1 Classical solutions and global monodromy

The three point function requires three twist vertices, $\sigma_{\vartheta_i}(z_i, \bar{z}_i)$, corresponding to the three relevant intersections of the D-branes. These vertices are attached to the boundary of the tree-level disc diagram which can be conformally mapped to the upper-half complex plane. Then our classical solution ∂X_{cl} is determined, up to a constant, by its holomorphicity (since it solves the string equation of motion) and asymptotic behaviour at each D-brane intersection, which is given by the OPEs in eq.(4.8). Hence we obtain,

$$\begin{aligned} \partial X_{cl}(z) &= a\omega(z), \quad \partial \bar{X}_{cl}(z) = \bar{a}\omega'(z), \\ \bar{\partial} X_{cl}(\bar{z}) &= b\bar{\omega}'(\bar{z}), \quad \bar{\partial} \bar{X}_{cl}(\bar{z}) = \bar{b}\bar{\omega}(\bar{z}), \end{aligned} \tag{4.14}$$

where,

$$\omega(z) = \prod_{i=1}^{3}(z - z_i)^{-(1-\vartheta_i)} \quad \omega'(z) = \prod_{i=1}^{3}(z - z_i)^{-\vartheta_i}, \tag{4.15}$$

and $a, \bar{a}, b, \bar{b}$ are normalisation constants. Using the doubling trick to define ∂X_{cl} on the entire complex plane, we require $a^* = \bar{b}$ and $\bar{a} = b^*$ (upto a phase). We can therefore write (4.13) as,

$$S_{cl} = \frac{1}{4\pi\alpha}\left(|a|^2 \int d^2z|\omega(z)|^2 + |b|^2 \int d^2z|\omega'(z)|^2\right). \tag{4.16}$$

The contribution to S_{cl} from $|\omega'(z)|$ diverges, hence we set $b = 0$.

The normalisation constants are determined from the global monodromy conditions, i.e. the transformation of X as it is transported around more than one twist operator such that the net twist is zero. We determine this from the action of a single twist operator, $\sigma_\vartheta(w, \bar{w})$. Ignoring the toroidal geometry for the moment, this action is given by

$$X(e^{2\pi i}z, e^{-2\pi i}\bar{z}) = e^{2\pi i\vartheta}X + (1 - e^{2\pi i\vartheta})f, \tag{4.17}$$

where f is the intersection point of the two D-branes. This can be seen from the local monodromy conditions (4.9) and the fact that f must be left invariant. Note, if we split X up into a classical and quantum part, then the classical field should have exactly the same behaviour as the full field.

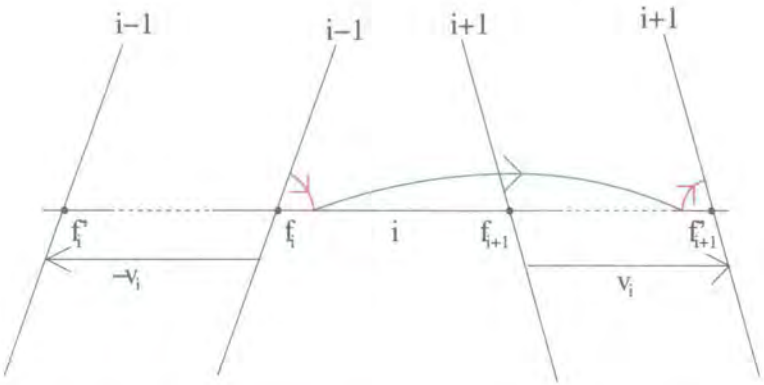

Figure 4.5: Transporting $X(z,\bar{z})$ around two twist fields

Hence, the boundary conditions for X_{qu} ignores the shift $(1-e^{2\pi i\vartheta})f$ leaving,

$$X_{qu}(e^{2\pi i}z, e^{-2\pi i}\bar{z}) = e^{2\pi i\vartheta}X_{qu}. \tag{4.18}$$

On introduction of toroidal geometry, the action of our twist operators must be generalised to not only rotate X_{cl} but also to shift by a lattice translation. Hence (4.17) is modified to

$$X(e^{2\pi i}z, e^{-2\pi i}\bar{z}) = e^{2\pi i\vartheta}X + (1-e^{2\pi i\vartheta})(f+v), \tag{4.19}$$

where $v \in \Lambda^*$, a coset of Λ. It follows that on integrating around two twist fields, the portion of integration around each vertex takes $X_{cl}(z,\bar{z})$ from one D-brane to another, while integrating between the two vertices introduces a shift along the i^{th} D-brane. Define $\vec{L}_{i,i+1}$ to lie in the direction $f_{i+1}-f_i$, with magnitude the distance along the i^{th} D-brane between successive copies of the $(i+1)^{th}$ D-brane. Then the shift must be of the form $f_{i+1}-f_i+v_i$ where,

$$v_i = q_i|I_{i,i+1}|\vec{L}_{i,i+1} \in \Lambda^*, \quad q_i \in \mathbb{Z}, \tag{4.20}$$

as illustrated in figure 4.5. Such lattice shifts give rise to polygons wrapping the torus, and hence to further contributions to the three-point function.

In the three point case we are considering, there is only one independent, net twist zero, closed curve. This is the Pochammer loop, shown in figure 4.6. We have set $z_1 = 0, z_2 = 1$ and $z_3 = x_\infty \to \infty$ using $SL(2,\mathbb{R})$ invariance and the dashed lines denote branch cuts. The global monodromy condition

is therefore,

$$\Delta_C X = \oint_C dz\partial X(z) + \oint_C d\bar{z}\bar{\partial} X(\bar{z}). \tag{4.21}$$

Evaluating the contour integral first, we obtain

$$\oint_C dz\omega(z) = -(-x_\infty)^{-(1-\vartheta_3)} 4\sin\pi\vartheta_2 \sin\pi\vartheta_1 e^{-\pi i\vartheta_1} \frac{\Gamma(\vartheta_1)\Gamma(\vartheta_2)}{\Gamma(1-\vartheta_3)}. \tag{4.22}$$

The left hand side of (4.21) is obtained by repeated action of (4.19),

$$\Delta_C X_{cl} = 4\sin\pi\vartheta_1 \sin\pi\vartheta_2 e^{-i\pi(\vartheta_1-\vartheta_2)}(f_2 - f_1 + v_1). \tag{4.23}$$

Substituting (4.22) and (4.23) into (4.21) we then determine,

$$|a|^2 = |-x_\infty|^{2(1-\vartheta_3)} |f_2 - f_1 + v_1|^2 \left(\frac{\Gamma(1-\vartheta_3)}{\Gamma(\vartheta_1)\Gamma(\vartheta_2)}\right)^2. \tag{4.24}$$

We also require the integral,

$$\int d^2z|\omega(z)|^2 = |-x_\infty|^{-2(1-\vartheta_3)} \sin\pi\vartheta_2 (\Gamma(\vartheta_2))^2 \frac{\Gamma(\vartheta_3)\Gamma(\vartheta_1)}{\Gamma(1-\vartheta_3)\Gamma(1-\vartheta_1)}, \tag{4.25}$$

which can be performed using the method of [92] to relate open and closed string amplitudes. The idea is to split the integral up into a product of holomorphic and anti-holomorphic contour integrals. This is described in more detail in appendix B.1. Finally, substituting (4.25) and (4.24) into (4.16) we obtain,

$$S_{cl} = \frac{1}{2\pi\alpha'}\left(\frac{\sin\pi\vartheta_1 \sin\pi\vartheta_2}{2\sin\pi\vartheta_3}|f_2 - f_1 + v_1|^2\right). \tag{4.26}$$

This is, as expected, the area of the triangle (or a triangle wrapped around the torus) defined by the intersecting D-branes that is swept out by the string worldsheet.

4.4.2 Wrapping contributions

To determine the shifts, we must consider triangles that wrap the torus and whose vertices are at the same intersection points. (Other shifts would contribute to other three point functions.). Without loss of generality, we keep f_2 fixed and extend the triangle as shown in figure 4.7. Then to obtain

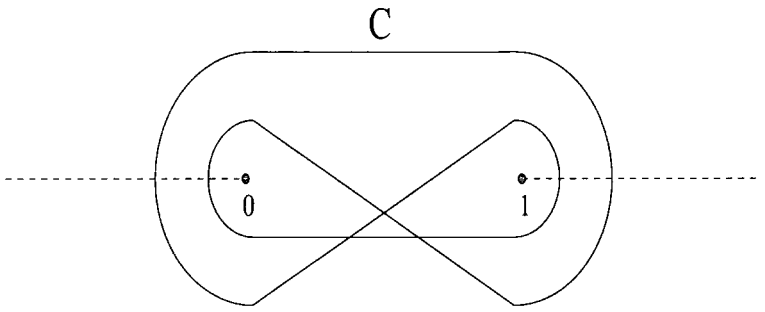

Figure 4.6: Closed curve with net twist zero required for global monodromy condition.

a contribution to our three point function, we must have

$$\sum_{i=1}^{3} v_i = 0. \tag{4.27}$$

Substituting (4.20) and the expression,

$$|I_{i,i+1}|\vec{L}_{i,i+1} = -(n_i v_x + m_i v_y), \tag{4.28}$$

into (4.27), we obtain the simple relations,

$$q_1 I_{21} = q_3 I_{32}, \quad q_2 I_{21} = q_3 I_{13}. \tag{4.29}$$

The q_1 and q_2 which allow for integer solutions are of the form,

$$q_1 = \frac{l|I_{32}|}{gcd(|I_{21}|,|I_{32}|,|I_{13}|)}, \quad q_2 = \frac{l|I_{13}|}{gcd(|I_{21}|,|I_{32}|,|I_{13}|)}, \tag{4.30}$$

where $l \in \mathbb{Z}$. This is similar to the case discussed in [93].

Finally, we can express the classical contribution to the three point amplitude as,

$$\mathcal{Z}_{cl} = \sum_l exp[-\frac{1}{2\pi\alpha'}\left(\frac{\sin\pi\vartheta_1 \sin\pi\vartheta_2}{2\sin\pi\vartheta_3}|f_2 - f_1 + v_1(l)|^2\right)]. \tag{4.31}$$

We will not explicitly determine the quantum part of the three point amplitude, as it may be obtained from the quantum part of the four point amplitude by a limiting process [55]. The complete four point amplitude is the subject of the next section.

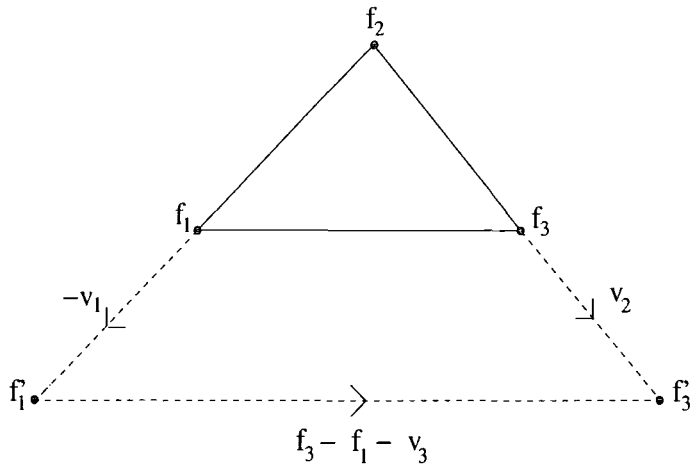

Figure 4.7: Determining the wrapped triangles

In the phenomenologically interesting case of Yukawa couplings, the quantum part is independent of the generation number and thus the behaviour of the Yukawa couplings is dominated by (4.31). Notice that this exponential dependence on worldsheet area leads to a natural mechanism for generation of hierarchies between quark masses, as observed in nature. This was first pointed out in [10].

4.5 The general four point function

We now proceed to a discussion of the four point function, with open string states located at the vertices of a four sided polygon, as depicted in figure 4.8. Firstly, we discuss the classical contribution and then proceed to an analysis of the quantum part using conformal field theory techniques.

4.5.1 The classical contribution to the four-point function

Our analysis will proceed in a similar manner to the three point case. The 4-point function requires 4 twist operators, $\sigma_{\vartheta_i}(z_i, \bar{z}_i)$, one for each polygon vertex or D-brane intersection. These twist operators are attached to the boundary of the tree-level disc diagram. Again, this can be conformally mapped to the upper-half complex plane and using $SL(2,\mathbb{R})$ invariance we set $z_1 = 0$, $z_2 = x_2$, $z_3 = 1$ and $z_4 = x_\infty$. The classical solution, ∂X_{cl}, is

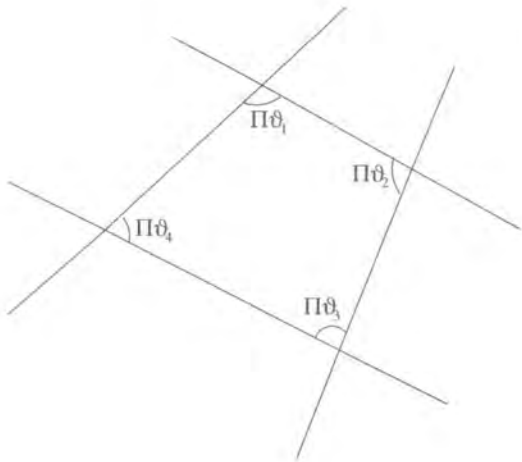

Figure 4.8: Generic 4 point diagram

again given by

$$\begin{aligned} \partial X_{cl}(z) &= a\omega(z), \quad \partial \bar{X}_{cl}(z) = \bar{a}\omega'(z), \\ \bar{\partial} X_{cl}(\bar{z}) &= b\bar{\omega}'(\bar{z}), \quad \bar{\partial} \bar{X}_{cl}(\bar{z}) = \bar{b}\bar{\omega}(\bar{z}), \end{aligned} \tag{4.32}$$

where this time we have,

$$\omega(z) = \prod_{i=1}^{4}(z - x_i)^{-(1-\vartheta_i)}, \quad \omega'(z) = \prod_{i=1}^{4}(z - x_i)^{-\vartheta_i}. \tag{4.33}$$

The extra factor coming from the fact we are now dealing with the four-point function. The classical action is still of the form (4.16), however the $|w'(z)|^2$ contribution no longer diverges. This is due to the fact that the integral, in polar coordinates, goes as

$$\int_0^\infty r^{-3} dr, \tag{4.34}$$

for large r. Hence, we can no longer set $b = 0$.

The normalisation of the classical solutions are again determined from the global monodromy conditions. However, we must now determine both a and b from the global monodromy conditions. To match this requirement, we now have two independent Pochammer loops to which we can apply our global monodromy condition (4.21). This arises as there are four twist vertices which we have set to the positions $0, x_2, 1$ and $x_\infty \to \infty$. Hence, we have a Pochammer contour, C_1, looping around 0 and x and another, C_2, looping around x and 1. Therefore, we have two conditions allowing us to determine

our two normalisation constants. These two independent global monodromy conditions are,

$$\begin{aligned}\Delta_{C_i} X_{cl} &= e^{-\pi i(\vartheta_i-\vartheta_{i+1})} 4\sin(\pi\vartheta_i)\sin(\pi\vartheta_{i+1})(f_{i+1}-f_i+v_i) \\ &= \oint_{C_i} dz\partial X_{cl}(z) + \oint_{C_i} d\bar{z}\bar{\partial} X_{cl}(\bar{z}).\end{aligned} \tag{4.35}$$

The contour integrals required can be written as,

$$\begin{aligned}\oint_{C_i} dz\omega(z) &= e^{-\pi i(\vartheta_i-\vartheta_{i+1})} 4\sin(\pi\vartheta_i)\sin(\pi\vartheta_{i+1})F_i, \\ \oint_{C_i} d\bar{z}\bar{\omega}'(\bar{z}) &= e^{-\pi i(\vartheta_i-\vartheta_{i+1})} 4\sin(\pi\vartheta_i)\sin(\pi\vartheta_{i+1})\bar{F}_i',\end{aligned} \tag{4.36}$$

where,

$$F_i = \int_{x_i}^{x_{i+1}} \prod_{j=1}^{4}(y-x_j)^{-(1-\vartheta_j)}dy \quad F_i' = \int_{x_i}^{x_{i+1}} \prod_{j=1}^{4}(y-x_j)^{-\vartheta_j}dy. \tag{4.37}$$

Hence (4.35) can be simplified to,

$$aF_i + b\bar{F}_i' = f_{i+1} - f_i + v_i \quad i = 1,2. \tag{4.38}$$

Using these conditions we can determine both a and b. Construct the classical solutions $\partial X_{cl,1}$ and $\partial X_{cl,2}$, with coefficients α_i, β_i as in (4.32) and which have the simple global monodromy,

$$\alpha_i F_j + \beta_i \bar{F}_j' = \delta_{ij}, \quad i,j = 1,2. \tag{4.39}$$

Then,

$$\begin{aligned}\alpha_1 &= \frac{\bar{F}_2'}{F_1\bar{F}_2' - F_2\bar{F}_1'}, \qquad \alpha_2 = -\frac{\bar{F}_1'}{F_1\bar{F}_2' - F_2\bar{F}_1'}, \\ \beta_1 &= -\frac{F_2}{F_1\bar{F}_2' - F_2\bar{F}_1'}, \quad \beta_2 = \frac{F_1}{F_1\bar{F}_2' - F_2\bar{F}_1'}.\end{aligned} \tag{4.40}$$

It follows, that to satisfy (4.38) for $i = 1,2$, we require,

$$\begin{aligned}a &= (f_2 - f_1 + v_1)\alpha_1 + (f_3 - f_2 + v_2)\alpha_2, \\ b &= (f_2 - f_1 + v_1)\beta_1 + (f_3 - f_2 + v_2)\beta_2.\end{aligned} \tag{4.41}$$

Using (4.16) the classical contribution to the 4-point function is given by,

$$S_{cl}(x_2) = \frac{1}{4\pi\alpha'}\left(|a|^2 I(x_2) + |b|^2 I'(x_2)\right), \tag{4.42}$$

where,

$$I(x_2) = \int d^2z|\omega(z)|^2 \quad I'(x_2) = \int d^2z|\omega'(z)|^2. \tag{4.43}$$

4.5.2 An explicit expression for the classical contribution

We now evaluate (4.42) more explicitly, relating it to the area of the four-sided polygon. Since S_{cl} is independent of x_∞, we can drop these factors arising in I, I' and F_i, F_i'. As before, we can split I into a product of holomorphic and anti-holomorphic contours obtaining,

$$I(x_2) = 2\sin(\pi\vartheta_2)|F_2||F_1| - \sin(\pi(\vartheta_2+\vartheta_3))|F_3||F_1| - \sin(\pi(\vartheta_1+\vartheta_2))|F_2||F_0|, \tag{4.44}$$

where,

$$F_3 = \int_1^\infty \prod_{j=1}^3 (y-x_j)^{-(1-\vartheta_j)}dy, \quad F_0 = \int_{-\infty}^0 \prod_{j=1}^3 (y-x_j)^{-(1-\vartheta_j)}dy. \tag{4.45}$$

We can write our F_i in terms of hypergeometric functions and thus obtain the relations,

$$\begin{aligned} |F_0| &= \tfrac{\sin(\pi\vartheta_2)}{\sin(\pi\vartheta_1)(1-\alpha\beta)}\left(|F_2| + \beta|F_1|\right), \\ |F_3| &= \tfrac{\sin(\pi\vartheta_2)}{\sin(\pi\vartheta_3)(1-\alpha\beta)}\left(|F_1| + \alpha|F_2|\right), \end{aligned} \tag{4.46}$$

where,

$$\alpha = -\tfrac{\sin(\pi(\vartheta_1+\vartheta_2))}{\sin(\pi\vartheta_1)}, \quad \beta = -\tfrac{\sin(\pi(\vartheta_2+\vartheta_3))}{\sin(\pi\vartheta_3)}. \tag{4.47}$$

This is explained in more detail in appendix B.2. Substituting into (4.44) we obtain,

$$I(x_2) = \frac{\sin(\pi\vartheta_2)}{1-\alpha\beta}(\beta|F_1|^2 + 2|F_1||F_2| + \alpha|F_2|^2). \tag{4.48}$$

Note that I' and F_i' are obtained from I and F_i by the substitution $\vartheta_i \to 1-\vartheta_i$. This allows us to also express the F_i' in terms of hypergeometric functions. Using the identities in B.2 we can then easily deduce that,

$$\begin{aligned} |F_1'| &= (1-x_2)^{1-\vartheta_2-\vartheta_3}x_2^{1-\vartheta_1-\vartheta_2}\gamma(|F_1| + \alpha|F_2|), \\ |F_2'| &= (1-x_2)^{1-\vartheta_2-\vartheta_3}x_2^{1-\vartheta_1-\vartheta_2}\gamma(|F_2| + \beta|F_1|), \end{aligned} \tag{4.49}$$

where,

$$\gamma = \frac{\Gamma(1-\vartheta_2)\Gamma(1-\vartheta_4)}{\Gamma(\vartheta_1)\Gamma(\vartheta_3)}. \tag{4.50}$$

Also, we define γ' by setting $\vartheta_i \to 1 - \vartheta_i$ in (4.50), then

$$\gamma\gamma' = \frac{1}{1-\alpha\beta} = \frac{\sin(\pi\vartheta_1)\sin(\pi\vartheta_3)}{\sin(\pi\vartheta_2)\sin(\pi\vartheta_4)}. \tag{4.51}$$

$I'(x_2)$ can now be obtained in terms of $|F_1|$ and $|F_2|$ simply by letting $\vartheta_i \to 1 - \vartheta_i$ in (4.48) and substituting in (4.49), we obtain

$$I'(x_2) = \gamma^2 \sin(\pi\vartheta_2)(1-x_2)^{2(1-\vartheta_2-\vartheta_3)} x_2^{2(1-\vartheta_1-\vartheta_2)} \left(\beta|F_1|^2 + 2|F_1||F_2| + \alpha|F_2|^2\right). \tag{4.52}$$

Finally, we require the expressions,

$$|a| = \left(\frac{v_{21}|F_2'| + v_{32}|F_1'|}{|F_1||F_2'| + |F_2||F_1'|}\right), \quad |b| = \left(\frac{v_{32}|F_1| - v_{21}|F_2|}{|F_1||F_2'| + |F_2||F_1'|}\right), \tag{4.53}$$

where $v_{21} = |f_2 - f_1 + v_1|$ and $v_{32} = |f_3 - f_2 + v_2|$. This allows us to obtain the following contribution to the classical action from a single T_2,

$$S_{cl}^{T_2}(\tau, v_{21}, v_{32}) = \frac{\sin(\pi\vartheta_2)}{4\pi\alpha'}\left(\frac{((v_{21}\tau - v_{32})^2 + \gamma\gamma'(v_{21}(\beta+\tau) + v_{32}(1+\alpha\tau))^2)}{(\beta + 2\tau + \alpha\tau^2)}\right), \tag{4.54}$$

where $\tau(x_2) = \left|\frac{F_2}{F_1}\right|$.

The complete expression for the action is just a sum of these contributions, one from each torus subfactor, i.e.

$$S_{cl} = \sum_{i=1}^{3} S_{cl}^{T^i}(\tau^i, v_{21}^i, v_{32}^i). \tag{4.55}$$

Now, if there is only non-zero worldsheet area in one subtorus, or if the angles (and hence τ^i) and ratios of lengths are the same in every subtorus (i.e. the polygons are identical up to a scaling), we may use a saddle point approximation to minimise the complete S_{cl}. The minimum of $S_{cl}^{T_2}$ is given by,

$$\tau_{min} = \frac{v_{32}}{v_{21}}, \tag{4.56}$$

and after some manipulation we find,

$$S_{cl}^{T_2}(\tau_{min}) = \frac{1}{2\pi\alpha'}\left(\frac{\sin\pi\vartheta_1 \sin\pi\vartheta_4}{\sin(\pi\vartheta_1 + \pi\vartheta_4)}\frac{v_{14}^2}{2} + \frac{\sin\pi\vartheta_2 \sin\pi\vartheta_3}{\sin(\pi\vartheta_2 + \pi\vartheta_3)}\frac{v_{23}^2}{2}\right). \tag{4.57}$$

We recognize this as the area/$2\pi\alpha'$ of the four-sided polygon. Note also that

at this minimum $b = 0$. Hence, in this case we see that S_{cl} is minimised to the sum of the areas of the quadrilaterals from each T^2 subfactor.

4.5.3 Wrapping contributions

To completely determine the classical contribution to the four-point amplitude, we must also include contributions from quadrilaterals which wrap the tori. As before, extending from f_2 we must have,

$$\sum_{i=1}^{4} v_i = 0. \tag{4.58}$$

Using (4.20) and (4.28), we then see that our wrapped polygons are given by integer solutions q_1, q_2 to the following system of diophantine equations,

$$\begin{pmatrix} q_1 I_{21} \\ q_2 I_{21} \end{pmatrix} = \begin{pmatrix} I_{32} & I_{42} \\ I_{13} & I_{14} \end{pmatrix} \begin{pmatrix} q_3 \\ q_4 \end{pmatrix}. \tag{4.59}$$

For any fixed q_3 and q_4 this solution is unique, since the determinant of the above matrix is non-zero. For the general case it is not possible to solve this for our wrapped polygons. This is due to the fact that a solution to a general system of diophantine equations can only be generated algorithmically. However, we see that the classical part of any wrapped polygon contribution to our four-point amplitude is essentially $e^{-\frac{1}{2\pi\alpha'}A}$, where A is the area of the wrapped polygon in the relevant T^2 torus. Hence, the leading contribution to the four-point function comes from the smallest polygon. This is the single unwrapped polygon from the planar case corresponding to the trivial solution to (4.59), i.e. all $q_i = 0$.

We can determine the wrapped polygons in more symmetrical situations where at least one pair of D-branes are parallel. In this situation however, our diophantine equation (4.59) no longer applies. If the i^{th} D-brane has D-branes which run parallel to it, we must modify our shift vector in (4.20) to $v_i = q_i gcd(\{|I_{k,i+1}||k \in P(i)\})\vec{L}_{i,i+1}$, where $P(i)$ is the set of all D-branes parallel to the i^{th} D-brane and gcd stands for the greatest common divisor. Therefore, the necessary modifications to our diophantine equation can be

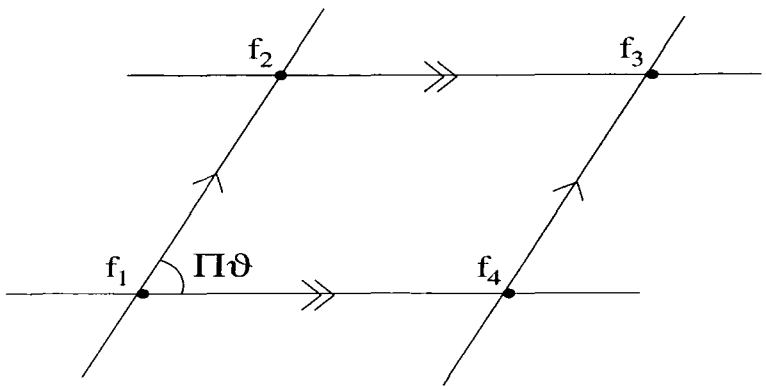

Figure 4.9: Two sets of parallel D-branes.

easily determined by substituting the generalised expression,

$$v_i = q_i gcd(\{|I_{k,i+1}||k \in P(i)\})\vec{L}_{i,i+1}, \tag{4.60}$$

into (4.58). To illustrate this we consider the following two cases.

One independent angle

Firstly, we consider the simple case of one independent angle as depicted in figure 4.9. Here we have two sets of parallel branes, the 1^{st} and 3^{rd}, and the 2^{nd} and 4^{th}. As usual, closure of the polygon results in the expression,

$$\sum_{i=1}^{4} v_i = 0. \tag{4.61}$$

Our shift vectors are now given by,

$$v_i = q_i gcd(|I_{i,i+1}|, |I_{i+2,i+1}|)\vec{L}_{i,i+1}, \tag{4.62}$$

for $i = 1, .., 4$. If we define $\vec{L}_{i,i-1}$ to lie in the direction $f_i - f_{i+1}$, with magnitude the distance along the i^{th} brane between successive $(i-1)^{th}$ branes, we obtain the the relation,

$$-|I_{i,i-1}|\vec{L}_{i,i-1} = |I_{i,i+1}|\vec{L}_{i,i+1} = -(n_i v_x + m_i v_y). \tag{4.63}$$

Substituting (4.62) and (4.63) into (4.61), we obtain the intuitively obvious result $q_1 = q_3$ and $q_2 = q_4$. Therefore q_1 and q_2 can take any integer values.

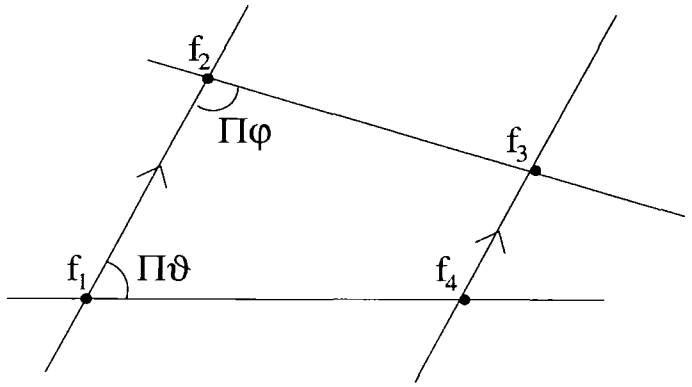

Figure 4.10: One set of parallel D-branes.

Two independent angles

Next consider the case of two independent angles as shown in figure 4.10. This time we have the 1^{st} and 3^{rd} branes parallel. Hence v_1 and v_3 are still given by (4.62), however now v_2 and v_3 are given by the 'non-parallel' expression (4.20). Again, substituting into (4.61) and simplifying using (4.63) we obtain,

$$q_1 A - q_3 A = q_4 I_{42}, \quad q_2 I_{12} = q_4 I_{41}, \tag{4.64}$$

where we have defined $gcd(|I_{12}|, |I_{23}|) = a_1|I_{12}| + b_1|I_{23}|$ and $A = a_1 I_{21} + b_1 I_{32}$. The second expression requires,

$$q_2 = \frac{lI_{41}}{gcd(I_{12}, I_{41})}, \quad q_4 = \frac{lI_{12}}{gcd(I_{12}, I_{41})}, \tag{4.65}$$

where $l \in \mathbb{Z}$. Defining,

$$c(l) := \frac{lI_{12}I_{42}}{gcd(I_{12}, I_{41})}, \tag{4.66}$$

we obtain an infinite set of diophantine equations,

$$(q_1 - q_3)A = c(l), \tag{4.67}$$

labelled by l. For a fixed l, a solution to (4.67) exits if and only if A divides $c(l)$. In which case, we have an infinite number of solutions given by,

$$q_1 = \frac{klI_{12}I_{42}}{Agcd(I_{12}, I_{41})}, \quad q_3 = \frac{(-1+k)lI_{12}I_{42}}{Agcd(I_{12}, I_{41})}, \tag{4.68}$$

where $k \in \mathbb{Z}$. Hence, our wrapped polygons are determined by extending from f_2 using,

$$q_1 = \frac{klI_{12}I_{42}}{Agcd(I_{12},I_{41})}, \quad q_2 = \frac{lI_{41}}{gcd(I_{12},I_{41})}, \tag{4.69}$$

and summing over $l, k \in \mathbb{Z}$ such that $q_1 \in \mathbb{Z}$.

4.5.4 The quantum contribution to the four-point function

Let us turn to the quantum contribution to the four point amplitude. As in the previous section, this amplitude is given by a disc diagram with four fermionic vertex operators in the $-1/2$ picture, $V^{(a)}$ on the boundary. The diagram is mapped to the upper half plane with vertices on the real axis. The positions of the vertices $(x_1 \dots x_4)$ will eventually be fixed by $SL(2,R)$ invariance to $0, x_2, 1, \infty$ (where x_2 is real), so that the 4 point ordered amplitude can be written

$$\begin{aligned} S_4(1,2,3,4) &= (2\pi)^4\delta^4(\textstyle\sum_a k_a)\, A(1,2,3,4) \\ &= \frac{-i}{g_o^2 l_s^4}\int_0^1 dx \langle V^{(1)}(0,k_1)V^{(2)}(x_2,k_2)V^{(3)}(1,k_3)V^{(4)}(\infty,k_4)\rangle. \end{aligned} \tag{4.70}$$

To get the total amplitude we sum over all possible orderings;

$$\begin{aligned} A_{total}(1,2,3,4) &= A(1,2,3,4) + A(1,3,2,4) + A(1,2,4,3) \\ &+ A(4,3,2,1) + A(4,2,3,1) + A(4,3,1,2). \end{aligned} \tag{4.71}$$

The vertex operators for the fermions are of the form

$$V_i^{(a)}(x_a,k_a) = const\, g_o l_s^{3/2} \lambda^a u_\alpha^{(i)} S_i^\alpha \sigma_{\vartheta_i} e^{-\phi/2} e^{ik_a.X}(x_a). \tag{4.72}$$

Here u_α is the space time spinor polarization, and S^α is the so called spin-twist operator discussed in subsection 2.2.5. This has the form

$$S_i^\alpha = \prod_{l=1}^{5} :\exp(iq_i^l H_l):, \tag{4.73}$$

where for D6 branes intersecting at angles we have in the Ramond sector,

$$q_i^l = \left(\pm\frac{1}{2}, \pm\frac{1}{2}, \vartheta_i^1 - \frac{1}{2}, \vartheta_i^2 - \frac{1}{2}, \vartheta_i^3 - \frac{1}{2}\right). \tag{4.74}$$

The relative sign of the first two entries is determined by the helicity, and $\vartheta_i^{m=1,2,3}$ are the angles of the i^{th} intersection in the m^{th} complex plane. This can be determined from the mode expansion of the fermionic fields, which is similar to (4.6). In what follows we will frequently drop the index m, when we consider what is happening in a single sub-torus. The spin fields have conformal dimension,

$$h_i = \frac{q_i^2}{2}. \tag{4.75}$$

Here σ_{ϑ_i} is the ϑ twist operator for the i^{th} vertex, with conformal dimension

$$h_i = \frac{1}{2}\vartheta_i.(1-\vartheta_i). \tag{4.76}$$

The evaluation of the expectation value of products of vertex operators is straightforward apart from the factor involving the bosonic twist operators. This calculation can be done analogously to the closed string case [11]. In contrast to the restricted cases discussed in [8, 55] with only one or two independent angles, we need to significantly modify the techniques. We now outline the derivation.

Consider the contribution from a single complex dimension in which the branes intersect with angles $\vartheta_i\pi$ where $\sum\vartheta_i = 2$ if there are no intersections. (Other topologies are possible. For example if there is a single intersection in the middle of the world-sheet we require $\sum_{i=left}\vartheta_i = \sum_{i=right}\vartheta_i$ where "left" and "right" indicate the vertices on opposing sides of the intersection.). We begin with the asymptotic behaviour of the Green function in the vicinity of the twist operators. The Green function can be written as,

$$g(z,w;x_i) = \frac{\langle -\frac{1}{2}\partial_z X \partial_w \overline{X} \prod_i \sigma_{\vartheta_i}\rangle}{\langle \prod_i \sigma_{\vartheta_i}\rangle}. \tag{4.77}$$

It has the following asymptotics,

$$\begin{aligned} g(z,w;x_i) &\sim \tfrac{1}{(z-w)^2} + \text{finite} \quad z \to w, \\ &\sim (z-x_i)^{-(1-\vartheta_i)} \quad z \to x_i, \\ &\sim (w-x_i)^{-\vartheta_i} \quad w \to x_i, \end{aligned}$$

which can be deduced from the OPEs (4.8). As we have seen the holomorphic fields are proportional to,

$$\begin{aligned} \partial X(z) &\equiv \omega(z) = \prod_i (z-x_i)^{-(1-\vartheta_i)}, \\ \partial \overline{X}(z) &\equiv \omega'(z) = \prod_i (z-x_i)^{-\vartheta_i}. \end{aligned} \tag{4.78}$$

Hence, the Green function may now be written generically upto an additional term usually denoted A,

$$g(z,w;x_i) = \omega(z)\omega'(w)\left\{\sum_{i<j} a_{ij}\frac{(z-x_i)(z-x_j)}{(w-x_i)(w-x_j)}\frac{\prod_k (w-x_k)}{(z-w)^2} + A\right\}, \tag{4.79}$$

where $a_{i<j}$ are constants and $A(\{x_i\})$ is a function of the positions of the vertex operators. This is the most general function with the desired conformal properties that can be written down as prescribed in [94]. Expanding in the various limits, we find by inspection that it has the required asymptotics if the constants satisfy

$$\begin{aligned} \sum_{i<j} a_{ij} &= 1, \\ \sum_{j=i+1}^{4} a_{ij} + \sum_{j=1}^{i-1} a_{ji} &= 1 - \vartheta_i. \end{aligned} \tag{4.80}$$

Note that summing the second of these conditions over i and using the $\sum_i (1-\vartheta_i) = 2$ condition automatically gives the first condition. Of course in the end any arbitrariness in the choice of a_{ij} and A must disappear from the amplitude which must be dependent on the ϑ_i's only.

Recall the operator product,

$$-\frac{1}{2}\partial_z X \partial_w \overline{X} \sim (z-w)^2 + T(z) + \dots , \tag{4.81}$$

this allows us to deduce the general form of $\langle \prod_i \sigma_{\vartheta_i} \rangle$ by considering,

$$\begin{aligned} \frac{\langle T(z) \prod_i \sigma_{\vartheta_i} \rangle}{\langle \prod_i \sigma_{\vartheta_i} \rangle} &= \lim_{w \to z} [g(z,w) - \frac{1}{(z-w)^2}] \\ &= -\frac{1}{2} \sum_{ij} \vartheta_i \vartheta_j \frac{1}{(z-x_i)(z-x_j)} \\ &\quad + \frac{1}{2} \sum_{i<j} a_{ij} \left(\frac{1}{z-x_k} + \frac{1}{z-x_{k'}} \right)^2 + \frac{A}{\prod_i (z-x_i)} \end{aligned} \tag{4.82}$$

where $k, k' \neq i, j$ and $k \neq k'$. Next, we compare this with the OPE of $T(z)$ with the twist operator,

$$T(z)\sigma_{\vartheta_i}(x_i) \sim \frac{h_i \sigma_{\vartheta_i}(x_i)}{(z-x_i)^2} + \frac{\partial_{x_i}\sigma_{\vartheta_i}(x_i)}{(z-x_i)} + \dots . \tag{4.83}$$

The leading $(z-x_i)^2$ divergences yield the correct conformal dimension of the twist operators;

$$h_i = \frac{1}{2}\vartheta_i(1-\vartheta_i).$$

Equating coefficients of $(z-x_i)^{-1}$ (in order to preserve generality we postpone using $SL(2,\mathbb{R})$ invariance to fix $(x_1, x_2, x_3, x_4) = (0, x_2, 1, x_\infty)$ for the moment) yields a set of differential equations for $\langle \prod_i \sigma_{\vartheta_i} \rangle$ of the form,

$$\partial_{x_k} \ln \left[\langle \prod_i \sigma_{\vartheta_i} \rangle \right] = \partial_{x_k} \ln \left[\prod_{i<j} (x_i - x_j)^{a_{ij} - (1-\vartheta_i)(1-\vartheta_j)} \right] + \frac{A}{\prod_{i \neq k} (x_k - x_i)}. \tag{4.84}$$

All that remains is to determine A which can be done using monodromy conditions for $\partial_z X \partial_w \overline{X}$. We proceed as for the classical calculation and consider the global monodromy conditions arising from the two independent Pochammer loops, $C_{l=1,2}$, encircling the prevertices x_l and x_{l+1}. From the local monodromy conditions for X_{qu} given in (4.18), we see that on completing these contours the quantum part should be left invariant,

$$\Delta_{C_l} X_{qu} = 0 = \oint_{C_l} dz \partial X_{qu} + \oint_{C_l} d\bar{z} \overline{\partial} X_{qu}. \tag{4.85}$$

Now we define the auxiliary Green function,

$$h(\bar{z},w)=\frac{\langle-\frac{1}{2}\bar{\partial}_{\bar{z}}X\partial_w\overline{X}\prod_i\sigma_{\vartheta_i}\rangle}{\langle\prod_i\sigma_{\vartheta_i}\rangle}. \tag{4.86}$$

This function has the following asymptotics,

$$\begin{aligned} h(\bar{z},w) &\sim \text{finite} && \text{as } z\to w,\\ &\sim(\bar{z}-x_i)^{-\vartheta_i} && \text{as } \bar{z}\to x_i,\\ &\sim(w-x_i)^{-\vartheta_i} && \text{as } w\to x_i, \end{aligned} \tag{4.87}$$

determining its form to be,

$$h(\bar{z},w)=B\bar{\omega}'(\bar{z})\omega'(w), \tag{4.88}$$

where $B(\{x_i\})$ is a function of the vertex positions. The monodromy condition applied to the Green functions is then,

$$\oint_{C_l}dz\,g(z,w)+\oint_{C_l}d\bar{z}\,h(\bar{z},w)=0. \tag{4.89}$$

We now use $SL(2,\mathbb{R})$ invariance to fix $(x_1,x_2,x_3,x_4)=(0,x_2,1,x_\infty)$. Taking the $w\to\infty$ limit, dividing by $w'(w)$ and extracting the leading x_∞ contributions, the monodromy condition (4.89) gives,

$$B\oint_{C_l}\overline{\omega}'(\bar{z})d\bar{z}+A\oint_{C_l}\omega(z)dz=x_\infty\oint_{C_l}\sum_i a_{i4}(z-x_i)\omega(z)dz \tag{4.90}$$

for both independent contours $C_{l=1,2}$. Defining $G_l=\int F_l(x_2)dx_2$ and $G_l'=\int F_l'(x_2)dx_2$ we can solve for A;

$$\frac{A}{x_\infty}=(1-\vartheta_4-a_{24})x_2-a_{34}-(1-\vartheta_4)\vartheta_2\left[G_1\partial_{x_2}\overline{G}_2'-G_2\partial_{x_2}\overline{G}_1'\right]/J, \tag{4.91}$$

where

$$J=F_1\overline{F_2'}-F_2\overline{F_1'}.$$

An alternative solution can be found by considering the monodromy condition,

$$\Delta_{C_l}\overline{X}_{qu}=0=\oint_{C_l}dw\partial\overline{X}_{qu}+\oint_{C_l}d\overline{w}\bar{\partial}\overline{X}_{qu}. \tag{4.92}$$

Applying this to our Green functions we obtain,

$$\oint_{C_l} dw\, g(z,w) + \oint_{C_l} d\overline{w}\, h(z,\overline{w}) = 0. \tag{4.93}$$

In a similar manner to above, noting the new form of $h(z,\overline{w})$, we take the $z \to \infty$ limit of the monodromy condition and divide by $\omega(z)$ to obtain;

$$B \oint_{C_l} \overline{\omega}(\overline{w}) d\overline{w} + A \oint_{C_l} \omega'(w) dw = x_\infty \oint_{C_l} \sum_{i<j\neq 4} a_{ij}(z - x_{k\neq,i,j,k})\omega'(w) dw. \tag{4.94}$$

Thus, we obtain a second expression for A;

$$\frac{A}{x_\infty} = (\vartheta_4 - a_{13})x_2 - a_{12} - (1-\vartheta_2)\vartheta_4 \left[G_2' \partial_{x_2}\overline{G_1} - G_1' \partial_{x_2}\overline{G_2}\right] / \overline{J}. \tag{4.95}$$

Now it is well known that integrals over the different Pochammer contours with integrands involving $\omega(z)$ generate solutions to the hypergeometric differential equation, which is discussed in appendix B.2. In the present case the required equation is that satisfied by the G_l and G_l' which (using $\partial_{x_2} G_l = F_l$) can be written;

$$\begin{aligned}(1-\vartheta_4)\vartheta_2 G_l &= x_2(1-x_2)\partial F_l + (-1)^l(\vartheta_1 + \vartheta_2 - 1 + (\vartheta_4 - \vartheta_2)x_2)F_l \\ (1-\vartheta_2)\vartheta_4 G_l' &= x_2(1-x_2)\partial F_l' - (-1)^l(\vartheta_1 + \vartheta_2 - 1 + (\vartheta_4 - \vartheta_2)x_2)F_l'.\end{aligned} \tag{4.96}$$

Substituting into (4.91) and (4.95) and summing yields the desired expression for A;

$$\frac{2A}{x_\infty x_2(1-x_2)} = -\partial_{x_2} \ln|J| + \frac{(a_{23}+a_{14})}{(1-x_2)} - \frac{(a_{34}+a_{12})}{x_2}, \tag{4.97}$$

where

$$|J| = |F_1||F_2'| + |F_2||F_1'|.$$

Note that, this expression may be deduced from (B.11) which also aids in the cancellation of terms in obtaining (4.97). We shall shortly give a closed expression for $|J|$ in terms of hypergeometric functions.

Finally, inserting (4.97) into (4.84), and using the relations in (4.80) gives,

$$\langle \prod_i \sigma_{\vartheta_i} \rangle = |J|^{-\frac{1}{2}} x_\infty^{-\vartheta_4(1-\vartheta_4)} x_2^{\frac{1}{2}(\vartheta_1+\vartheta_2-1)-\vartheta_1\vartheta_2} (1-x_2)^{\frac{1}{2}(\vartheta_2+\vartheta_3-1)-\vartheta_2\vartheta_3}. \tag{4.98}$$

Note that as promised there is no arbitrariness in the choice of a_{ij}. The function $|J|$ may be evaluated as;

$$\begin{aligned}|J| = & \frac{x_2^{1-\vartheta_1-\vartheta_2}}{(1-x_2)^{1-\vartheta_2-\vartheta_3}} \frac{\Gamma(1-\vartheta_1)\Gamma(\vartheta_3)}{\Gamma(\vartheta_3+\vartheta_4)\Gamma(\vartheta_2+\vartheta_3)} \times \\ & {}_2F_1[1-\vartheta_1, \vartheta_3, \vartheta_2+\vartheta_3; 1-x_2]\, {}_2F_1[1-\vartheta_1, \vartheta_3, \vartheta_3+\vartheta_4; x_2] + \\ & \frac{(1-x_2)^{1-\vartheta_2-\vartheta_3}}{x_2^{1-\vartheta_1-\vartheta_2}} \frac{\Gamma(\vartheta_1)\Gamma(1-\vartheta_3)}{\Gamma(\vartheta_1+\vartheta_2)\Gamma(\vartheta_1+\vartheta_4)} \times \\ & {}_2F_1[\vartheta_1, 1-\vartheta_3, \vartheta_1+\vartheta_4; 1-x_2]\, {}_2F_1[\vartheta_1, 1-\vartheta_3, \vartheta_1+\vartheta_2; x_2].\end{aligned} \tag{4.99}$$

This is for a single sub-T^2 torus of the compactified space. The contributions from the three complex planes should be multiplied together with the appropriate angles ϑ_i^m for each. As a check, note that when there is only one independent angle, $\vartheta_1 = \vartheta_3 = \vartheta$ and $\vartheta_2 = \vartheta_4 = 1-\vartheta$ the function reduces to that found in [8]. In addition we recover the result with two independent angles derived in [55] by setting $\vartheta_1 = 1-\vartheta_2$ and $\vartheta_4 = 1-\vartheta_3$. Note that the function has crossing symmetry; it is invariant under $\vartheta_1 \leftrightarrow \vartheta_3$ and $x_2 \leftrightarrow 1-x_2$. Finally note that the entire expression is invariant if we swap interior for exterior angles, $\vartheta_i \to 1-\vartheta_i$.

4.6 Summary

We have discussed the calculation of three and four point amplitudes for open strings localised at D-brane intersections. In both cases, the classical contribution to the amplitude is dominated by $e^{-\frac{1}{2\pi\alpha'}A}$, where A is the area of the polygon associated with the interaction. In the case of Yukawa couplings this leads to a natural mechanism for the generation of a mass hierarchy. For the quantum part of the four point amplitude, we were able to adapt the techniques of [11] to the open string case. Hence, by considering the conformal field theory we obtained the correlation function of four twist operators. This allows the computation of four fermion interactions.

An application of these results may be used to not only explore the phenomenology of intersecting brane models, but also to discuss or support more generic field theoretic ideas in set-ups with fermions localized in extra dimensions. For example, our results have been used to demonstrate that very low (TeV) string scales are incompatible with the experimental absence of FCNCs [95]. Further, these results aid in the analysis of flavour structure in

intersecting brane models [96].

In the next chapter, we generalise our calculations to determine the N-point function for open string at D-brane intersections. Then we proceed to discuss a phenomenological application of our results in the context of four fermion interactions on four independent sets of D-branes.

Chapter 5

N-point Amplitudes in Intersecting Brane Models

We now proceed to generalise the calculations of the previous chapter to the case of N-point amplitudes. That is we consider the interaction of N open string states localised at D-brane intersections. In particular, we calculate the classical contribution and the correlation function of N twist vertices. As a consistency check, we show that we can obtain the $(N-1)$-point amplitude from the N-point amplitude as a limiting case. Finally we will discuss some phenomenological applications of our results.

5.1 The classical contribution to the N-point function

Let us begin with a discussion of the classical contribution to the N-point function. We will use the notation and develop the methods from the previous chapter.

5.1.1 The classical contribution in the planar case

For simplicity we first concentrate on the planar case, i.e. ignoring the wrapping contributions which will be dealt with in the next section. The N-point function requires N twist operators, $\sigma_{\vartheta_i}(x_i)$, where $x_1 = 0$, $x_{N-1} = 1$ and $x_N = x_\infty \to \infty$. The classical solution is again determined up to a normalisation constant by it's holomorphicity and asymptotic behaviour at each

D-brane intersection. However, in this case we may generalise our expressions for the classical solutions to,

$$\begin{aligned} \partial X_{cl}(z) &= a\omega(z), & \partial \bar{X}_{cl}(z) &= \rho(z)\omega'(z), \\ \bar{\partial} X_{cl}(\bar{z}) &= \bar{\rho}(\bar{z})\bar{\omega}'(\bar{z}), & \bar{\partial} \bar{X}_{cl}(\bar{z}) &= a^*\bar{\omega}(\bar{z}), \end{aligned} \tag{5.1}$$

where $\rho(z)$ is a polynomial of degree p and,

$$\omega(z) = \prod_{i=1}^{N}(z-x_i)^{-(1-\vartheta_i)}, \quad \omega'(z) = \prod_{i=1}^{N}(z-x_i)^{-\vartheta_i}. \tag{5.2}$$

This modification obviously does not change the asymptotics of X_{cl} at the D-brane intersections. However, if we consider the contribution to S_{cl},

$$\int d^2z \bar{\partial} X_{cl} \partial \bar{X}_{cl} = \int d^2z |\rho(z)|^2 |\omega'(z)|^2, \tag{5.3}$$

we see that this converges only if $p \leq N-4$. Notice that for $N=4$ the expressions in (5.1) reduce to those of our previous case in (4.32). We can define a useful basis for $\rho(z)$ given by,

$$\rho^i(z) = \prod_{\substack{j=2 \\ (j \neq i)}}^{N-2}(z-x_j), \quad i = 2,..,N-2. \tag{5.4}$$

Our generalised classical solutions can then be expressed in the form,

$$\bar{\partial} X_{cl}(\bar{z}) = b_i^* \bar{\Omega}'^i(\bar{z}), \quad \partial \bar{X}_{cl}(z) = b_i \Omega'^i(z), \tag{5.5}$$

where,

$$\Omega'^i = \omega'(z)\rho^i(z). \tag{5.6}$$

In the N-point case our classical solutions require $N-2$ normalisation constants. However, we now have $N-2$ Pochammer loops, C_i, as depicted in figure 5.1. To each loop we can apply the global monodromy condition,

$$\Delta_{C_l} X_{cl} = \oint_{C_l} dz \partial X(z) + \oint_{C_l} d\bar{z} \bar{\partial} X(\bar{z}). \tag{5.7}$$

The required contour integrals are given by the $(N-2)\times(N-2)$ matrix

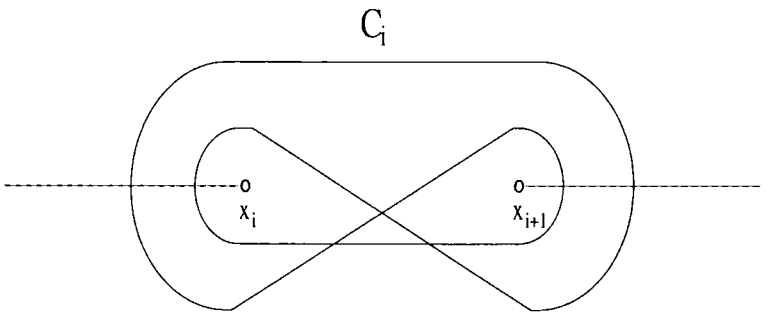

Figure 5.1: The $N-2$ Pochammer loops

W_l^i, defined by

$$\begin{aligned} W_l^1 &= \oint_{C_l} dz\omega(z) = e^{-i\pi(\vartheta_l-\vartheta_{l+1})} 4\sin(\pi\vartheta_l)\sin(\pi\vartheta_{l+1})F_l^1, \\ W_l^i &= \oint_{C_l} d\bar{z}\bar{\Omega}'^i(\bar{z}) = e^{-i\pi(\vartheta_l-\vartheta_{l+1})} 4\sin(\pi\vartheta_l)\sin(\pi\vartheta_{l+1})F_l^i, \end{aligned} \tag{5.8}$$

where,

$$\begin{aligned} F_l^1 &= \int_{x_l}^{x_{l+1}} \omega(y)dy, \\ F_l^i &= \int_{x_l}^{x_{l+1}} \bar{\omega}'(y)\rho^i(y)dy, \quad i = 2,..,N-2. \end{aligned} \tag{5.9}$$

Substituting into (5.7) and using the usual expression for the local monodromy of X around a twist vertex (4.17), we obtain

$$c_i F_l^i = f_{l+1} - f_l \quad l = 1,..,N-2, \tag{5.10}$$

with $c = (a, b_2^*, .., b_{N-2}^*)$. So we now have $N-2$ conditions for $N-2$ constants, giving

$$c_i(x_2,..,x_{N-2}) = \sum_{l=1}^{N-2}(f_{l+1} - f_l)(F^{-1})_i^l. \tag{5.11}$$

Finally, we determine the classical contribution to the N-point function in the planar case to be,

$$S_{cl}(x_2,..,x_{N-2}) = \frac{1}{4\pi\alpha'}\left(|a|^2 I(x_2,..,x_{N-2}) + \sum_{i,j} b_i^* b_j I'_{ij}(x_2,..,x_{N-2})\right), \tag{5.12}$$

where,

$$I(x_2,..,x_{N-2}) = \int d^2z|\omega(x)|^2, \quad I'_{ij}(x_2,..,x_{N-2}) = \int d^2z\bar{\Omega}'^i(\bar{z})\Omega'^j(z). \tag{5.13}$$

Note that for $N = 4$ this reduces to (4.42).

5.1.2 Wrapping contributions to the N-point function

We next consider the more phenomenologically interesting case of $M = T^2 \times T^2 \times T^2$, and consider wrapping contributions from strings winding around the tori. As always we restrict our attention to a single T^2 subfactor. As discussed in subsection 4.4.1, on introduction of toroidal geometry the action of our twist operators must be generalised to not only rotate X_{cl} but also to shift by a lattice translation. That is

$$X(e^{2\pi i}z, e^{-2\pi i}\bar{z}) = e^{2\pi i\vartheta}X + (1 - e^{2\pi i\vartheta})(f + v), \tag{5.14}$$

where $v \in \Lambda^*$, a coset of Λ. As mentioned previously, such shifts are of the form $v_i = q_i|I_{i,i+1}|\vec{L}_{i,i+1}$, with $q_i \in \mathbb{Z}$ (provided no D-branes are parallel). Hence the global monodromy conditions are now generalised to,

$$\begin{aligned} \Delta_{C_i}X_{cl} &= e^{-\pi i(\vartheta_i - \vartheta_{i+1})}4\sin(\pi\vartheta_i)\sin(\pi\vartheta_{i+1})(f_{i+1} - f_i + v_i) \\ &= \oint_{C_i} dz\partial X_{cl}(z) + \oint_{C_i} d\bar{z}\bar{\partial}X_{cl}(\bar{z}). \end{aligned} \tag{5.15}$$

Using the contour integrals (5.8) we obtain,

$$c_i F_l^i = f_{l+1} - f_l + v_l, \quad l = 1, .., N-2. \tag{5.16}$$

Hence we now have,

$$c_i(x_2, .., x_{N-2}, q_1, .., q_{N-2}) = \sum_{l=1}^{N-2}(f_{l+1} - f_l + v(l))(F^{-1})_i^l. \tag{5.17}$$

Our normalisation constants are now dependent on the q_l as well as the x_i. The q_l define the wrapped polygons, and take values determined by the intersection numbers of the D-branes.

To determine the wrapped polygons which contribute to the N-point amplitude, consider extending (w.l.o.g) from vertex f_2 as depicted in figure 5.2. Closure of the polygon requires,

$$\sum_{i=1}^{N} v_i = 0. \tag{5.18}$$

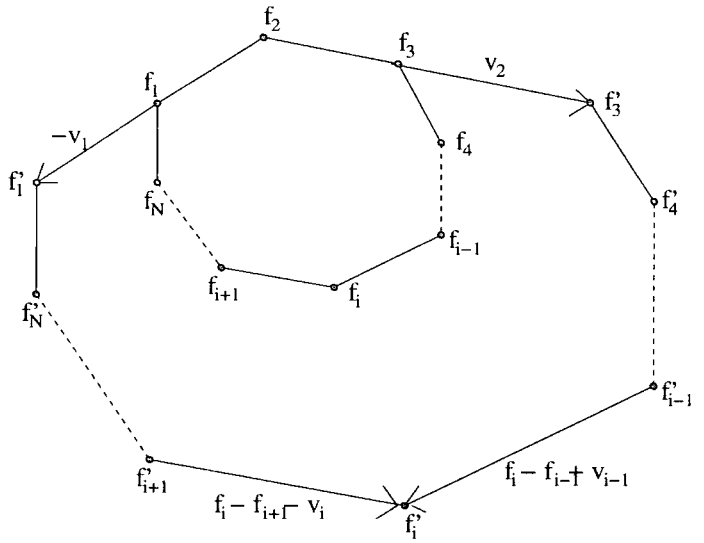

Figure 5.2: Determining the wrapped polygons

Assuming there are no D-branes parallel to one another and substituting,

$$|I_{i,i+1}|\vec{L}_{i,i+1} = -(n_i v_x + m_i v_y), \tag{5.19}$$

into (5.18) we obtain the linear diophantine equations,

$$\begin{pmatrix} q_N I_{N,N-1} \\ q_{N-1} I_{N,N-1} \end{pmatrix} = \begin{pmatrix} I_{N-1,1} & \cdots & I_{N-1,N-2} \\ I_{1,N} & \cdots & I_{N-2,N} \end{pmatrix} \begin{pmatrix} q_1 \\ \vdots \\ q_{N-2} \end{pmatrix}. \tag{5.20}$$

We can now determine our wrapped polygons by extending from f_2, taking all values of q_i, $i = 1, .., N-2$ that allow for integer solutions to (5.20). Each such solution defines a wrapped polygon contributing to the N-point function. For example, consider the $N = 3$ case. Then (5.20) reduces to,

$$q_1 I_{21} = q_3 I_{32}, \quad q_2 I_{21} = q_3 I_{13}. \tag{5.21}$$

The q_1 and q_2 which allow for integer solutions are then of the form,

$$q_1 = \frac{l|I_{32}|}{gcd(|I_{21}|,|I_{32}|,|I_{13}|)}, \quad q_2 = \frac{l|I_{13}|}{gcd(|I_{21}|,|I_{32}|,|I_{13}|)}, \tag{5.22}$$

where $l \in \mathbb{Z}$. This reproduces the result (4.30) found in chapter 4.

Unfortunately, it is not possible to solve (5.20) in the general case, only

for concrete examples. This is due to the fact that diophantine equations are usually solved algorithmically, however it is possible to make some general remarks. We require the following result from linear algebra [97, 98],

THEOREM. Let $A \in M_{m,n}(\mathbb{Z})$. There exists $L \in SL_m(\mathbb{Z})$ and $R \in SL_n(\mathbb{Z})$ such that,

$$LAR = D = diag(d_1, d_2, .., d_s, 0, .., 0), \tag{5.23}$$

where $d_i > 0$, $i = 1, .., s$ and $d_i | d_{i+1}$, $i = 1, .., s-1$.

Denoting our diophantine matrix equation as $b = Ax$, we can therefore write our solution as $x = Ry$ where y is a solution to the diagonal system of equations, $Dy = e$, with $e = Lb$. Since A is of size $2 \times (N-2)$, we have in general two distinct cases for the form of D, corresponding to $s = 1$ and $s = 2$ above. However, our assumption of a convex polygon means that we only need to consider the case $s = 2$. This can be deduced from the fact that the dimension of the row space of A is the same as that of D. Hence we have the general solution,

$$\begin{pmatrix} q_1 \\ \vdots \\ q_{N-2} \end{pmatrix} = R \begin{pmatrix} e_1/d_1 \\ e_2/d_2 \\ l_1 \\ \vdots \\ l_{N-4} \end{pmatrix}, \tag{5.24}$$

where l_i are free integer parameters and e_1 and e_2 are functions of q_N and q_{N-1}. Unfortunately, it is not possible to determine L and R for a general matrix A.

We can now write the classical contribution to the N-point function in the toroidal case as,

$$Z_{cl}(x_2, .., x_{N-2}) = \sum_{q_1,..,q_{N-2}} e^{-Scl(x_2,..,x_{N-2},q_1,..,q_{N-2})}, \tag{5.25}$$

where,

$$S_{cl}(x_2,..,x_{N-2},q_1,..,q_{N-2}) = \\ \frac{1}{4\pi\alpha'}\left(|a|^2 I(x_2,..,x_{N-2}) + \sum_{i,j} b_i^* b_j I'_{ij}(x_2,..,x_{N-2})\right). \tag{5.26}$$

Note that we sum over $N-2$ variables corresponding to the $N-2$ independent sides of an N-sided polygon and only include q_i such that (5.20) has a solution. This sum incorporates all possible wrapped polygon contributions to our classical amplitude.

5.1.3 The Schwarz-Christoffel map and the area rule

Let us denote the classical contribution from a single torus subfactor by $S_{cl}^{T_2}$. As we have seen in chapter 4, at the minimum of $S_{cl}^{T_2}$ for $N=4$, $b_2=0$ (previously denoted, b), and we obtain the area of the polygon involved in the interaction. An analogous situation also occurs in the three point case, where again $b_2=0$ and the action is the area of a triangle. Furthermore, it seems intuitively obvious that for general N, the area of the worldsheet (i.e. S_{cl}) has as its minimum value the area of the polygon associated with the amplitude, provided only one $S_{cl}^{T_2^i}$ is non-zero. That this is indeed the case, and this occurs when the $b_i=0$, can be motivated as follows.

We can express X_{cl} as,

$$X_{cl}(z,\bar{z}) = A + a\int^z \prod_{i=1}^N (\zeta - x_i)^{-(1-\vartheta_i)} d\zeta + b_l^* \int^{\bar{z}} \prod_{i=1}^N \overline{(\bar{\zeta}-x_i)^{-\vartheta_i}}\rho^l(\bar{\zeta})d\bar{\zeta}, \tag{5.27}$$

with $X_{cl}(x_i)=f_i$ and $A\in\mathbb{C}$. The lower integration limits are left unspecified as they affect only the value of A. Differentiating gives ∂X_{cl} and $\bar{\partial}X_{cl}$, as in section 5.1. Note that we expect X_{cl} to be, at least locally, one to one and hence if $f_j=f_i$ we must have $x_j=x_i$. Using (5.27) and $X_{cl}(x_i)=f_i$ allows us immediately to obtain the relation,

$$c_l F_i^l = f_{i+1} - f_i \quad i=1,..,N-2, \tag{5.28}$$

which are simply the global monodromy conditions (5.10).

Now inserting $b_i=0$ in (5.27), we obtain a Schwarz-Christoffel map. This is the general form of a map from the upper-half complex plane to an N-

sided polygon. Hence, integrating this over the complex plane as in (4.13) just gives back the area of the polygon as the classical action. In summary, we have motivated the simple rule,

> *The minimum of the classical action equals the sum of the polygon areas projected in each T^2 when the non-zero polygons are the same up to an overall scaling.*

From now on, in keeping with the literature on Schwarz-Christoffel mappings we will refer to the x_i as prevertices.

5.2 The quantum contribution to the N-point amplitude

The correlator of N twist vertices can be computed using the stress tensor method described in section 4.5.4. We also employ techniques discussed in [99], although here modified to the tree level case. Generalising the $N = 4$ case, the Green function should now take the form,

$$g(z,w;x_i) = \omega(z)\omega'(w)\left\{\sum_{i<j} a_{ij}\frac{(z-x_i)(z-x_j)}{(w-x_i)(w-x_j)}\frac{\prod_k(w-x_k)}{(z-w)^2} + A(w)\right\}, \tag{5.29}$$

where the a_{ij} satisfy the same conditions as in (4.80). However, $A(w)$ is now a function of the form

$$A(w) = \sum_{i>j>i'>j'} b_{iji'j'}\frac{\prod_k(w-x_k)}{(w-x_i)(w-x_j)(w-x_{i'})(w-x_{j'})},$$

where $b_{iji'j'}$ are some coefficients.

It is useful in what follows to define

$$g_s(z,w) = \omega(z)\omega'(w)\sum_{i<j} a_{ij}\frac{(z-x_i)(z-x_j)}{(w-x_i)(w-x_j)}\frac{\prod_k(w-x_k)}{(z-w)^2}, \tag{5.30}$$

and from the asymptotics of $h(\overline{z}, w)$, it can be seen that

$$h(\overline{z}, w) = \sum_{i,j=2}^{N-2} c_{ij} \overline{\Omega}'^{i}(\overline{z}) \Omega'^{j}(w) \,, \tag{5.31}$$

where $\Omega'^{i}(z)$ is given by (5.6). In order to write down a solution to the monodromy conditions we again require the $(N-2) \times (N-2)$ matrix W_l^i defined in (5.8), where l labels the $N-2$ independent Pochammer contours. With these definitions a solution to the global monodromy conditions with g and h in the prescribed form can be written down as follows,

$$\begin{aligned} g(z,w) &= g_s(z,w) - \omega(z) \sum_{l=1}^{N-2} (W^{-1})_1^l \oint_{C_l} dy \, g_s(y,w), \\ h(\overline{z},w) &= -\sum_{i=2}^{N-2} \overline{\Omega}'^{i}(\overline{z}) \sum_{l=1}^{N-2} (W^{-1})_i^l \oint_{C_l} dy \, g_s(y,w). \end{aligned} \tag{5.32}$$

To simplify the calculation of the twist field correlators, we leave the x_i as $z_i \in \mathbb{C}$ in the above expressions and postpone the use of $SL(2,\mathbb{R})$ invariance. We shall compute both holomorphic and antiholomorphic contributions to the correlator, and then employ $\partial_{x_k} = \frac{1}{2}(\partial_{z_k} + \partial_{\bar{z}_k})$ to obtain our final answer relevant to twist fields on the boundary of an open string diagram.

Now following the method in section 4.5.4, we may insert the expression for $g(z,w)$ into

$$\frac{\langle T(z) \prod_i \sigma_{\vartheta_i} \rangle}{\langle \prod_i \sigma_{\vartheta_i} \rangle} = \lim_{w \to z} [g(z,w) - \frac{1}{(z-w)^2}], \tag{5.33}$$

and extract the singular holomorphic behaviour at any one of the poles, $(z - z_k)^{-1}$, to find the holomorphic contribution

$$H = \partial_{z_k} \ln \left[\prod_{i<j} (z_i - z_j)^{-(1-\vartheta_i)(1-\vartheta_j)} \right] - \sum_{l=1}^{N-2} (W^{-1})_1^l \partial_{z_k} W_l^1. \tag{5.34}$$

To evaluate the trailing term, following [99], we note that

$$\partial_{z_k} \ln |W| = \sum_{l=1}^{N-2} (W^{-1})_i^l \partial_{z_k} W_l^i + \sum_{\substack{j=1 \\ (j \neq i)}}^{N-2} \sum_{l=1}^{N-2} (W^{-1})_j^l \partial_{z_k} W_l^j. \tag{5.35}$$

By comparing the singularities as $z \longrightarrow z_k$ we can evaluate the second piece,

$$\sum_{\substack{j=1\\(j\neq i)}}^{N-2}\sum_{l=1}^{N-2}(W^{-1})^l_j\partial_{z_k}W^j_l = \partial_{z_k}\ln\prod_{\substack{j=1\\(j\neq k,i)}}^{N-2}(z_k-z_j)^{1-\vartheta_k}. \tag{5.36}$$

Inserting this back into (5.34) we obtain the holomorphic contribution to the correlator,

$$H = \partial_{z_k}\ln\left[|W|^{-1}\prod_{i<j}(z_i-z_j)^{-(1-\vartheta_i)(1-\vartheta_j)}\prod_{\substack{j=2\\(j\neq k)}}^{N-2}(z_k-z_j)^{1-\vartheta_k}\right]. \tag{5.37}$$

In order to compute the antiholomorphic contribution, we complex conjugate the coordinates and exchange $\vartheta_i \longrightarrow 1-\vartheta_i$ everywhere. Thus we obtain,

$$\bar{H}' = \partial_{\bar{z}_k}\ln\left[|\overline{W}'|^{-1}\prod_{i<j}(\bar{z}_i-\bar{z}_j)^{-\vartheta_i\vartheta_j}\prod_{\substack{j=2\\(j\neq k)}}^{N-2}(\bar{z}_k-\bar{z}_j)^{\vartheta_k}\right]. \tag{5.38}$$

Note that $|W|$ is invariant (up to a sign) under complex conjugation accompanied by interchange of differentials of the type $\omega(z)$ with $\Omega'(z)$, so that it is compatible with the antiholomorphic differential equations. Hence, upon adding the two contributions, multiplying by $\frac{1}{2}$ and setting the coordinates of the twist fields to be real, we get the total contribution

$$\partial_{x_k}\ln\langle\prod_i\sigma_{\vartheta_i}\rangle = \partial_{x_k}\ln\left[|W|^{-\frac{1}{2}}\prod_{\substack{j=2\\(j\neq k)}}^{N-2}(x_k-x_j)^{\frac{1}{2}}\prod_{i<j}(x_i-x_j)^{-\frac{1}{2}(1-\vartheta_i)(1-\vartheta_j)-\frac{1}{2}\vartheta_i\vartheta_j}\right]. \tag{5.39}$$

Finally we can write down the correlator which solves the differential equations in all variables $\{x_k\}$,

$$\langle\prod_i\sigma_{\vartheta_i}\rangle = |W|^{-\frac{1}{2}}\prod_{\substack{i<j\\(i,j\neq 1)}}^{N-2}(x_i-x_j)^{\frac{1}{2}}\prod_{i<j}^{N}(x_i-x_j)^{\frac{1}{2}(\vartheta_i+\vartheta_j-1)-\vartheta_i\vartheta_j}. \tag{5.40}$$

One may verify that when $N = 4$ it gives the earlier 4 point result[1], the W_l^i matrix is now a 2×2 matrix of the usual hypergeometric integrals in (4.36) whose determinant is proportional to $|J|$.

5.3 Obtaining the $(N-1)$-point amplitude from the N-point amplitude

Consistency requires that the $(N-1)$-point amplitude be obtainable from the N-point amplitude as a limiting case. We can reduce the N-point amplitude down to an $(N-1)$-point amplitude as depicted in figure 5.3. Take a single prevertex, x_i say, and let it coalesce with x_{i+1}. Shifting a single prevertex of course potentially adjusts the entire polygon. However, we may keep each of the $N-2$ independent sides fixed by adjusting the $N-2$ constants c_i. Thus, we are able to coalesce f_i and f_{i+1} by adjusting only the lengths of the two adjacent sides $f_{i-1,i}$ and $f_{i,i+1}$, whilst leaving the rest of the polygon and all the angles unchanged.

Let us begin by considering how the classical contribution reduces in this case. We denote by $\bar{S}_{cl}$, the classical action for the N-point amplitude with the identification $x_i = x_{i+1}$, and by $\tilde{S}_{cl}$ the action we would expect for the $(N-1)$-point amplitude obtained by reduction from the N-point amplitude. This notation will also be employed in this section to distinguish other quantities between the two cases. We now show that $\bar{S}_{cl} = \tilde{S}_{cl}$. From the diagram, the following relations are easily determined by the geometry of the parent amplitude,

$$\begin{array}{llll} f'_j = f_j & \vartheta'_j = \vartheta_j & x'_j = x_j & \text{For } j = 1,..,i-1, \\ f'_j = f_{j+1} & \vartheta'_j = \vartheta_{j+1} & x'_j = x_{j+1} & \text{For } j = i+1,..,N-1, \end{array} \tag{5.41}$$

and also,

$$f'_i = f_{i+1} = f_i \quad \vartheta'_i = -1 + \vartheta_i + \vartheta_{i+1} \quad x'_i = x_{i+1}. \tag{5.42}$$

[1]To explicitly obtain the $N = 4$ expression, we must extract the $(-x_\infty)$ term out of $|W|^{-1/2}$.

Using these expressions it is simple to deduce that $\bar{I} = \tilde{I}$ and furthermore,

$$\begin{aligned} \bar{I}'_{lm} &= \tilde{I}'_{\overline{g(l)g(m)}}, \quad l,m = 1,..,i-1,i+1,..,N-2, \\ \bar{I}'_{im} &= \bar{I}'_{\overline{i+1},m}, \end{aligned} \tag{5.43}$$

where,

$$g(k) = \begin{cases} k & k = 1,..,i-1 \\ k-1 & k = i+1,..,N-2. \end{cases} \tag{5.44}$$

We also need to examine the global monodromy conditions in the N-point and $(N-1)$-point cases. For this we require the following easily obtained relations,

$$\begin{aligned} \bar{F}^k_j &= \tilde{F}^{g(k)}_{g(m)}, \quad k,j = 1,..,i-1,i+1,..,N-2, \\ \bar{F}^i_j &= \bar{F}^{i+1}_j, \quad F^k_i = 0. \end{aligned} \tag{5.45}$$

Then we can see that the monodromy conditions are the same in both cases, with the identification

$$\begin{aligned} &\bar{c}_k = \tilde{c}_{g(k)}, \qquad k = 1,..,i-1,i+2,..,N-2, \\ &\bar{c}_{i+1} + \bar{c}_i = \tilde{c}_i. \end{aligned} \tag{5.46}$$

Finally, substituting (5.43) and (5.46) into our expression for $\bar{S}_{cl}$ given in (5.12) we obtain $\tilde{S}_{cl}$.

The quantum contribution in (5.40) should also reduce in the correct manner as the two prevertices coalesce, and indeed it does. The discussion is similar to the one loop closed string diagram discussion of [99]. When the two twist fields at x_i and x_{i+1} come together we should recover an amplitude consistent with,

$$\sigma_{\vartheta_i}(x_i)\sigma_{\vartheta_{i+1}}(x_{i+1}) \sim (x_i - x_{i+1})^{k_i}\sigma_{\vartheta_i+\vartheta_{i+1}-1} \tag{5.47}$$

where k_i is to be determined by equating the conformal dimensions on each side. We find that $k_i = -(1-\vartheta_i)(1-\vartheta_{i+1})$ when $\vartheta_i + \vartheta_{i+1} \geq 1$ and $k_i = -\vartheta_i\vartheta_{i+1}$ when $\vartheta_i + \vartheta_{i+1} \leq 1$. We must verify that the amplitude yields the correct factors asymptotically. The basis of $N-2$ Pochammer loops evolves into $N-3$ loops as two points coalesce. When the two adjacent points come together the local behaviour of ∂X is given by $\omega(z) \sim z^{-(1-\vartheta_i)}(z-\delta)^{-(1-\vartheta_{i+1})}$ where the first prevertex we arbitrarily set to 0 and the second

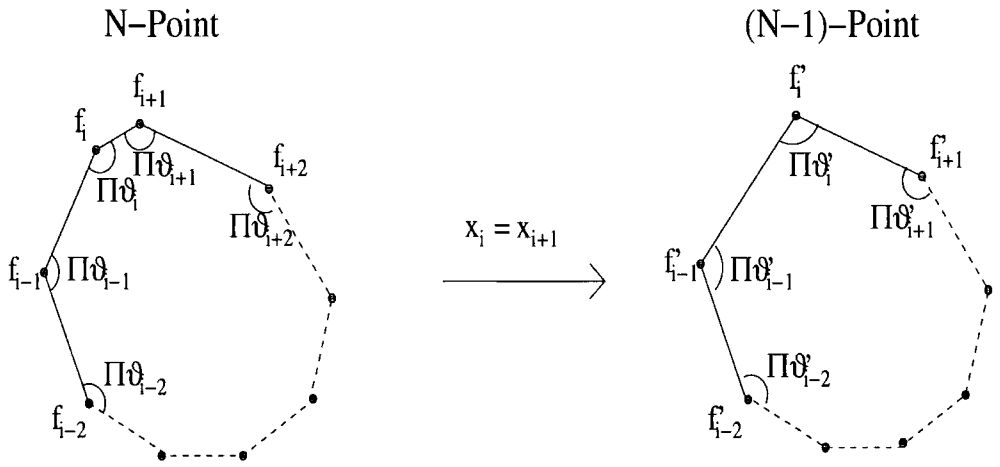

Figure 5.3: Reducing the N-point amplitude to the $(N-1)$-point amplitude.

to δ. One can check, from our expressions (B.10) for the F_i^1, that the ω contour integrals around the loop "trapped" between the two vertices diverge as $(x_i - x_{i+1})^{\vartheta_i+\vartheta_{i+1}-1}$ if $\vartheta_i + \vartheta_{i+1} < 1$ and are convergent otherwise. The opposite is true for the Ω' integrals so that at coalescence, including the divergent factors from $|W|^{-1/2}\prod_{i<j}(x_i - x_j)^{1/2}$, we have

$$\langle \prod_j \sigma_{\vartheta_j} \rangle \sim (x_i - x_{i+1})^{\frac{1\pm1}{2}(\vartheta_i+\vartheta_{i+1}-1)-\vartheta_i\vartheta_{i+1}} \langle \prod_{j\neq i} \sigma_{\vartheta_j} \rangle, \tag{5.48}$$

where we take a plus sign if $\vartheta_i + \vartheta_{i+1} \geq 1$ and minus if $\vartheta_i + \vartheta_{i+1} < 1$, yielding the expected behaviour in (5.47).

Combining the above results we see that the expression for an N-point amplitude reduces to that of an $(N-1)$-point amplitude as required.

5.4 Higgs exchange

We now discuss an application of our results. In particular, the general 4-point amplitude is required when there are four independent branes. In models which reproduce the Standard Model (or supersymmetric variants thereof) the relevant processes are therefore $q_L q_R \to e_L e_R$ as shown in figure 5.4, and necessarily involve 2 left and 2 right chirality fields.

The full four-point amplitude can be easily obtained from our previous results. We are interested in the four fermion operator, $(\overline{q}_L^{(3)} q_R^{(2)})(\overline{e}_R^{(1)} e_L^{(4)})$.

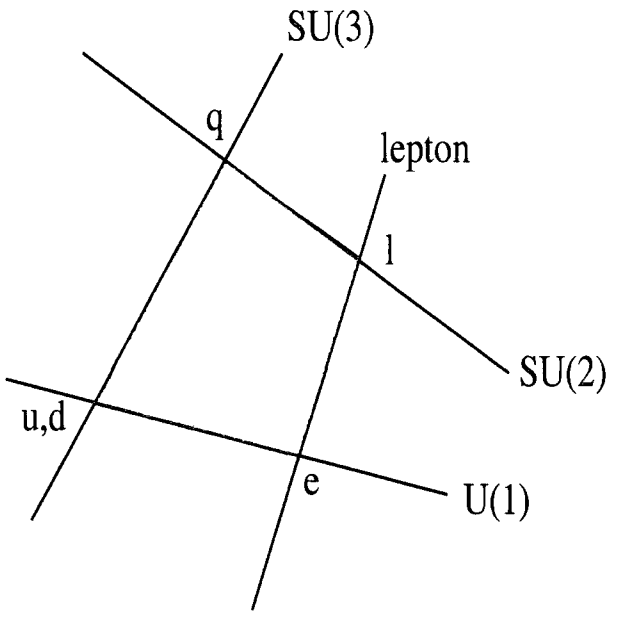

Figure 5.4: Instanton contribution to the four point amplitude

The uncompactified part of the fermions have the charges,

$$\begin{aligned} \widetilde{q_1} &= -\tilde{q}_4 = \pm(\frac{1}{2},\frac{1}{2}), \\ \widetilde{q_2} &= -\tilde{q}_3 = \pm(\frac{1}{2},-\frac{1}{2}), \end{aligned} \tag{5.49}$$

and the compactified part has the charge $q_i^m = \vartheta_i^m - \frac{1}{2}$, as mentioned in (4.74). Collecting the simpler correlators together, we have

$$\begin{aligned} ghosts \times \langle e^{-\phi/2}(0)e^{-\phi/2}(x)e^{-\phi/2}(1)e^{-\phi/2}(x_\infty)\rangle &= x_\infty^{\frac{5}{4}}x^{-\frac{1}{4}}(1-x)^{-\frac{1}{4}}, \\ \langle e^{-ip_1.X}e^{-ip_2.X}e^{-ip_3.X}e^{-ip_4.X}\rangle &= x^{2\alpha' p_1.p_2}(1-x)^{2\alpha' p_2.p_3}, \end{aligned} \tag{5.50}$$

and

$$\begin{aligned} \langle e^{-iq_1.H}e^{-iq_2.H}e^{-iq_3.H}e^{-iq_4.H}\rangle_{non-cmp} &= x_\infty^{\tilde{q}_4.(\tilde{q}_1+\tilde{q}_2+\tilde{q}_3)}x^{\tilde{q}_1.\tilde{q}_2}(1-x)^{\tilde{q}_2.\tilde{q}_3} \\ &= x_\infty^{-\frac{1}{2}}x^{\tilde{q}_1.\tilde{q}_2}(1-x)^{\tilde{q}_2.\tilde{q}_3} = x_\infty^{-\frac{1}{2}}(1-x)^{-\frac{1}{2}}. \end{aligned} \tag{5.51}$$

For the compactified tori factors, we have

$$\langle e^{-iq_1.H}e^{-iq_2.H}e^{-iq_3.H}e^{-iq_4.H}\rangle_{cmp} = \prod_m^3 x_\infty^{\vartheta_4^m(1-\vartheta_4^m)-\frac{1}{4}} x^{\vartheta_1^m\vartheta_2^m-\frac{1}{2}(\vartheta_1^m+\vartheta_2^m)+\frac{1}{4}} \times (1-x)^{\vartheta_2^m\vartheta_3^m-\frac{1}{2}(\vartheta_2^m+\vartheta_3^m)+\frac{1}{4}}. \tag{5.52}$$

Note that, particles of one chirality take the opposite Weyl index to that of the opposing chirality. Hence, using Weyl notation, in $\overline{u}_{\dot{\alpha}}^{(3)}u_{\dot{\beta}}^{(2)}\overline{u}_{\gamma}^{(1)}u_{\delta}^{(4)}$ we now have opposite $\dot{\alpha}\dot{\beta}$ and $\gamma\delta$ indices which (writing as $\varepsilon_{\dot{\alpha}\dot{\beta}}\varepsilon_{\gamma\delta}$) just contracts the $\overline{q}_L q_R$ and $\overline{e}_L e_R$ fermions. Piecing together all the separate contributions and including the twist field correlators determined in (4.98), we obtain the final expression for the amplitude (up to an overall normalisation),

$$\begin{aligned} A(1,2,3,4) &= -g_o^2\alpha' \int_0^1 dx\, x^{-1-\alpha' s}(1-x)^{-1-\alpha' t}\frac{(1-x)^{-\frac{1}{2}}}{\prod_m^3 |J^m|^{1/2}} \\ &\quad \times \left[(\overline{u}^{(3)}u^{(2)})(\overline{u}^{(1)}u^{(4)})\right]\sum e^{-S_{cl}(x)}, \end{aligned} \tag{5.53}$$

where $s = -(k_1+k_2)^2$, $t = -(k_2+k_3)^2$, $u = -(k_1+k_3)^2$ are the usual Mandlestam variables. Note that, the dependence on ϑ_i^m cancels between the bosonic twist fields and the spin-twist fields. The classical action is given by (4.55) in terms of the different τ in each sub-torus.

Now consider the geometry depicted in figure 5.4. The $SU(2)$ and $U(1)$ branes will intersect and a Higgs field appears at that intersection. Then from subsection 4.5.2 (assuming for simplicity that the projected areas are zero in the other sub-tori), the minimum of the action is the area of the polygon, which is simply the difference in the two triangular areas defined by the $SU(2)$, $U(1)$ branes and either the lepton or $SU(3)$ brane. Since this is a stringy process (5.53) gives a contribution of the form,

$$\frac{Y_u/Y_e}{M_s^2}. \tag{5.54}$$

This is a significantly larger contribution than one would expect in field theory. In this case, the process would occur via Higgs exchange and be suppressed by the product of two Yukawa couplings, i.e. we would expect the amplitude to go as,

$$\frac{Y_u Y_e}{t-M_h^2}, \tag{5.55}$$

or the s channel equivalent. In fact, in the limit that the lepton brane is lying

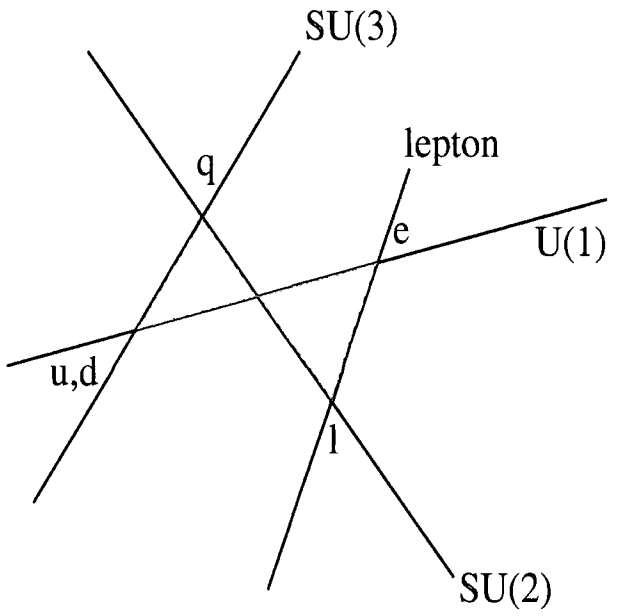

Figure 5.5: t-channel Higgs exchange as "double instanton"

on top of the SU(3) brane in all sub-T_2tori, there is no Yukawa suppression at all in this process. Thus, at low string scales this stringy exchange can potentially be important.

However, the geometry of our D-branes may also be as depicted in figure 5.5, with the lepton brane lying to the right of the $SU(2) - U(1)$ intersection. In this case (5.53) gives the equivalent of Higgs exchange in the field theory limit. Indeed, since the instanton suppression goes as $e^{-Area/2\pi\alpha'}$, we expect to find the product of two Yukawas. This feature and the appearance of a Higgs pole will now be verified.

From here on, we shall denote x_2 by x. It is easy to show that when the diagram has an intersection in a particular sub-torus, as in figure 5.5, the contribution to the action from that subtorus is a monotonically decreasing function of x. Hence the sum of the contributions is minimized by taking the limit $x \longrightarrow 1$. Assuming that $1 - \vartheta_2 - \vartheta_3 > 0$, the relevant limits are

$$\begin{aligned} &Lim_{x\to 1}\tau = -\beta, \\ &Lim_{x\to 1}|J| = (1-x)^{(-1+\vartheta_2+\vartheta_3)} \frac{1}{(\gamma\gamma')^{\frac{1}{2}}}\, \eta(\vartheta_2,\vartheta_3)\eta(1-\vartheta_1,1-\vartheta_4), \end{aligned} \tag{5.56}$$

where

$$\eta(\vartheta_i,\vartheta_j)=\left(\frac{\Gamma(\vartheta_i)\Gamma(\vartheta_j)\Gamma(1-\vartheta_i-\vartheta_j)}{\Gamma(1-\vartheta_i)\Gamma(1-\vartheta_j)\Gamma(\vartheta_i+\vartheta_j)}\right)^{\frac{1}{2}}. \tag{5.57}$$

Then up to an overall normalisation we have,

$$\begin{aligned}A(1,2,3,4)= \; & -g_o^2\alpha'\left[(\overline{u}^{(3)}u^{(2)})(\overline{u}^{(1)}u^{(4)})\right]\, e^{-S_{cl}(1)}\times \\ & \int_0^1 dx\,(1-x)^{-\alpha' t-\sum\frac{1}{2}(\vartheta_2^m+\vartheta_3^m)}.\end{aligned} \tag{5.58}$$

The contribution to the classical action from each sub-torus becomes,

$$S_{cl}(1)=\frac{1}{2\pi\alpha'}\left(\frac{\sin\pi\vartheta_1\sin\pi\vartheta_4}{\sin(\pi\vartheta_2+\pi\vartheta_3)}\frac{v_{14}^2}{2}+\frac{\sin\pi\vartheta_2\sin\pi\vartheta_3}{\sin(\pi\vartheta_2+\pi\vartheta_3)}\frac{v_{23}^2}{2}\right). \tag{5.59}$$

Bearing in mind that the angle at the intersection is $\pi-\pi\vartheta_2-\pi\vartheta_3$, we see that the result is just the sum of the area$/2\pi\alpha'$ of the two triangles. Finally the pole term now arises from the x integral,

$$-\alpha'\int_0^1 dx\,(1-x)^{-\alpha' t-\sum\frac{1}{2}(\vartheta_2^m+\vartheta_3^m)}=\frac{1}{t-M_h^2}, \tag{5.60}$$

where (recalling that $0<\vartheta_2^m+\vartheta_3^m<1$) we recognize the mass of a scalar Higgs state in the spectrum at the intersection,

$$\alpha' M_h^2=1-\frac{1}{2}\sum_m(\vartheta_2^m+\vartheta_3^m). \tag{5.61}$$

Hence identifying the Yukawa couplings with the areas of the two triangles, as in section 4.4, we obtain the expected form

$$\frac{Y_u Y_e}{t-M_h^2}, \tag{5.62}$$

up to a normalisation factor. This factor maybe computed using the normalisation of the Yukawa couplings discussed in [55, 100]. The above discussion was carried out for intersecting D6-branes, but it is straightforward to translate it to other set-ups.

5.5 Conclusion

In summary, we have analysed the N-point amplitude at tree level for open strings localised at D-brane intersections. We were able to generalise the techniques used for three and four point amplitudes discussed in the previous chapter. Thus, we obtained both the classical and quantum contributions to the general N-point amplitude, including those contributions that wrap the internal space. For consistency, we checked that the N-point amplitude is reduced down to the $(N-1)$-point amplitude when two prevertices coalesce. We have also shown that for general N, *the minimum of the classical action is given by the sum of the polygon areas projected in each torus subfactor, when the non-zero polygons are identical up to an overall scaling.*

Our results are applicable to all orbifold, orientifold and toroidal compactifications. Orbifolds and orientifolds would require a modification of the counting over wrapped polygons, but the leading contributions would be the same.

We examined the process $q_L q_R \to e_L e_R$, on four independent sets of D-branes. This process, depending as it does on the geometry of the D-branes, has a purely stringy contribution, as well as a sensible field theory limit corresponding to Higgs exchange. In the former case, the amplitude is of the form $\frac{Y_q/Y_e}{M_s^2}$ which should be compared to the field theory case $\frac{Y_q Y_e}{t-m_h^2}$. Thus at low string scales the stringy exchanges are potentially important.

These calculations provide a starting point for discussing general interactions in intersecting brane models and hence understanding their phenomenology in more detail. In addition they may prove useful in addressing questions to do with the possible introduction of a realistic flavour structure in these models [96]. Further processes including for example Higgstrahlung, can also be treated.

Chapter 6

A summary and discussion

As we have seen, string theory is a powerful framework within which we are able to describe both the gauge interactions of the Standard Model and a description of gravity at the quantum level. However, it is still restricted to being a framework for the construction of models, as opposed to a single fundamental theory of nature. This is similar to the sense in which quantum field theory is a framework within which one can construct the Standard Model. This arises as a consequence of the fact that our current understanding of the fundamental structure of string theory is limited, and at present there is no thorough understanding of the string moduli space depicted in figure 1.1. Therefore, it is impossible to deduce a ground state and suitable compactification from first principles. It follows that, in order to compare string theory to nature, we must make assumptions and 'simply' construct models that seem to contain features shared with our observable universe. In one sense, this is perfectly reasonable and a similar process was used in discovering the Standard Model. On the other hand, this may result in us ignoring or not recognising important lessons that could be learnt from string theory. It is therefore important that both approaches are taken and lessons are learnt and shared between them. The aim of this thesis, was to contribute to this effort.

We began in chapter 3, by exploring a model constructed using the bottom-up approach [7] to string model building. This approach has the extremely useful feature of removing a substantial proportion of the dependence of the low energy physics of the model on the global details of the compactification space. This allows us to focus on more generic features of

these models without the need for analysing different geometries in detail. Some interesting features arise, for instance locating the D-branes on a simple orbifold singularity, containing a $\mathbb{Z}_3$ group factor, leads to a model with three generations of quark-leptons. Essentially, because the $\mathbb{Z}_3$ 'twists' each internal complex dimension equally. Again, we see that geometry in string theory can lead to insights into our 'why' questions discussed in chapter 1.

The model constructed utilised a new method for obtaining CP violation in the low energy field theory. Such a phenomenon is only accommodated and not explained in the Standard Model, leading to a longstanding puzzle in particle physics. Here, CP was broken spontaneously through the action of discrete torsion, thus providing the possibility of a geometric explanation of CP violation. This motivated a simple ansatz for the Kähler metric, whose actual form is unknown due to our desire to separate out as much of the low energy physics as possible from our choice of compactification, and also the difficulty in its computation for anything other than the simplest geometries. Our ansatz resulted in a phenomenologically viable CKM matrix, with mixing angles and a complex phase close to those measured experimentally. This shows that physics close to that of the Standard Model can be obtained as a feature of a class of models with a relatively simple construction. These models also had the added benefit of separating out the generation of flavour structure and supersymmetry breaking. This leads to the possibility of avoiding the traditional supersymmetric CP and flavour problems, although more work needs to be done to establish this concretely.

The remaining two chapters covered the formalism required to calculate scattering amplitudes in intersecting brane models [56]. These models are based on the fact that it is possible to obtain chiral fermions at the intersection of two D-branes at an arbitrary angle [57]. Thus, these models are somewhat more general than those constructed in the bottom-up approach, where D-branes are always either parallel or perpendicular. An intersecting brane model generically contains a number of different stacks of D-branes which upon wrapping a compact internal space generally intersect repeatedly. Thus, such models have the generic feature of replication of the fermion spectrum. An attractive feature of these models is thus the relative ease of constructing a model with three generations of quark-leptons.

To fully compare these models to experiment and to establish if they are

capable of describing our universe, it is necessary to compute scattering amplitudes between string states localised at brane intersections. The starting point for this is elucidated in detail in chapters 4 and 5. We began in chapter 4, with the simple case of Yukawa interactions and showed that the classical contribution went as $e^{-\frac{1}{2\pi\alpha'}\Delta}$, where Δ is the area of the triangle described by the intersecting branes (or more accurately, the sum of the projected areas in each sub-tori). As first pointed out in [10], this leads to a natural mechanism for the generation of a mass hierarchy. Next, we proceeded to the general four point amplitude, first presented in [9]. Again, the classical action can be minimised to obtain the area of a quadrilateral (when restricted to a single sub-torus). The correlator of twist fields was computed using a generalisation of methods developed for closed strings on orbifolds. In chapter 5, these results were generalised to N-point scattering amplitudes, thus securing a framework for discussing general interactions in intersecting brane models and hence understanding their phenomenology in more detail.

As a first step towards this aim, we analysed general $N = 4$ amplitudes on four independent sets of D-branes. The relevant process was $q_L q_R \to e_L e_R$. This process, depending as it does on the geometry of the D-branes, has a purely stringy contribution, as well as sensible field theory limit contributions corresponding to s and t-channel Higgs exchange. In the former case, the amplitude is of the form $\frac{Y_q/Y_e}{M_s^2}$ which should be compared to the field theory case $\frac{Y_q Y_e}{t-m_h^2}$. Thus, at low string scales the stringy exchanges are potentially important. Also, applications of our result may be used to establish constraints on the string scale through flavour changing neutral currents [96].

To conclude, we have contributed to the understanding of the phenomenological viability of certain string models based on D-brane configurations. In the long term, this will aid in either the construction of a new string model to replace the physics of the Standard Model, or show that such a model is not possible. Both scenarios will lead to an improved understanding of the fundamental structure of string theory.

Appendix A

Determination of zeros in $\tilde{K}_{33}$

As discussed in the main text, the zeros in $\tilde{K}_{33}$ are inherited from the hermitian matrix,

$$Z_{ij} = Tr((X_{33}^{(i)})^{\dagger} X_{33}^{(j)}). \tag{A.1}$$

The Chan-Paton factors were calculated in (3.52). However the $X_{33}^{(i)}$ are not determined uniquely. Therefore we choose the nth principal root of γ_{ω_k} defined by,

$$\gamma_{\omega_k}^{\frac{1}{n}} \equiv S^{\dagger} (\gamma_{\omega_k}^{diag})^{\frac{1}{n}} S, \tag{A.2}$$

with S the unitary matrix which diagonalises γ_{ω_k} and,

$$(\gamma_{\omega_k}^{diag})_{ij} = \delta_{ij} \lambda_i^{\frac{1}{n}}. \tag{A.3}$$

Here λ_i is the i^{th} eigenvalue of γ_{ω_k}, $\lambda_i^{1/n} \equiv e^{\frac{1}{n}\log(\lambda_i)}$ and we restrict $\arg(\lambda_i)$ to the interval $(-\pi, \pi]$, thus taking the principal value of $\log(\lambda_i)$.

With these choices the $X_{33}^{(i)}$ are uniquely determined, and we have

$$\begin{aligned} Z_{12} = \; & \tfrac{1}{s}(\textstyle\sum_{l=1}^{g(s)} e^{-4\pi i(l-1)/ns} + e^{4\pi i/n} \sum_{l=g(s)+1}^{s} e^{-4\pi i(l-1)/ns}) \\ & \times (\textstyle\sum_{p=0}^{p_{max}} e^{2\pi i p/n} \sum_{u(p)>j\geq l(p)} e^{-2\pi i(j-1)/M}), \end{aligned} \tag{A.4}$$

$$\begin{aligned} Z_{13} = \; & \tfrac{1}{s}(\textstyle\sum_{l=1}^{g(s)} e^{-2\pi i(l-1)/ns} + e^{2\pi i/n} \sum_{l=g(s)+1}^{s} e^{-2\pi i(l-1)/ns}) \\ & \times (\textstyle\sum_{p=0}^{p_{max}} e^{-2\pi i p/n} \sum_{u(p)>j\geq l(p)} e^{2\pi i(j-1)/M}), \end{aligned} \tag{A.5}$$

and,

$$\begin{aligned} Z_{23} = \; & \tfrac{1}{s}\left(\sum_{l=1}^{g(s)} e^{2\pi i(l-1)/ns} + e^{-2\pi i/n} \sum_{l=g(s)+1}^{s} e^{2\pi i(l-1)/ns}\right) \\ & \times \left(\sum_{p=0}^{p_{max}} e^{-4\pi ip/n} \sum_{u(p)>j\geq l(p)} e^{4\pi i(j-1)/M}\right), \end{aligned} \tag{A.6}$$

where,

$$\begin{aligned} p_{max} &= [\tfrac{(s-1)n}{M} + \tfrac{1}{2}], \\ u(p) &= (2p+1)\tfrac{M}{2n} + 1, \\ l(p) &= (2p-1)\tfrac{M}{2n} + 1, \\ g(s) &= \begin{cases} k & \text{if s=2k,} \\ k+1 & \text{if s=2k+1,} \end{cases} \end{aligned} \tag{A.7}$$

with [..] denoting rounding to the nearest integer. Furthermore, since the $X_{33}^{(i)}$ are unitary $s \times s$ matrices, we have

$$Z = \begin{pmatrix} s & Z_{12} & Z_{13} \\ Z_{12}^* & s & Z_{23} \\ Z_{13}^* & Z_{23}^* & s \end{pmatrix}. \tag{A.8}$$

Finally, it can be easily seen from (A.4), (A.5) and (A.6) that $Z_{12} = Z_{13} = Z_{23} = 0$ for $n = 1$, $Z_{12} = Z_{23} = 0$ and $Z_{13} \neq 0$ for $n = 2$ and for $n \geq 3$ all elements of Z are non-zero.

Appendix B

Computations for N-point functions in intersecting brane models

B.1 Computation of integrals in the classical action

We now generalise the methods in [92] to evaluate the integral,

$$I(x_2,..,x_{N-2}) = \int d^2z \prod_{j=2}^{N-2} |z-x_j|^{-2(1-\vartheta_j)} |z|^{-2(1-\vartheta_1)} |z-1|^{-2(1-\vartheta_{N-1})}. \quad \text{(B.1)}$$

This is required in the computation of the classical contribution to the N-point function for open strings at D-brane intersections.

If we introduce the new variables, $\xi = z$ and $\eta = \bar{z}$, we can rewrite (B.1) as

$$\begin{aligned} &I = \tfrac{i}{2} \textstyle\int_{-\infty}^{\infty} d\xi \int_{-\infty}^{\infty} d\eta |\xi\eta|^{-(1-\vartheta_1)} |(1-\xi)(1-\eta)|^{-(1-\vartheta_{N-1})} \times \\ &\textstyle\prod_{j=2}^{N-2} |(x_j-\xi)(x_j-\eta)|^{-(1-\vartheta_j)} exp[i\pi(f(-(1-\vartheta_1);\xi,\eta) + \\ &f(-(1-\vartheta_{N-1});(1-\xi),(1-\eta)) + \textstyle\sum_{j=2}^{N-2} f(-(1-\vartheta_j);(x_j-\xi),(x_j-\eta)))], \end{aligned} \quad \text{(B.2)}$$

where

$$f(a;x,y) = \begin{cases} 0 & xy > 0 \\ a & xy < 0. \end{cases} \quad \text{(B.3)}$$

	$\eta < 0$	$x_p < \eta < x_{p+1}$	$\eta > 1$
$\xi < 0$	0	$-\sum_{l=1}^{p}(1-\vartheta_l)$	$-\sum_{l=1}^{N-1}(1-\vartheta_l)$
$x_j < \xi < x_{j+1}$	$-\sum_{l=1}^{j}(1-\vartheta_l)$	$p > j$, $-\sum_{l=j+1}^{p}(1-\vartheta_l)$ $p = j$, 0 $p < j$, $-\sum_{l=p+1}^{j}(1-\vartheta_l)$	$-\sum_{l=j+1}^{N-1}(1-\vartheta_l)$
$\xi > 1$	$-\sum_{l=1}^{N-1}(1-\vartheta_l)$	$-\sum_{l=p+1}^{N-1}(1-\vartheta_l)$	0

Table B.1: Complex phases in $I(x_i)$

This phase convention results in the phases in table B.1 for the differing regions of the integration parameters. Now we split up the integral over ξ into the regions given in the table and regard the η integration as a complex integral. Then the phase choice in (B.2) corresponds to the integration contours in the complex η plane as shown in figure B.1. With a careful analysis of the branch cuts these contours give phases consistent with those in table B.1. In the cases $\xi < 0$ and $\xi > 1$, we can close the contour to give a zero contribution to the integral. In the remaining cases of $x_j < \xi < x_{j+1}$, we can deform the contour as depicted in figure B.2 (or equivalently, we could deform the bottom half of the contour in the opposite direction). On splitting the new contour into a sum over integrals between x_p and x_{p+1}, the phase factor for each integrand is,

$$\begin{array}{ll} \sum_{l=j+1}^{p}(1-\vartheta_l) & \text{top of contour,} \\ -\sum_{l=j+1}^{p}(1-\vartheta_l) & \text{bottom of contour.} \end{array} \tag{B.4}$$

This allows us to split I into a product of line integrals,

$$\begin{array}{l} I = \sum_{p=2}^{N-2}\sin(\pi\sum_{m=2}^{l}(1-\vartheta_m))\int_0^{x_2}d\xi h(\xi)\int_{x_p}^{x_{p+1}}d\eta h(\eta) + \\ \sin(\pi\sum_{m=2}^{N-1}(1-\vartheta_m))\int_0^{x_2}d\xi h(\xi)\int_1^{\infty}d\eta h(\eta) + \\ \sum_{j=2}^{N-2}\sum_{p=1}^{j-1}\sin(\pi\sum_{m=p+1}^{j}(1-\vartheta_m))\int_{x_j}^{x_{j+1}}d\xi h(\xi)\int_{x_p}^{x_{p+1}}d\eta h(\eta) + \\ \sum_{j=2}^{N-2}\sin(\pi\sum_{m=1}^{j}(1-\vartheta_m))\int_{x_j}^{x_{j+1}}d\xi h(\xi)\int_{-\infty}^{0}d\eta h(\eta), \end{array} \tag{B.5}$$

where,

$$h(y) = |y|^{-(1-\vartheta_1)}|1-y|^{-(1-\vartheta_{N-1})}\prod_{j=2}^{N-2}|x_j-y|^{-(1-\vartheta_j)}. \tag{B.6}$$

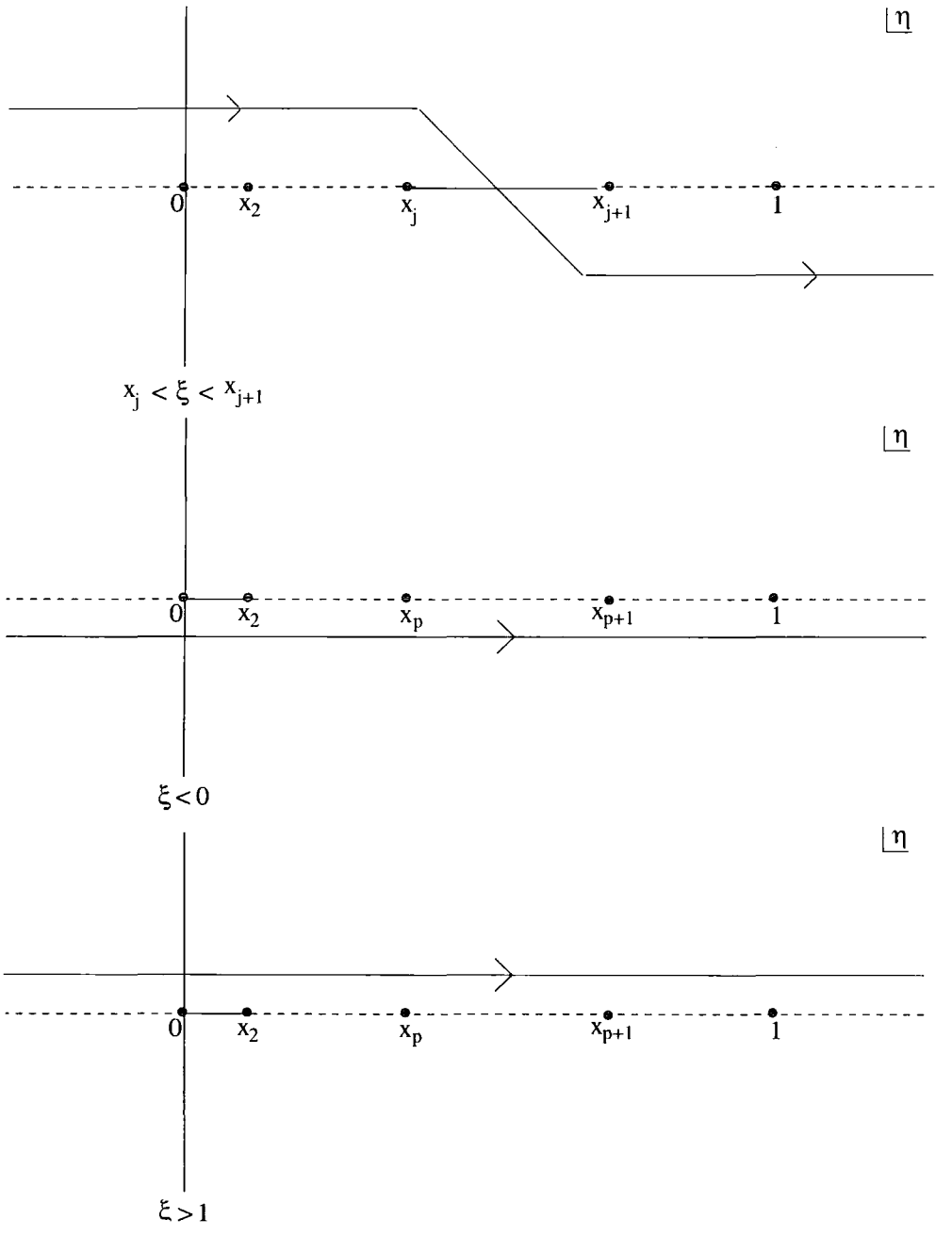

Figure B.1: The contour integrals for the cases a) $x_j < \xi < x_{j+1}$; b) $\xi < 0$, and c) $\xi > 1$. The dotted lines denote branch cuts.

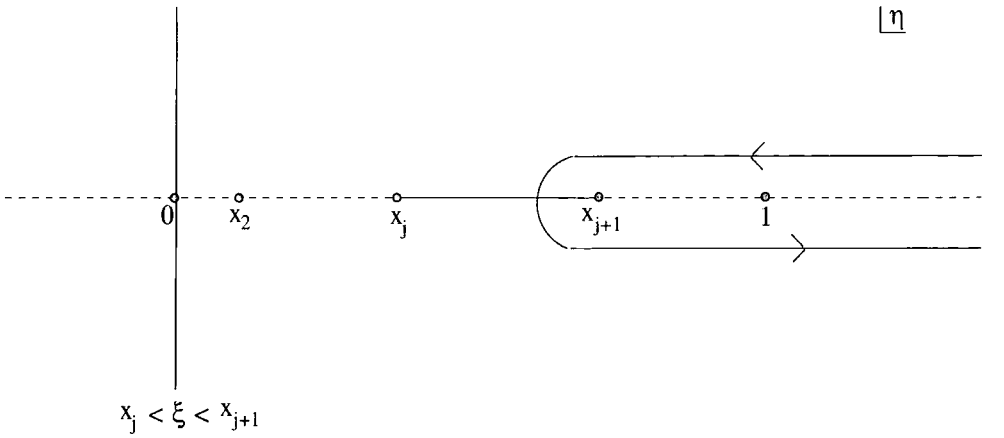

Figure B.2: Deformed contour for $x_j < \xi < x_{j+1}$.

Thus we obtain,

$$I(x_2,..,x_{N-2}) = \sum_{p=2}^{N-1}(-1)^p \alpha_{2,p}|F_p^1||F_1^1| + \sum_{j=2}^{N-2}\sum_{p=0}^{j-1}(-1)^{j-(p+1)}\alpha_{p+1,j}|F_j^1||F_p^1|, \tag{B.7}$$

where we have defined $\alpha_{ij} = \sum_{l=i}^{j}\vartheta_l$ and the following line integrals,

$$\begin{aligned} F_i^1 &= \int_{x_i}^{x_{i+1}} \prod_{j=1}^{N-1}(y-x_j)^{-(1-\vartheta_j)}, \quad i = 1,..,N-2, \\ F_0^1 &= \int_{-\infty}^{0} \prod_{j=1}^{N-1}(y-x_j)^{-(1-\vartheta_j)}, \quad F_{N-1}^1 = \int_1^{\infty} \prod_{j=1}^{N-1}(y-x_j)^{-(1-\vartheta_j)}. \end{aligned} \tag{B.8}$$

Note that in the four point case this reduces to (4.44), with the identification $F_i^1 = F_i$, and to (4.25) in the three point case. Also, this result is consistent with similar expressions used in [11, 92].

B.2 Lauricella and hypergeometric functions

Lauricella functions are the generalisations of hypergeometric functions to multiple variables. The Type D Lauricella function has the integral representation,

$$\begin{aligned} &B(a,c-a)F_D^{(n)}(a,b_1,..,b_n;c;x_1,..,x_n) = \\ &\int_0^1 u^{a-1}(1-u)^{c-a-1}(1-ux_1)^{-b_1}..(1-ux_n)^{-b_n}du, \end{aligned} \tag{B.9}$$

when $Re(a), Re(c-a) > 0$ and $B(p,q)$ is the beta function. Hence we can express the line integrals (B.8) in terms of Type D Lauricella functions. It is easily shown that,

$$\begin{aligned} F_i^1 =& e^{i\pi\vartheta_i}(x_i - x_{i+1})^{-1+\vartheta_i+\vartheta_{i+1}} \prod_{\substack{j=1 \\ (j\neq i,i+1)}}^{N-1} (x_i - x_j)^{-(1-\vartheta_j)} B(\vartheta_i, \vartheta_{i+1}) \times \\ & F_D^{(N-3)}(\vartheta_i, 1-\vartheta_1, .., 1-\vartheta_{i-1}, 1-\vartheta_{i+2}, .., 1-\vartheta_{N-1}; \vartheta_i + \vartheta_{i+1}; \\ & \tilde{x}_{i,1}, .., \tilde{x}_{i,i-1}, \tilde{x}_{i,i+2}, .., \tilde{x}_{i,N-1}), \end{aligned}$$

where $i = 1, .., N-2$ and,

$$\begin{aligned} F_0^1 =& e^{-i\pi(\vartheta_N+1)} B(\vartheta_N, \vartheta_1) \times \\ & \times F_D^{(N-3)}(\vartheta_N, 1-\vartheta_2, .., 1-\vartheta_{N-2}; \vartheta_1 + \vartheta_N; 1-x_2, .., 1-x_{N-2}), \\ F_{N-1}^1 =& B(\vartheta_N, \vartheta_{N-1}) F_D^{(N-3)}(\vartheta_N, 1-\vartheta_2, .., 1-\vartheta_{N-2}; \vartheta_N + \vartheta_{N-1}; x_2, .., x_{N-2}), \end{aligned} \tag{B.10}$$

where $\tilde{x}_{ij} = \frac{x_i - x_{i+1}}{x_i - x_j}$. These are required in the computation of the classical part of N-point amplitudes in intersecting brane models.

Consider the case $N = 4$, then our Lauricella functions reduce to the standard hypergeometric functions,

$$\begin{aligned} F_0^1 &= e^{-i\pi(1+\vartheta_4)} B(\vartheta_4, \vartheta_1) {}_2F_1(\vartheta_4, 1-\vartheta_2; \vartheta_1 + \vartheta_4; 1-x_2), \\ F_1^1 &= e^{-i\pi(\vartheta_2+\vartheta_3)} x_2^{-1+\vartheta_1+\vartheta_2} B(\vartheta_1, \vartheta_2) {}_2F_1(\vartheta_1, 1-\vartheta_3; \vartheta_1 + \vartheta_2; x_2), \\ F_2^1 &= e^{-i\pi(-1+\vartheta_3)} (1-x_2)^{-1+\vartheta_2+\vartheta_3} B(\vartheta_2, \vartheta_3) {}_2F_1(\vartheta_3, 1-\vartheta_1; \vartheta_2 + \vartheta_3; 1-x_2), \\ F_3^1 &= B(\vartheta_4, \vartheta_3) {}_2F_1(\vartheta_4, 1-\vartheta_2; \vartheta_4 + \vartheta_3; x_2), \end{aligned} \tag{B.11}$$

where ${}_2F_1(a,b,c;x) = F_D^1(a,b;c;x)$. Due to the simpler form of these hypergeometric functions, they satisfy a number of identities,

1. ${}_2F_1(a,b;c;x) = (1-x)^{c-a-b} {}_2F_1(c-a, c-b; c; x)$.
2. ${}_2F_1(a,b;c;x) = (1-x)^{-a} {}_2F_1(a, c-b; c; \frac{x}{x-1})$.
3. ${}_2F_1(a,b;c;x) = \frac{\Gamma(c)\Gamma(a+b-c)}{\Gamma(a)\Gamma(b)} {}_2F_1(c-a, c-b; c-a-b+1; 1-x) \times$
   $(1-x)^{c-a-b} + \frac{\Gamma(c)\Gamma(c-a-b)}{\Gamma(c-a)\Gamma(c-b)} {}_2F_1(a, b; a+b-c+1; 1-x)$.
4. ${}_2F_1(a,b;c;x) = \frac{\Gamma(c)\Gamma(b-a)}{\Gamma(b)\Gamma(c-a)} {}_2F_1(a, c-b; a-b+1; \frac{1}{1-x}) \times$
   $(1-x)^{-a} + \frac{\Gamma(c)\Gamma(a-b)}{\Gamma(a)\Gamma(c-b)} {}_2F_1(b, c-a; b-a+1; \frac{1}{1-x})(1-x)^{-b}$.

(B.12)

These identities are utilised in the simplification of the classical action in section 4.5.2. In particular, they can be used to deduce (4.46) and (4.49).

Of further use in the computation of the four-point amplitude in section 4.5.4, is the hypergeometric differential equation,

$$(1-x)xy'' + (c-(a+b+1)x)y' - aby = 0. \tag{B.13}$$

This has the solution,

$$y = {}_2F_1(a,b;c;x)c_1 + x^{1-c}{}_2F_1(a-c+1,b-c+1;2-c;x)c_2. \tag{B.14}$$

So, in our case we define $G_l = \int F_l(x_2)dx_2$, which can be expressed as

$$\begin{aligned} G_1 &\sim x_2^{\vartheta_1+\vartheta_2}{}_2F_1(\vartheta_1, 1-\vartheta_3; 1+\vartheta_1+\vartheta_2; x_2), \\ G_2 &\sim (1-x_2)^{\vartheta_2+\vartheta_3}{}_2F_1(\vartheta_3, 1-\vartheta_1; 1+\vartheta_2+\vartheta_3; 1-x_2). \end{aligned} \tag{B.15}$$

These two expressions are of the form (B.14) with $c_1 = 0$. Hence, identifying a, b and c we obtain,

$$(1-\vartheta_4)\vartheta_2 G_l = x_2(1-x_2)\partial F_l + (-1)^l(\vartheta_1+\vartheta_2-1+(\vartheta_4-\vartheta_2)x_2)F_l, \tag{B.16}$$

and letting $\vartheta_i \to 1-\vartheta_i$ we obtain,

$$(1-\vartheta_2)\vartheta_4 G_l' = x_2(1-x_2)\partial F_l' - (-1)^l(\vartheta_1+\vartheta_2-1+(\vartheta_4-\vartheta_2)x_2)F_l'. \tag{B.17}$$

Bibliography

[1] E.Cremmer, B.Julia, and J.Scherk. Supergravity Theory in Eleven-Dimensions. *Phys.Lett.*, B76:409–412, 1978.

[2] M.J.Duff. M-Theory (The Theory Formly Known as Strings). *Int.J.Mod.Phys.*, A11:5623–5642, 1996. hep-th/9608117.

[3] J.H.Schwarz. Lectures on Superstring and M-Theory Dualities. *Nucl.Phys.Proc.Suppl.*, B55:1–32, 1997. hep-th/9607201.

[4] P.Candelas, G.T.Horowitz, A.Strominger, and E.Witten. Vacuum Configurations for Superstrings. *Nucl.Phys.*, B258:46–74, 1985.

[5] M.Atiyah and E.Witten. M-Theory Dynamics On A Manifold of G_2 Holonomy. *Adv.Theor.Math.Phys.*, 6:1–106, 2003. hep-th/0107177.

[6] P.Horava and E.Witten. Eleven-Dimensional Supergravity on a Manifold with Boundary. *Nucl.Phys.*, B475:94–114, 1996. hep-th/9603142.

[7] G.Aldazabal, L.E.Ibáñez, F.Quevedo, and A.M.Uranga. D-branes at Singularities: A Bottom-Up Approach to the String Embedding of the Standard Model. *JHEP*, 008:002, 2000. hep-th/0005067.

[8] S.A.Abel and A.W.Owen. Interactions in Intersecting Brane Models. *Nucl.Phys.*, B663:197–214, 2003. hep-th/0303124.

[9] S.A.Abel and A.W.Owen. N-point Amplitudes in Intersecting Brane Models. *Nucl.Phys.*, 682:183–216, 2004. hep-th/0310257.

[10] G.Aldazabal, S.Franco, L.E.Ibáñez, R.Rabadán, and A.M.Uranga. Intersecting Brane Worlds. *JHEP*, 0102:047, 2001. hep-th/0011132.

[11] L.Dixon, D.Friedan, E.Martinec, and S.Shenker. The Conformal Field Theory of Orbifolds. *Nucl.Phys.*, B282:13–73, 1987.

[12] S.Hamidi and C.Vafa. Interactions on Orbifolds. *Nucl.Phys*, B279:465, 1987.

[13] M.B.Green, J.H.Schwartz, and E.Witten. *Superstring Theory, volumes 1 and 2.* Cambridge University Press, Cambridge, 1987.

[14] J.Polchinski. *String Theory, volumes 1 and 2.* Cambridge University Press, Cambridge, 1998.

[15] R.J.Szabo. BUSSTEPP LECTURES ON STRING THEORY:An Introduction to String Theory and D-Brane Dynamics. hep-th/0207142.

[16] C.V.Johnson. D-Brane Primer. hep-th/0007170.

[17] J.Polchinski. TASI Lectures on D-branes. hep-th/9611050.

[18] J.Polchinski. Dirichlet Branes and Ramond-Ramond Charges. *Phys.Rev.Lett*, 75:4724–4727, 1995. hep-th/9510017.

[19] D.Bailin and A.Love. Orbifold Compactifications of String Theory. *Phys.Rept.*, 315:285–408, 1999.

[20] E.Gimon and J.Polchinski. Consistency Conditions for Orientifolds and D-Manifolds. *Phys.Rev.*, D54:1667–1676, 1996. hep-th/9601038.

[21] S.A.Abel and J.Santiago. Constraining the string scale: from Planck to Weak and back again. *J.Phys.*, G30:R83–R111, 2004. hep-ph/0404237.

[22] E.Cremmer, S.Ferrara, L.Girardello, and A.Van Proeyen. Coupling Supersymmetric Yang-Mills Theories to Supergravity. *Phys.Lett*, B116:231, 1982.

[23] E.Cremmer, S.Ferrara, L.Girardello, and A.Van Proeyen. Yang-Mills Theories with Local Supersymmetry:Lagrangian, Transformation Laws and Superhiggs Effect. *Nucl.Phys.*, B212:413, 1983.

[24] M.Dine and N.Seiberg. Couplings and Scales in Superstring Models. *Phys.Rev.Lett.*, 55:366, 1985.

[25] E.Witten. New Issues in Manifolds of $SU(3)$ Holonomy. *Nucl.Phys.*, B268:79, 1986.

[26] C.P.Burgess, A.Font, and F.Quevedo. Low Energy Effective Action for the Superstring. *Nucl.Phys.*, B272:661, 1986.

[27] S.A.Abel and A.W.Owen. CP violation and CKM predictions from Discrete Torsion. *Nucl.Phys.*, B651:191–210, 2003. hep-th/0205031.

[28] B.Aubert et al. Observation of CP Violation in the B0 Meson System. *Phys.Rev.Lett*, 87:091801. *hep-ex/0107013.*

[29] K.Abe et al. Observation of Large CP Violation in the Neutral B Meson System. *Phys.Rev.Lett*, 87:091802. *hep-ex/0107061.*

[30] T.Affolder et al. A Measurement of $\sin 2\beta$ from B $\rightarrow$ J / Ψ K0(S) with the CDF Detector. *Phys.Rev.*, D61:072005. *hep-ex/9909003.*

[31] M.Dine, R.G.Leigh, and D.A.MacIntire. Of CP and other Gauge Symmetries in String theory. *Phys.Rev.Lett*, 69:2030–2032, 1992. hep-th/9205011.

[32] K.Choi, D.B.Kaplan, and A.E.Nelson. Is CP a Gauge Symmetry? *Nucl.Phys.*, B391:515, 1993. *hep-ph/9205202.*

[33] S.Khalil, O.Lebedev, and S.Morris. CP Violation and Dilaton Stabilization in Heterotic String Models. *Phys.Rev.*, D65:115014, 2002. *hep-th/0110063.*

[34] O.Lebedev and S.Morris. Towards a Realistic Picture of CP Violation in Heterotic String Models. *JHEP*, 0208:007, 2002. *hep-th/0203246.*

[35] S.A.Abel and G.Servant. CP and Flavour in Effective Type I Strings Models. *Nucl.Phys.*, B611:43. *hep-ph/0105262.*

[36] S.A.Abel and G.Servant. Dilaton Stabilization in Effective Type I String Models. *Nucl.Phys.*, B597:3. *hep-th/0009089.*

[37] D.Bailin, G.V.Kraniotis, and A.Love. The Effect of Wilson Line Moduli on CP Violation by Soft Supersymmetry Breaking Terms. *Phys.Lett*, B422:343–352. *hep-th/98041325.*

[38] D.Bailin, G.V.Kraniotis, and A.Love. CP Violating Phases in the CKM Matrix in Orbifold Compactifications. *Phys.Lett*, B435:323–330. *hep-th/9805111.*

[39] D.Bailin, G.V.Kraniotis, and A.Love. CP Violation by Soft Supersymmetry Breaking terms in Orbifold Compactifications. *Phys.Lett*, B414:269. *hep-th/9707105.*

[40] T.Dent. Breaking CP and Supersymmetry with Orbifold Moduli Dynamics. *Nucl.Phys.*, B623:73–96. *hep-th/0110110.*

[41] E.Sharpe. Recent Developments in Discrete Torsion. *Phys.Lett.*, B498:104–110, 2002. hep-th/0008191.

[42] Y.Nir. CP Violation In and Beyond the Standard model. hep-ph/9911321.

[43] C.Jarlskog. Commutator of the Quark Mass Matrices in the Standard Electroweak model and a Measure of Maximal CP Nonconservation. *Phys.Rev.Lett*, 55:1039, 1985.

[44] M.Kobayashi and T.Maskawa. CP Violation in the Renormalizable Theory of Weak Interaction. *Prog.Theo.Phys.*, 49:652–657, 1973.

[45] C.Vafa. Modular Invariance and Discrete Torsion in Orbifolds. *Nucl. Phys*, B273:592–606, 1986.

[46] C.Vafa and E.Witten. On Orbifolds with Discrete Torsion. *J.Geom.Phys*, 15:189–214. *hep-th/9409188.*

[47] M.E.Angulo, D.Bailin, and H.Yang. Tadpole and Anomally Cancellation Conditions in D-brane Orbifold models. *Int.J.Mod.Phys*, A18:3637–3694, 2003. hep-th/'0210150.

[48] G.Aldazabal, A.Font, L.E.Ibáñez, and G.Violero. D=4, N=1, Type IIB Orientifolds. *Nucl.Phys.*, B536:29–68, 1998. hep-th/9804026.

[49] M.R.Douglas. D-branes and Discrete Torsion. *hep-th/9807235.*

[50] M.Klein and R.Rabadán. Orientifolds with Discrete Torsion. *JHEP*, 0007:040, 2000. hep-th/0002103.

[51] L.E.Ibáñez, R.Rabadán, and A.M.Uranga. Anomalous $U(1)$'s in Type I and Type IIB $D = 4$, $N = 1$ string vacua. *Nucl.Phys.*, B542:112, 1999. hep-th/9808139.

[52] E.Poppitz. On the One Loop Fayet-Iliopoulos Term in Chiral Four Dimensional Type I Orbifolds. *Nucl.Phys.*, B542:31–44, 1999. hep-th/9810010.

[53] V.Kaplunovsky and J.Louis. On Gauge Couplings in String Theory. *Nucl.Phys.*, B444:191–244, 1995. *hep-th/9502077.*

[54] K.Hagiwara *et al.* Particle Data Group. *Phys.Rev.*, D66:010001, 2002.

[55] M.Cvetič and I.Papadimitriou. Conformal Field Theory Couplings for Intersecting D-branes on Orientifolds. *Phys.Rev.*, D68:046001, 2003. hep-th/0303083.

[56] R.Blumenhagen, L.Göerlich, B.Körs, and D.Lüst. Non-commutative Compactifications of Type I Strings on Tori with Magnetics Background Flux. *JHEP*, 0010:006, 2000. hep-th/0007024.

[57] M.Berkooz, M.R.Douglas, and R.G.Leigh. Branes Intersecting at Angles. *Nucl.Phys.*, B480:265–278, 1996. hep-th/9606139.

[58] G.Aldazabal, S.Franco, L.E.Ibáñez, R.Rabadán, and A.M.Uranga. D=4 Chiral String Compactifications from Intersecting Branes. *J.Maths.Phys.*, 42:3103–3126, 2001. hep-th/0011073.

[59] R.Blumenhagen, B.Körs, and D.Lüst. Type I Strings with F- and B-Flux. *JHEP*, 0102:030, 2001. hep-th/0012156.

[60] R.Blumenhagen, B.Körs, and D.Lüst. Moduli Stabilization for Intersecting Brane Worlds in Type 0' String Theory. *Phys.Lett.*, B532:141–151, 2002. hep-th/0202024.

[61] R.Blumenhagen, B.Körs, D.Lüst, and T.Ott. Hybrid Inflation in Intersecting Brane Worlds. *Nucl.Phys.*, B641:235–255, 2002. hep-th/0202124.

[62] R.Blumenhagen, V.Braun, B.Körs, and D.Lüst. Orientifolds of K3 and Calabi-Yau Manifolds with Intersecting D-Branes. *JHEP*, 0207:026, 2002. hep-th/0206038.

[63] J.Ellis, P.Kanti, and D.V.Nanopoulos. Intersecting Branes Flip SU(5). *Nucl.Phys.*, B647:235–251, 2002.

[64] Christos Kokorelis. Standard Model Compactifications from Intersecting Branes. hep-th/0211091.

[65] D.Cremades, L.E.Ibáñez, and F.Marchesano. More about the Standard Model at Intersecting Branes. hep-th/0212048.

[66] D.Bailin, G.V.Kraniotis, and A.Love. Intersecting D5-Brane Models with Massive Vector-like Leptons. *JHEP*, 0302:052, 2003. hep-th/0212112.

[67] M.Cvetič, I.Papadimitriou, and G.Shiu. Supersymmetric Three Family $SU(5)$ Grand Unified Models from Type IIA Orientifolds with Intersecting D6-Branes. hep-th/0212177.

[68] R.Blumenhagen, D.Lüst, and T.R.Taylor. Moduli Stabilization in Chiral Type IIB Orientifold Models with Fluxes. *Nucl.Phys.*, B663:319–342, 2003. hep-th/0303016.

[69] T.Li and T.Liu. Quasi-Supersymmetric G^3 Unification from Intersecting D6-Branes on Type IIA Orientifolds. hep-th/0304258.

[70] M.Axenides, E.Floratos, and C.Kokorielis. SU(5) Unified Theories from Intersecting Branes. hep-th/0307255.

[71] L.E.Ibáñez, F.Marchesano, and R.Rabadán. Getting Just the Standard Model at Intersecting Branes. *JHEP*, 0111:002, 2001. hep-th/0105155.

[72] R.Blumenhagen, B.Körs, D.Lüst, and T.Ott. The Standard Model from Stable Intersecting Brane World Orbifolds. *Nucl.Phys.*, B616:3–33, 2001. hep-th/0107138.

[73] D.Cremades, L.E.Ibáñez, and F.Marchesano. Standard Model at Intersecting D5-branes: Lowering the String Scale. *Nucl.Phys.*, B643:93–130, 2002. hep-th/0205074.

[74] C.Kokorelis. New Standard Model vacua from Intersecting Branes. *JHEP*, 0209:029, 2002. hep-th/0205147.

[75] C.Kokorelis. Exact Standard Model Compactifications From Intersecting Branes. *JHEP*, 0208:036, 2002. hep-th/0206108.

[76] M.Cvetič, P.Langacker, and G.Shiu. Three Family Standard-like Orientifold model: Yukawa Couplings and Hierarchy. *Nucl.Phys.*, B642:139, 2002. hep-th/0206115.

[77] C.Kokorelis. Exact Standard Model Structures From Intersecting D5-Branes. hep-th/0207234.

[78] M.Cvetič, G.Shiu, and A.M.Uranga. Three-family Supersymmetric Standard-like Models from Intersecting Brane Worlds. *Phys.Rev.Lett.*, 87:201801, 2001. hep-th/0107143.

[79] M.Cvetič, G.Shiu, and A.M.Uranga. Chiral Four-Dimensional N=1 Supersymmetric Type IIA Orientifolds from Intersecting D6-Branes. *Nucl.Phys.*, B615:3, 2001. hep-th/0107166.

[80] R.Blumenhagen, L.Göerlich, and T.Ott. Supersymmetric Intersecting Branes on the Type IIA $T^6/\mathbb{Z}_4$ orientifold. *JHEP*, 0301:021, 2003. hep-th/0211059.

[81] G.Honecker. Chiral Supersymmetric Models on an Orientifold of $\mathbb{Z}_4 \times \mathbb{Z}_2$ with Intersecting D6-branes. hep-th/0303015.

[82] M.Cvetič and I.Papadimitriou. More Supersymmetric Standard-Like Models from Intersecting D6-Branes on Type IIA Orientifolds. *Phys.Rev.*, D67:126006, 2003. hep-th/0303197.

[83] M.Cvetič, P.Langacker, and J.Wang. Dynamical Supersymmetry Breaking in Standard-Like Models with Intersecting D6-Branes. *Phys.Rev.*, D68:046002, 2003. hep-th/0303208.

[84] K.Behrndt and M.Cvetič. Supersymmetric Intersecting D6-Branes and Fluxes in Massive Type IIA String Theory. hep-th/0308045.

[85] C.Kokorelis. N=1 Locally Supersymmetric Standard Models from Intersecting Branes. hep-th/0309070.

[86] C.Kokorelis. Deformed Intersecting D6-brane GUTS and N=1 SUSY. hep-th/0212281.

[87] D.Lüst and S.Stieberger. Gauge Threshold Corrections in Intersecting Brane World Models. hep-th/0302221.

[88] I.R.Klebanov and E.Witten. Proton Decay in Intersecting D-Brane Models. *Nucl.Phys.*, B664:3–20, 2003. hep-th/0304079.

[89] R.Blumenhagen, D.Lüst, and S.Stieberger. Gauge Unification in Supersymmetric Intersecting Brane Worlds. *JHEP*, 0307:036, 2003. hep-th/0305146.

[90] J.A.Casas, F.Gomez, and C.Muñoz. World-sheet instanton contribution to $\mathbb{Z}_7$ Yukawa couplings. *Phys.Lett.B*, 251:99–104.

[91] T.Kobayashi and O.Lebedev. Heterotic Yukawa couplings and continuous Wilson lines. hep-th/0303009.

[92] H.Kawai, D.C.Lewellen, and S.-H.H.Tye. A relation between tree amplitudes of closed and open strings. *Nucl.Phys.*, B269:1, 1986.

[93] D.Cremades, L.E.Ibáñez, and F.Marchesano. Yukawa couplings in intersecting D-brane models. *JHEP*, 0307:038, 2003. hep-th/0302105.

[94] A.A.Belavin, A.M.Polyakov, and A.B.Zamolodchikov. Infinite Conformal Symmetry in Two-Dimensional Qunatum Field Theory. *Nucl.Phys.*, B241:333–380, 1984.

[95] S.Abel, M.Masip, and J.Santiago. Flavour Changing Neutral Currents in Intersecting Brane Models. *JHEP*, 0304:057, 2003. hep-ph/0303087.

[96] S.A.Abel, O.Lebedev, and J.Santiago. Flavour in Intersecting Brane Models and Bounds on the String Scale. hep-ph/0312157.

[97] F.Lazebnik. On Systems of Linear Diophantine Equations. *The Mathematics Magazine*, 69:261–266, 1996.

[98] B.L.van der Waerden. *Algebra, Volume 2.* Frederick Ungar Publishing Co., New York, 1970.

[99] J.J.Atick, L.J.Dixon, and P.A.Griffin. Multi-loop Twist Field Correlation Functions for $\mathbb{Z}_N$ Orbifolds. *Nucl.Phys.*, B298:1–35, 1988.

[100] D.Lüst, P.Mayr, R.Richter, and S.Stieberger. Scattering of Gauge, Matter, and Moduli Fields from Intersecting Branes. hep-th/0404134.